Electrochemical Carboxylation of Aldehydes with CO_2: Mechanistic Insights and Enantioselective Synthesis

Thesis by

Thu Nu Minh Ton

In Partial Fulfillment of the Requirements for

the degree of

Doctor of Philosophy in Chemistry

CALIFORNIA INSTITUTE OF TECHNOLOGY

Pasadena, California

2026

(Defended May 20th, 2026)

Thu Nu Minh Ton
ORCID: 0000-0003-0134-2435

ACKNOWLEDGMENTS

My graduate journey would not have been possible without the support of those around me.

First, I would like to thank my advisor, Prof. Karthish Manthiram. When I first joined the group, I had zero knowledge of electrochemistry. It is through Karthish's mentorship and encouragement that I can call myself an electrochemist today. He consistently encouraged me to develop my own research interests and to voice my perspectives with confidence, knowing that I often preferred to listen rather than speak. Above all, Karthish entrusted me with the independence to grow as a scientist, and that trust became the foundation of my own self-confidence. I am grateful to have had the opportunity to conduct my graduate studies in the Manthiram group.

I am also grateful for the support of my committee members. My committee chair, Prof. Kim See, has been incredibly supportive ever since I joined Caltech as a first-year student. It was a privilege to take her electrochemical course and learn electrochemistry from a different perspective. Kim always advised me to pursue bigger and crazier ideas, something I hope to keep striving for in the future. I have also learned a great deal from Prof. Brian Stoltz, who was always willing to offer an organic chemist's perspective on my work. Brian has also been incredibly encouraging in my pivot to a patent law career and provided invaluable support throughout my job search. Lastly, I am grateful to Prof. Scott Cushing for his valuable feedback on my work. His straightforward approach pushed me to think more clearly about my work and decide what I want to prioritize.

Next, I would like to acknowledge my mentors in the Manthiram group. Prof. Rachel Baker was my mentor during my first year and I learned so much from her, both inside and outside the lab. Not only is Rachel an incredible chemist, but she is also incredibly kind and humble. No matter how frustrated or discouraged I felt, she had a remarkable gift for keeping things in perspective. Dr. Haochen Zhang was my mentor in my later years at Caltech and his guidance greatly shaped who I am as a scientist. Under Haochen's guidance, I became a more meticulous and careful thinker. Most important, Haochen believed in me more than I

believed in myself, and that belief helped me through the harder moments of graduate school more than he probably realizes.

Other members of the Manthiram group also helped me in various ways. I learned a great deal about electrochemical carboxylation from Dr. Nathan Corbin, whose work inspired me to join the group. Prof. Minju Chung and Prof. Joy Cho were so supportive and helpful in my first years and taught me so much about how to do electrochemistry research. It was a pleasure to work with Emma Cosner and Spencer Delgado-Kukuczka, my fellow Sub-C members. I always consider them the cool kids of Sub-C and am grateful for our many conversations and Sub-C lunches. Thank you to Dr. Gangsan Lee for being a great listener while I discuss my problems at our benches and for always giving good advice.

I have had many opportunities to work with many collaborators, whose scientific inputs were tremendously valuable. Dr. Paul Oyala helped me with my EPR experiments and provided helpful feedback on the data interpretation. Dr. Nathan Dalleska helped me with UPLC-UV Vis and was incredibly patient when I made mistakes.

Many members of the Caltech community helped me throughout my Ph.D. I would like to thank Martha Hepworth and Matt Buga for ensuring that things are always running smoothly in the Manthiram lab. Thank you to the administrative assistants, namely Aracely Sustaita, Tomomi Kano, and Elisha Okawa for their help with scheduling all my committee meetings.

I want to thank my undergraduate research advisor, Prof. Jarad Mason, as well as my mentors Dr. Grant Stec, Dr. Suren Thapa, and Dr. Jae Lee. I learned so much about research during this time and their guidance inspired me to pursue my Ph.D.

I entered Caltech with an amazing cohort of scientists, who later became great friends. Thank you to Mengdi Li and Colin Morrell for being in my group during Chem 112 and making the class more enjoyable. I always enjoy our conversations whenever we have the chance to catch up. My fellow lab mates Chenyu Jiang, Channing Klein, and James Wang have been my greatest support and best friends in the Manthiram lab. They are truly the most loyal crew, and I am forever grateful that graduate school brought us together.

I always looked forward to spending time with my Vietnamese friends because our hangouts always involved great food and even better conversations. Thank you to Hai Dong, Linh Le, Ha Vu, Vy Nguyen, and Mai Nguyen for joining me on my food adventures and for suggesting great new restaurants.

I am grateful for my family's support during my Ph.D. Thank you to my parents for listening to my worries and for always encouraging me. Their unconditional support allowed me to keep striving for bigger goals and I would not be where I am today without them. Thank you to my brother, Thanh, for always listening to my problems and for being the voice of reason. Thank you for treating me to good food despite being the younger sibling.

Lastly, my partner, Khoa. Meeting you was the best thing that happened during my Ph.D. I am so grateful for your never-ending patience and your unfailing ability to make me laugh. Graduate school was a thousand times better with you by my side, and I look forward to many more adventures with you.

ABSTRACT

The electrochemical carboxylation of organic substrates with CO_2 is a promising strategy for the sustainable synthesis of value-added carboxylic acids, offering mild operating conditions and avoiding the need for highly reactive organometallic reagents. As the electrical grid transitions toward renewable energy sources, electrochemical activation of CO_2 is poised to become an increasingly carbon-negative process, further improving the sustainability of chemical manufacturing. Despite these advantages, the scope of electrochemical carboxylation remains limited, and a deeper mechanistic understanding is needed to guide rational improvements in selectivity and efficiency. This thesis addresses these gaps by investigating the electrochemical carboxylation of aldehydes, an underexplored but industrially relevant substrate class, and demonstrating for the first time that this transformation can be performed enantioselectively.

For aromatic aldehydes, electroanalytical and spectroscopic studies support a mechanism in which a substrate-derived ketyl radical couples with CO_2 to form the α-hydroxy carboxylic acid product. EPR spectroscopy provided direct evidence for formation of the ketyl radical intermediate under electrolytic conditions, and kinetic studies identified the coupling step as the rate-determining step. Lewis acidic additives such as $MgCl_2$ were found to play a key role in promoting ketyl radical formation. Extending this chemistry to aliphatic aldehydes revealed that their more negative reduction potentials open an alternative CO_2 reduction pathway towards electrochemical carboxylation. However, it was also found that polymerization of the substrate under reductive conditions limits carboxylation selectivity, prompting future works to understand and develop strategies towards mitigating the polymerization pathway.

Building on this mechanistic foundation, the first enantioselective electrochemical carboxylation of an aldehyde was demonstrated using chiral metal salen complexes as homogeneous catalysts, affording optically active mandelic acid with up to 43% enantiomeric excess. Both the applied potential and metal center identity were found to strongly influence enantioselectivity, pointing to an electronic basis for stereocontrol. Cyclic

voltammetry studies further suggest that the most effective catalysts readily undergo reductive activation under the applied conditions, enabling coordination with CO_2 to initiate the enantioselective pathway. Taken together, the insights developed in this thesis provide a foundation for the rational design of more selective, efficient, and enantiocontrolled electrochemical CO_2 incorporation strategies.

PUBLISHED CONTENT AND CONTRIBUTIONS

Ton, T. N.; Baker, R. J.; Manthiram, K.; Recent Progress in the Development of Electrode Materials for Electrochemical Carboxylation with CO_2. *J. Catal.* **2024**, 432, 115371. https://doi.org/10.1016/j.jcat.2024.115371.

T.N.T. participated in the participated in the conception of the manuscript, analyzed the literature, and participated in the writing of the manuscript.

Ton, T. N.; Zhang, H.; Oyala, P. H.; Lee, G. S.; Manthiram, K.; Electrochemical Benzaldehyde Carboxylation for Sustainable Mandelic Acid Synthesis via Radical Intermediates. *Chem. Catal.* **2025**, 5(12), 101519. https://doi.org/10.1016/j.checat.2025.101519.

T. N. T. participated in the conception of the project, conducted the experiments, analyzed the data, and participated in the writing of the manuscript.

TABLE OF CONTENTS

LIST OF FIGURES AND TABLES

Chapter 1

INTRODUCTION

1.1 UTILIZATION OF CO_2 IN CHEMICAL SYNTHESIS

Carbon dioxide (CO_2) is a crucial component of Earth's atmosphere and plays a critical role in sustaining life. However, anthropogenic activities such as industrial manufacturing, deforestation, and agriculture have led to unprecedent levels of CO_2 in the atmosphere, contributing to global climate change, ocean acidification, and extreme weather events. These shifts result in widespread biodiversity loss and pose significant risks to human health and economy, making it critical to pursue strategies to reduce CO_2 emissions. Among these emerging strategies, the utilization of CO_2 as a chemical feedstock for the synthesis of fuel and high-value chemical has been gaining great interest. Not only does this help to sequester CO_2 from the atmosphere, taking advantage of CO_2 as a carbon source would facilitate the transition away from fossil fuel-derived chemical precursors. These changes will allow for the transition to a more sustainable, carbon neutral economy.[1,2]

One strategy to convert CO_2 to a value-added product is to incorporate it onto an existing molecule in the form of a carboxyl group,[3] as shown here:

$$R - H + CO_2 \rightarrow R - COOH$$

Carboxylic acids are versatile functional groups in organic chemistry, serving as key intermediates in the synthesis of a wide range of chemical products. Their resonance-stabilized structure imparts stability and ease of handling, while the carbonyl group enables efficient transformations into derivatives such as esters, amides, and anhydrides. Consequently, carboxylic acids have widespread applications across various industries, including pharmaceuticals, plastics, and consumer products.[4,5]

Despite the promise of CO_2 as a nontoxic and abundant building for the synthesis of valuable carboxylic acids, its practical use is limited by its thermodynamic stability and kinetic

inertness. As a result, reactions involving CO_2 have typically required significant energy input to overcome the high activation barrier. Typically, these reactions are performed at elevated temperatures and pressures conditions, which is energy-intensive and unsafe. For instance, the Kolbe-Schmitt reaction for the industrial synthesis of hydroxybenzoic acids from phenols is performed with 100 bar of CO_2 pressure at 125 ºC (**Figure 1**).[6,7] Even in cases where such harsh conditions are avoided, carboxylation reactions often require the use of highly reactive organometallic nucleophiles, such Grignard reagents, to activate CO_2 (**Figure 1**).[3,8] Due to their reactive nature, these reagents pose significant challenges in preparation, handling, and functional group tolerance, which limits their practical application in chemical synthesis. The use of organometallic species also requires additional waste removal steps, which can be costly and inefficient. Alternative strategies that avoid unsafe conditions and the use highly reactive reagents are needed to perform the conversion of CO_2 to value-added carboxylation acids.

One strategy that has garnered a great deal of interest is the electrochemical carboxylation reaction, which relies on voltage as a powerful driving force to overcome the inertness of CO_2 (**Figure 1**). As a result, the reaction can be performed under ambient conditions without requiring the use of organometallic reagents. Functional group tolerance is expected to improve, as the applied voltage can be tuned to target the desired carboxylation reaction and limit any unwanted side reactivity. The reaction can also be performed heterogeneously at the surface of an electrode, avoiding costly catalyst recovery and separation processes. As electricity becomes increasing renewable in the future, electrochemical activation of CO_2 is shifting towards becoming a carbon-negative process, further improving the sustainability of the reaction. Given these advantages, electrochemical carboxylation presents a promising strategy to synthesize value-added carboxylic acids from CO_2.

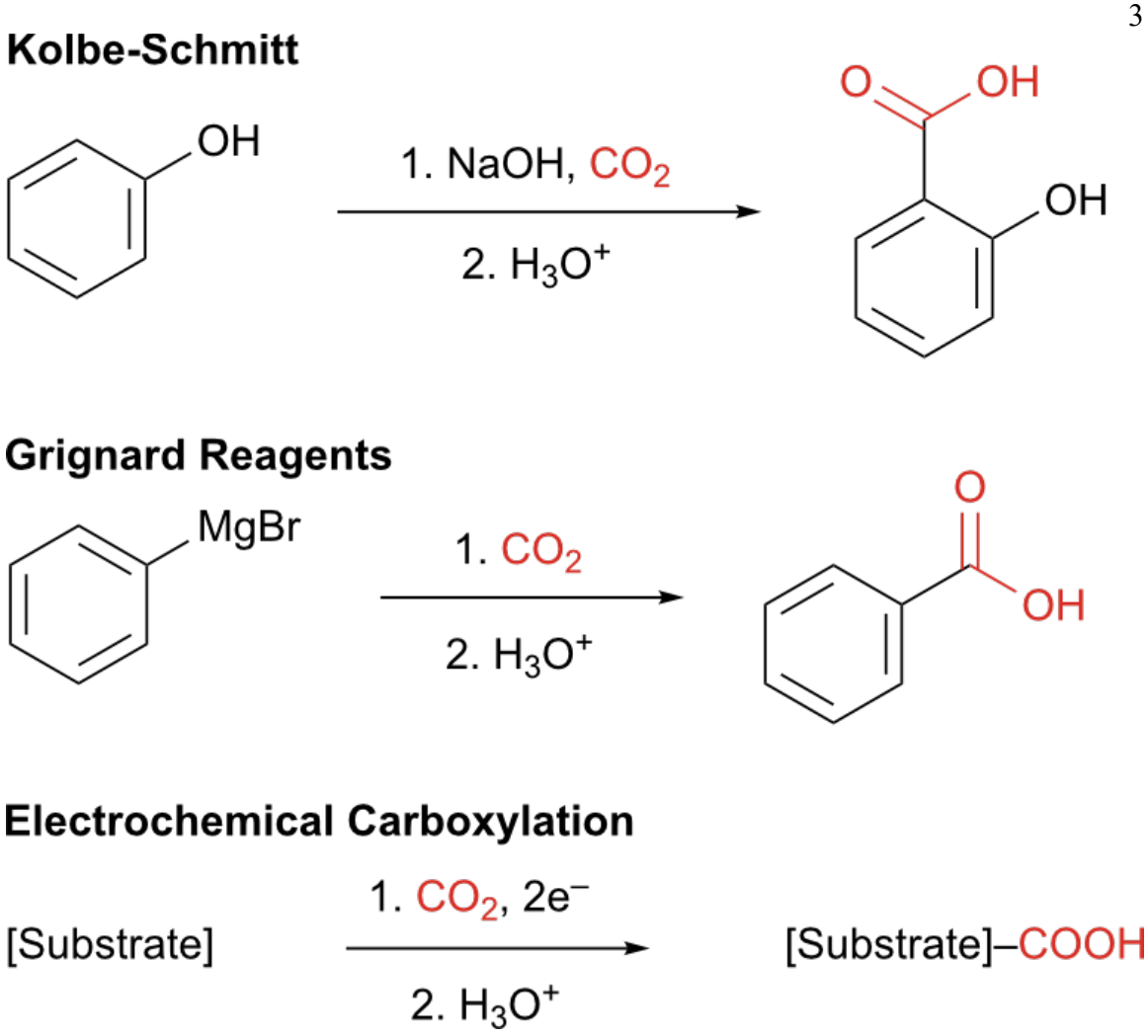

Figure 1. Industrial routes to synthesize carboxylic acids using CO_2 include the Kolbe-Schmitt reaction and the use of reactive Grignard reagents. Electrochemical carboxylation offers a safer and more sustainable alternative.

1.2 ELECTROCHEMICAL CARBOXYLATION WITH CO_2

Since CO_2 contains carbon at its highest oxidation state, electrochemical carboxylation is a reductive process, occurring at the cathode. The reaction occurs via two main pathways. In one pathway, reduction of the organic substrate generates either a radical anion via one-electron reduction or carbanion via two-electron reduction, followed by nucleophilic attack on CO_2 (**Figure 2, top**). Alternatively, if the reduction potential of the organic molecule is very negative, the reduction of CO_2 dominates, generating a CO_2 radical anion that reacts

with the organic substrate (**Figure 2, bottom**). The predominant mechanistic pathway often depends on the identity of the organic substrate and cathode material.[9,10]

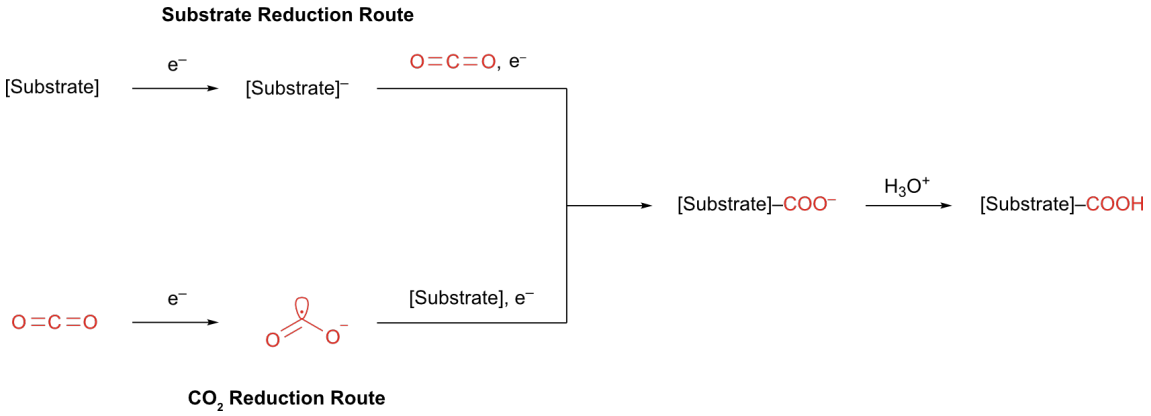

Figure 2. Electrochemical carboxylation can occur via a substrate reduction route (top) or a CO_2 reduction route (bottom).

On the anodic side, it has been established that the use of a sacrificial anode, such as aluminum or zinc, is optimal to produce the best carboxylic acid yields.[11] Facile oxidation of the sacrificial anode helps to prevent undesired oxidation of other species in the system. Additionally, cationic species generated from dissolution of the anode stabilize the carboxylate intermediate, driving the reaction forward and suppressing competitive side reactions.

The first electrochemical carboxylation reaction was reported in patent by Loveland[12], which described the dicarboxylation of 1,3-butadiene to make 3-hexenedioic acid. Since then, common classes of substrates that have been extensively used in electrochemical carboxylation reactions include organic halides, olefins, and carbonyl compounds.[9] Organic halides are among the most widely studied substrates, providing many of the foundation mechanistic understandings in the field. In general, the reactivity of organic halides towards electrochemical carboxylation differs between aliphatic and aryl halides and also trends with the halide identity.[13–16] Meanwhile, electrochemical carboxylation studies involving olefins have focused on conjugated systems, such as styrene. In these systems, monocarboxylation at the α- or β-position, as well as dicarboxylation have all been reported, with selectivity for

a particular product influenced by the substrate identity, cathode material, solvent composition, and applied potential.[17–22] Ketones and other carbonyl compounds are interesting as they can be used to access α-hydroxy acids, but their scope has been mostly limited to aromatic substrates.[23–25] Overall, these studies demonstrate that electrochemical carboxylation is most effective for substrates capable of stabilizing reactive intermediates, while less activated systems remain more challenging.

Beyond these examples, there remain opportunities further expand the synthetic toolbox for electrochemical carboxylation. First, being able to perform selective carboxylation of more challenging substrates will enable the synthesis of more diverse compounds. One such example is the aldehyde substrate, which are underexplored compared to ketones and other carbonyl substrates. Secondly, since carboxylic acid motifs are often found in many pharmaceuticals or biologically active compounds, achieving high enantioselectivity is crucial for future applications. These considerations guide the electrochemical carboxylation work discussed in this thesis.

1.3 BRIEF OVERVIEW OF THIS THESIS

From this perspective, this thesis work focuses on expanding both the scope and fundamental understanding of the electrochemical carboxylation reaction. A central theme is the use of mechanistic insight to rationalize and improve reaction selectivity and efficiency. By examining how factors such as the electrode environment and electrolyte additives influence the formation of key intermediates, this work develops a more detailed picture of the steps underlying CO_2 incorporation. In doing so, it identifies the key parameters that govern product formation and reactivity, with the goal of enabling more controlled, selective, and broadly applicable electrochemical carboxylation processes.

Chapter 2 is a review on the development of electrode materials used in electrochemical carboxylation. This review discusses the importance of the electrode material in controlling reaction selectivity and how mechanistic understanding is important in improving electrode

performance. The review also briefly touches upon the role of the electrode in controlling reaction regio- and stereoselectivity.

Chapter 3 focuses on an underexplored organic substrate in the electrochemical carboxylation literature: aldehydes. Specifically, benzaldehyde is used as a model substrate to study the electrochemical carboxylation of aromatic aldehydes towards α-hydroxy carboxylic acids. This works explores the effect of Lewis acidic additives, which help to promote the formation of the aldehyde-derived ketyl radical intermediate. Spectroscopic evidence for the formation of this ketyl radical intermediate was acquired using electron paramagnetic spectroscopy. Kinetic dependence studies showed that the rate determining step of this reaction was coupling between the ketyl radical and CO_2, and that maintaining moderate activities of both species is most important to improve selectivity and rates.

Chapter 4 further expands the electrochemical carboxylation substrate scope towards aliphatic aldehydes, which have historically shown lower selectivity compared to their aromatic counterparts. Mechanistic investigations suggest that reduced efficiency arises in part from their more negative reduction potentials, surpassing that of CO_2. Additionally, it was observed aliphatic aldehydes are prone to polymerization under the reaction conditions, introducing an alternative decomposition pathway that further diminishes carboxylation selectivity.

Chapter 5 expands upon the mechanistic understanding established in the previous works by investigating the enantioselective electrochemical carboxylation of aldehydes, a transformation that has not been previously reported. Chiral metal ligands are employed to perform asymmetric electrochemical carboxylation of benzaldehyde, affording optically active mandelic acid. It was found that both the applied potential and metal center identity influenced enantioselectivity, highlighting underlying electronic effects. Mechanistic studies using cyclic voltammetry suggest that the most effective catalysts undergo reductive activation under the optimized reaction conditions, generating an active intermediate capable of binding CO_2 and initiating the enantioselective pathway.

Chapter 6 provides a summary of the works discussed above and explores future research directions.

Chapter 2

RECENT PROGRESS IN THE DEVELOPMENT OF ELECTRODE MATERIALS FOR ELECTROCHEMICAL CARBOXYLATION WITH CO_2

Ton, T. N.; Baker, R. J.; Manthiram, K.; Recent Progress in the Development of Electrode Materials for Electrochemical Carboxylation with CO_2. *J. Catal.* **2024**, 432, 115371. https://doi.org/10.1016/j.jcat.2024.115371.

2.1 ABSTRACT

The desire to reduce carbon emissions in chemical synthesis has spurred research interest in leveraging CO2 as an abundant, non-toxic, and renewable carbon source. Electrochemical carboxylation, a strategy employing clean electricity for the sustainable synthesis of value-added carboxylic acids from CO2, represents a promising avenue. In this context, the careful selection of electrode material emerges as an important factor influencing the efficiency and selectivity of electrocarboxylation reactions. This review delves into the current landscape of developing high-performing electrocatalysts, guided by fundamental mechanistic understanding. Additionally, it examines how the choice of cathode material impacts reaction regioselectivity and explores the role of the anode in elevating performance and sustainability. The review concludes with perspectives on the future directions of the field and proposes strategies for further improvements.

2.2 INTRODUCTION

Chemical manufacturing is an integral part of modern society, responsible for the production of fertilizers, uels, medications, and consumer goods that contribute to improved life expectancy and quality of life. However, the industry's reliance on fossil fuels, both as an energy source to drive chemical reactions and feedstocks to synthesize commodity chemicals, has made it a dominant driver of global climate change. According to the

International Energy Agency, the chemical industry is the largest industrial energy consumer and the third-largest industrial source of CO_2 emissions in the world.[26] Faced with these challenges, research efforts have focused on the valorization of CO_2 into fuels and chemical products, which would simultaneously decrease society's reliance on fossil fuels and help sequester a greenhouse gas from the atmosphere, allowing for the transition to a more sustainable carbon neutral economy.

Despite these benefits, conversion of CO_2 into useful chemical products is challenging due to its thermodynamic stability and kinetic inertness. Consequently, previous strategies to activate CO_2 have often relied on harsh conditions, involving high temperatures and pressures. For instance, the industrial synthesis of urea from CO_2 and ammonia requires pressures of up to 350 bar and temperatures up to 220 ^oC.[27,28] The Kolbe-Schmitt reaction for the industrial synthesis of hydrobenzoic acid is performed with 100 bar of CO_2 pressure at 125 ^oC.[6,7] Even in instances where harsh conditions are avoided, the use of highly reactive reagents are required, such as organolithium and Grignard reagents, to drive C–C coupling with CO_2.[1,8,29]

Since then, milder and less-energy intensive conditions have been explored for the incorporation of CO_2 as a chemical building block in organic synthesis. These strategies have focused on the development of improved thermo- [16], photo- [30,31], and electrocatalysts [32,33]. Out of these, thermocatalytic and photocatalytic methods still rely on homogeneous catalysts and stoichiometric chemical reductants, which are less ideal for industrial applications. Alternatively, electrochemical methods offer a milder route by providing the necessary energy in the form of voltage-driven electrons.[34] They can also be performed heterogeneously at the surface of an electrode, avoiding costly catalyst recovery and separation processes. And, as electricity becomes increasingly renewable in the future, electrochemical activation of CO_2 is shifting towards becoming a carbon-negative process.

To date, most literature reports on electrochemical conversion of CO_2 discuss electroreduction of CO_2 into useful C_1 (CO, methanol, formate), C_2 (ethylene, ethanol), and C_{3+} (propane, propanol) products. A great deal of progress has been made in the development

of catalysts to improve selectivity, yield, and Faradaic efficiency (FE) towards the desired product,[35–38] although achieving higher molecular weight products remains a challenge. One way to further increase molecular weights of products is to append CO_2 onto carbon scaffolds via a process called electrochemical carboxylation (or electrocarboxylation), generating carboxylic acids. The electrocarboxylation substrates range from organic halides (aryl and alkyl), carbonyls (ketones, aldehydes, imines), olefins, and alkynes. The diversity of substrate offers countless opportunities for the synthesis of industrially relevant carboxylic acids under mild conditions, using CO_2 as a renewable carbon feedstock and clean electricity as a driving force.

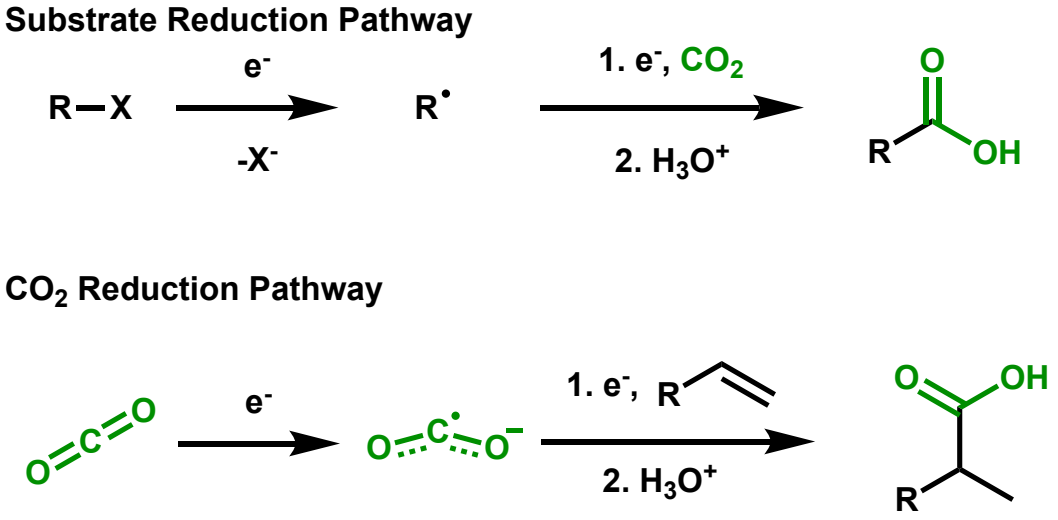

Figure 3. Electrocarboxylation can either occur through a substrate reduction pathway (top) or CO_2 reduction pathway (bottom).

The choice of electrode material plays a key role in controlling the selectivity and efficiency of electrocarboxylation reactions. On the cathodic side, there are two generally accepted classes of mechanism for the electrocarboxylation of organic substrates.[9,39] Mechanism 1 **(Figure 3, top)** involves cathodic reduction of the organic scaffold, forming a nucleophilic species that can react with the electrophilic carbon in CO_2. Activation of the substrate can either involve a one or two electron transfer, depending on the identity of the substrate. Alternatively, CO_2 can be reduced in mechanism 2 **(Figure 3, bottom)**, forming a radical anion, $CO_2^{\bullet-}$, that reacts with an electrophilic substrate. Due to the inertness of CO_2, it was

generally accepted that substrate activation was the dominant route towards electrocarboxylation. However, advances in the CO_2 reduction literature have dramatically lowered the overpotential for CO_2 reduction, making mechanism 2 a more viable strategy, and in certain cases, a preferred strategy. This review highlights the current state of the art in the development of high performing electrocatalyst guided by the mechanistic understanding. There will also be brief discussions about the role of the cathode material in controlling reaction regio- and stereoselectivity, as well as the role of the anode in improving performance and sustainability. Finally, our perspectives on the outlook for the field and proposed strategies for further improvements will be discussed.

2.3 MECHANISTICALLY INFORMED CATALYST DESIGN

2.3.1 Substrate Activating Catalysts

Given the relative kinetic inertness of CO_2, the electrocarboxylation substrate is often more readily activated under an applied reduction potential. In a substrate activation mechanism, the substrate can either be singly or doubly reduced, generating a nucleophilic species that subsequently reacts with CO_2. Efforts in electrocatalyst design have predominantly focused on lowering the onset reduction potential required to activate these substrates.

An example of a substrate that predominantly goes through the substrate activation pathway are organic halides. For these species, silver has traditionally been used as an electrocarboxylation cathode.[9] This is because the reduction potential of organic halides on silver is more positive relative to other cathode materials due to the strong X–Ag interaction, driving formation of the radical anion species. However, recent efforts have attempted to move away from using expensive, pure silver as an electrocatalyst, with focus shifting toward transition metal catalysts made from cheap and abundant materials.

One such strategy is the alloying of Ag with transition metals. Suryanarayanan et al.[40] synthesized trimetallic alloy nanomaterials made of different ratios of silver, copper, and nickel ($Ag_xCu_yNi_z$) and electrodeposited their materials on glassy carbon electrodes. They found that for the electrocarboxylation of benzyl bromide, a common electrocarboxylation

model substrate, the best performing alloy was $Ag_{46}Cu_{40}Ni_{14}$, giving a yield of 95% under constant potential electrolysis with a charge of 2.1 F/mole. In general, it was observed that the alloy materials produced yields between 75-95%, which was comparable or better than the best performing monometallic system (Ag_{100}, with yield of 75%). X-ray diffraction and atomic force microscopy analysis (AFM) showed that the presence of Cu and Ni in the alloy generated a more porous structure that had greater surface roughness. This, in turn, led to lower reduction potentials for the benzyl bromide substrate and improved carboxylation performance, as confirmed by voltammetry data.

Research efforts have also focused on completely moving away from silver. Yimin et al.[41] showed that a Cu-Ni alloy electrode led to improved carboxylation performance over monometallic Ag, also citing greater porosity as the cause of improved performance. Using benzyl bromide as the substrate, the best performing Cu-Ni alloy produced a product yield of 39.4%, compared to 28.7% on Ag alone. The lower yield compared to work by Suryanarayanan[40] might be attributed to differences in electrolysis conditions (electrolyte solvent, run time, anode material). However, these works demonstrate the promise of using transition metals as carboxylation cathodes, with work by Yimin et al. showing potential for systems that only contain transition metals.

Considering the importance of high surface area electrocarboxylation catalysts, more recent catalyst design efforts have focused on increasingly porous catalyst materials. A carbazole-derived porous organic polymer embedded with Cu (Cu@Cz-POP) showed promising performance towards the electrocarboxylation of benzyl bromide, delivering yield of 65% with a current density of 120 mA/cm^2.[42] It was proposed that the porous structure help to promote mass and electron transport to the catalytically active Cu sites. Additionally, the electron-rich carbazole functionalization has high CO_2 affinity that is thought to promote CO_2 transport and coupling with the reduced benzyl bromide species, making carboxylation more favorable compared to side reactions such as hydrogenation.

These examples highlight some of the guiding principles that have allowed for the design of improved electrocarboxylation catalysts, including alloying, increasing surface roughness,

and using porous structures with high surface areas. Since then, research efforts have also expanded to the electrocarboxylation of substrates that are more challenging to activate compared to benzyl bromide, such as aryl chlorides and alkyl bromides. Due to the high onset reduction potentials of these substrates, direct reduction routes are often unviable. To that end, research efforts have focused on indirect reduction routes, either with the use of transition metal complexes or organic mediators.

In 2021, Yu et al.[43] studied the electrocarboxylation of a series of unactivated organic halides, using nickel as their catalyst. The optimized Ni-catalyst, containing a combination of ditertbutylbipyridine (L, dtbbpy) and 4-dimethylaminopyridine (DMAP) ligands, was able to perform electrocarboxylation of 4-chlorobiphenyl in 70% yield. They also performed electrocarboxylation of a wide range of aryl chloride, bromides, iodine and sulfonate substrates with yields reaching up to 90%. Mechanistic investigation found that rather than being directly reduced by the cathode, the organic halide substrate undergoes an oxidative addition step to the reduced Ni-catalyst. Consequently, the presence of the catalyst allows for the carboxylation of difficult to reduce species that have previously been inaccessible.

More recently, there has been a shift towards metal-free electrocarboxylation, especially for applications in the pharmaceutical industry that has strict limits on metal impurities. Work by Xue and Qiu et al.[44] demonstrated that naphthalene could act as an organic mediator for the electrocarboxylation of a wide range of aryl and alkyl bromide and aryl chloride substrates. Specifically, aryl chlorides containing electron-donating groups, which are especially challenging to reduce, showed respectable yields between 30-60%. Cyclic voltammetry data indicated that the naphthalene is first reduced, generating a radical anion that goes on to reduce the organic halide species. Density functional theory (DFT) was performed to confirm the thermodynamic viability of this process.

2.3.2 CO_2 Activating Catalysts

It was previously proposed that under electrocarboxylation conditions, CO_2 could also be reduced to generate the radical anion $CO_2^{\bullet-}$ that goes on to react with the organic scaffold. However, it was believed that this CO_2 reduction route was the minor pathway due to high

overpotentials required for CO_2 reduction. More recently, as CO_2 reduction catalysts become increasing efficient and selective, there has been emerging interest in applying these catalysts towards electrocarboxylation.

In 2022, Zheng et al.[45] reported on a double activation strategy for the electrocarboxylation of acetophenone via silver-doped CeO_2 nanowires (Ag-CeO_2 NWs). They observed that compared to its monometallic counterparts (Ag foil, Ag nanoparticles, and CeO_2 nanowires), the Ag-CeO_2 NWs produced the 2-phenyllactic acid product at 91% Faradaic efficiency and 83% yield. In the CO_2 reduction literature, Ag has been shown to promote the formation of the adsorbed $CO_2^{\bullet-}$ radical anion.[46,47] Under aqueous conditions, $CO_2^{\bullet-}$ is protonated, subsequently forming CO. In contrast, under the non-aqueous conditions typically employed in electrocarboxylation, the highly reactive $CO_2^{\bullet-}$ intermediate is expected to react with other species in solution, including the ketones employed in this work. Additionally, the authors found that using CeO_2 as a support further lowered the onset reduction potential of CO_2, such that the difference in onset reduction potential between CO_2 and acetophenone was only 0.13 V (compared to a difference of 0.95 V with the use of Ag foil). By bringing the onset reduction potential of CO_2 closer to that of acetophenone, the authors were able to optimize a double activation strategy by promoting the CO_2 reduction mechanism on top of the existing ketone reduction mechanism.

Performing electrocarboxylation via CO_2 reduction is also a promising strategy for substrates that have high reduction potentials. One such substrate is styrene, which has a reduction potential similar to that of CO_2.[18,48] Previous studies of styrene carboxylation have employed bulk metal cathodes such as nickel or titanium,[17,19,48] but yields remained low due to the high onset reduction potentials of both starting materials. To circumvent this issue, Zheng and coworkers[20] proposed to use nitrogen-coordinated single atom Cu catalysts, which had also been shown to lower the overpotential of CO_2 reduction to $CO_2^{\bullet-}$,[49–51] towards the electrocarboxylation of styrene. Under optimized conditions, the reaction achieved a FE of 92%, with the rest of the current density going towards CO_2 reduction products (CO and CH_4). More impressively, the performance of the single atom catalyst was dramatically better than that of Cu foil alone (34% FE). The findings of this work pave the way towards rational

catalyst design, drawing inspiration from the CO_2 reduction literature to improve carboxylation performance.

Similarly, Mita et al.[52] proposed a strategy to carboxylate heteroaromatic compounds that exhibit high reduction potentials (-2.50 to -2.94 V vs. SCE) by taking advantage of the less negative reduction potential of CO_2 (-2.2 V vs. SCE in aprotic solvents).[53] They were able to perform dicarboxylation of a wide range of heteroaromatic compounds with up to 90% yield. Prior to this work, electrochemical dicarboxylation was limited to styrene and 1,3-diene derivatives. Furthermore, they were able to apply their optimized conditions towards the synthesis of bioactive compounds, demonstrating the viability of electrocarboxylation for a wide range of applications.

Performing electrocarboxylation via CO_2 reduction is also a viable strategy to avoid unwanted side products. For instance, previous routes to activate benzyl halides for carboxylation would often lead to side reactions such as hydrogenolysis or reductive coupling of the radical halide.[54] However, Mellah et al.[55] showed that by using a Sm(II)-catalyst to activate CO_2 for electrocarboxylation, they were able to avoid the formation of these side products. They reported the highest to date yield for the electrocarboxylation of benzyl chloride at 99%. This strategy is also viable for substrates that are challenging to reduce, as demonstrated by their substrate scope study of a wide range of benzyl chlorides and bromides.

One shortcoming of the CO_2 activation strategy is the formation of CO_2 reduction side products. To address this issue, a bimetallic copper–silver catalyst was recently developed for the electrocarboxylation of aryl bromide, using bromobenzene as the model substrate.[56] Mechanistic studies revealed that both bromobenzene and CO_2 undergo a one-electron reduction, followed by a radical cross-coupling step to form the desired product **(Figure 4)**. Control experiments suggest that Cu was responsible for CO_2 activation, while Ag both activated the aryl bromide and promoted radical cross-coupling step. The use of this bimetallic system helped to suppress electroreduction side reactions, leading to a high FE of 98%. However, further improvements are required as yields remained at around 60%.

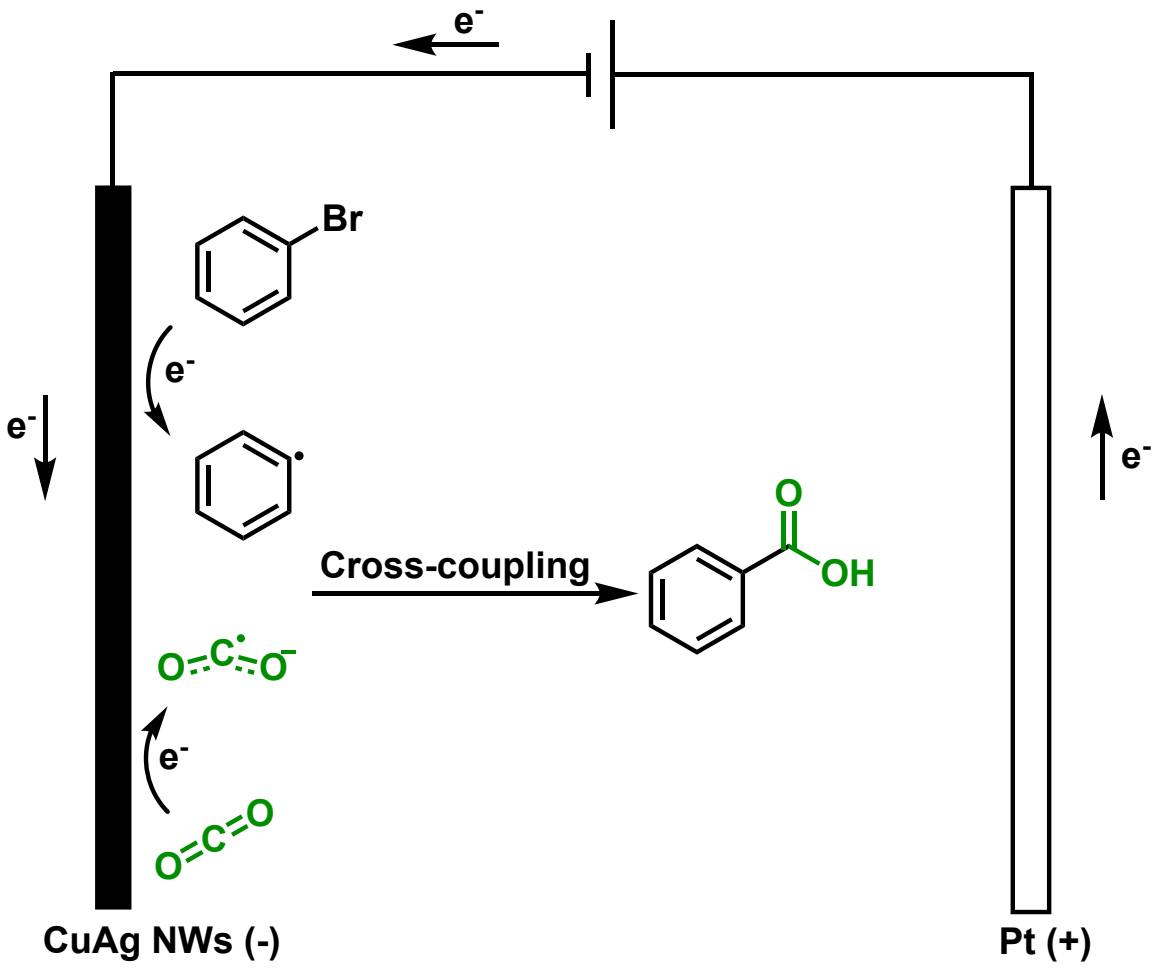

Figure 4. Proposed electrocarboxylation mechanism via the double activation of CO_2 and bromobenzene with the use bimetallic CuAg NWs. Reproduced from Ref. 56 with permission from American Chemical Society.

2.3.3 Regioselectivity

The catalyst material can also play a crucial role in controlling reaction regioselectivity. The electrocarboxylation of styrene derivatives is a well-studied reaction.[17–19,48,57] One of the challenges of styrene carboxylation is controlling reaction regioselectivity, as carboxylation at either α- or β-position, as well as dicarboxylation, have all been observed.[53] Previous attempts to perform carboxylation of styrene have mainly produced the branched product, via carboxylation at the α-position. This is because activation of styrene with metal catalysts

lead to the formation of stable η^3-benzylic metal intermediates that produce the branched product.[22,58–60]

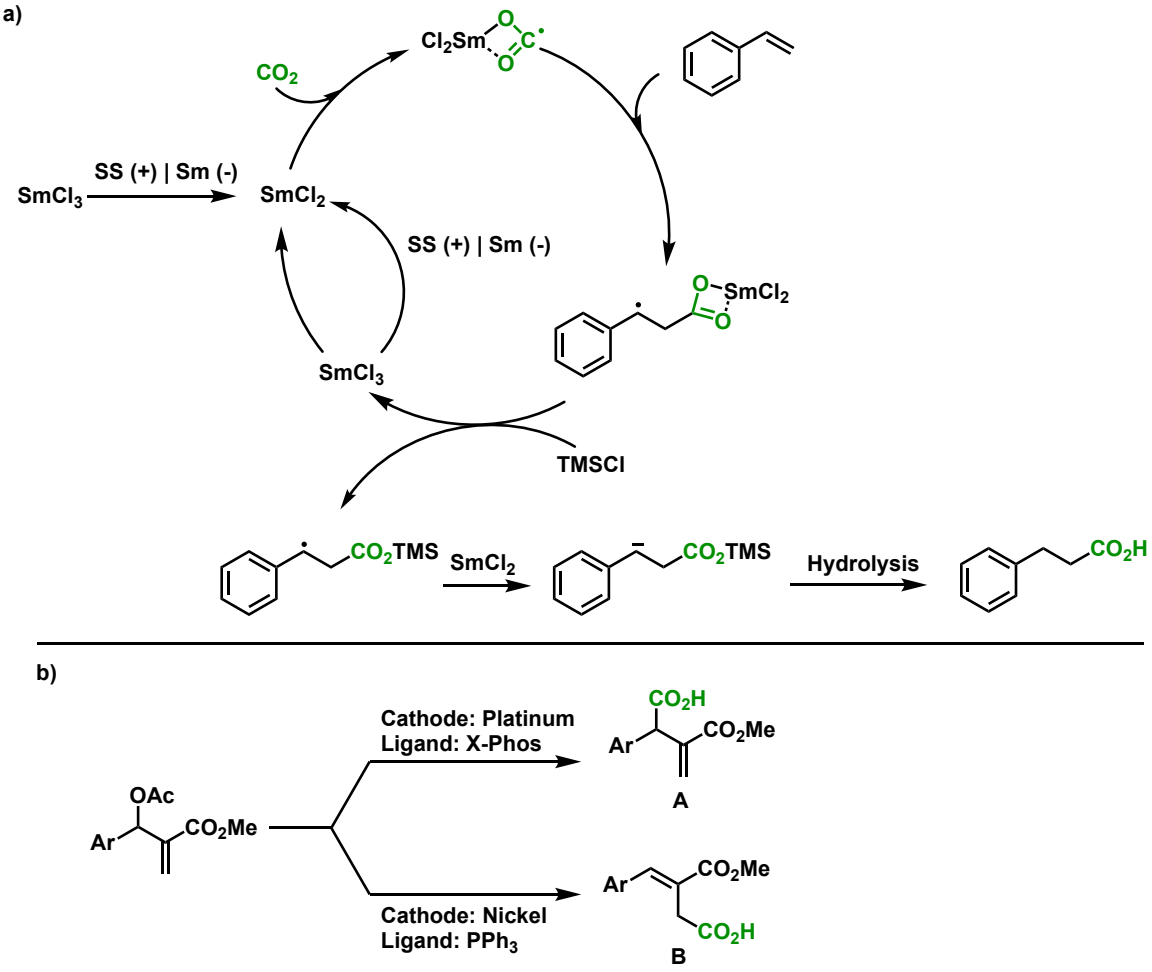

Figure 5. Regioselective electrocarboxylation reactions. (a) Proposed mechanism for the Sm-catalyzed regioselective electrocarboxylation of styrene with CO_2. Reproduced from Ref. 21 with permission from American Chemical Society. (b) Switchable regioselectivity of of Baylis-Hillman acetates carboxylation with the choice of cathode material. Reproduced from Ref. 61 with permission from Elsevier.

Recently, Mellah and co-workers[21] developed an alternative route to carboxylate styrene and its derivatives, producing exclusively the β-carboxylated product. Rather than activating styrene, their Sm(II)-catalyst was used to activate CO_2, forming a samarium carboxylate species **(Figure 5a)**. This radical species then adds to the olefin at the β-position, forming

the more stable benzylic radical species that is subsequently reduced. Using this strategy, they were able to exclusively synthesize the linear, β-carboxylated product.

The choice of electrode material can also lead to a switch in reaction regioselectivity. Tummanapalli and coworkers[61] studied the electrocarboxylation of Baylis-Hillman acetates and found that a Pt cathode predominantly led to carboxylation at the benzylic position. Meanwhile, the use of a Ni cathode produced the *E*-isomer as the major product **(Figure 5b)**. The team proposed that this observed switch in regioselectivity, was due to a difference in mechanism favored by each electrode. Mechanistic studies found that the Pt cathode favored a direct two electron reduction of the acetate, generating an allyl carbanion that goes on to attack CO_2. Meanwhile, the Ni cathode favors two single electron reductions of both the acetate and CO_2. In this case, the product is formed via a radical coupling step. This was the first report of a regioselectivity switch due to the choice of electrode material alone.

2.3.4 Stereoselectivity

When synthesizing chiral compounds, the ability to selectively produce the desired stereoisomer is highly desirable as it avoids costly separation processes during the production of pharmaceuticals and agrochemicals, among other applications.[62] Asymmetric electrocarboxylation is inherently challenging due to the achiral nature of the electron. Some of the earliest strategies employed to perform asymmetric electrocarboxylation was by using chiral starting materials to produce the desired chiral products. However, this chemistry is limited by the substrate, and strategies to perform enantioselective carboxylation of achiral substrates must be explored. This section will focus on the progress that has been made towards developing electrocatalysts that can perform enantioselective electrocarboxylation at high yields and FEs.

In 2014, Wang and Lu et al.[63] reported on the use of a chiral Co(II)salen complex for the electrocarboxylation of 1-phenylethylchloride. When the Co(II)salen complex was present, they were able to synthesize the chiral 2-phenylpropionic acid product at 83% enantiomer excess (ee), though only with a yield of 16%. Furthermore, they were able to invert the

favored stereoisomer by the choice of chiral catalyst Co(II)-(R,R)(salen) versus Co(II)-(S,S)(salen).

While the findings of this work were promising for advancing asymmetric synthesis in electrochemistry, there were improvements that needed to be made. One shortcoming was the use of a homogeneous catalyst, which presents challenges in separations and recyclability. To address this issue, Wang and Lu et al.[64] proposed to incorporate their chiral cobalt complex into silver nanoparticles **(Figure 6)**. Their [Co]@Ag composite was used as the cathode for their system, performing both carboxylation and asymmetric synthesis on one heterogeneous surface. With this system, they were able to carboxylate 1-phenylethylchloride at 73% ee and 58% yield. Compared to their original work, the ee was lower but the yield was a lot higher, due to the use of silver as the cathode material instead of glassy carbon. The composite material also exhibited great recyclability, lasting through seven cycles without Co leaching.

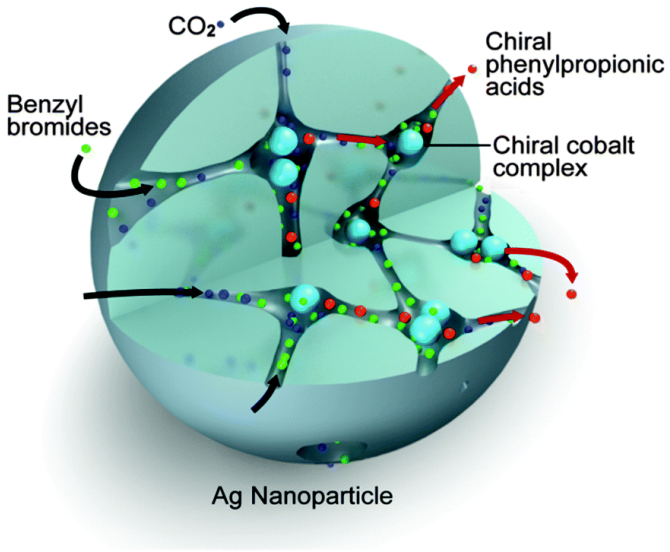

Figure 6. [Co]@Ag composite for the asymmetric carboxylation of benzyl bromides. Reprinted from Ref. 64 with permission from Royal Society of Chemistry.

Since then, the incorporation of chiral metal complexes into electrode materials have been employed to perform electrocarboxylation of other types of substrates, such as ketones.[65–67] More recently, this work has been improved upon through further screening of metal centers

and chiral ligands. The most optimized catalyst was a Ni(II)L1 complex (L1 = salen functionalized with tBu groups), which could perform electrocarboxylation of acetophenone with an ee of 90% and yield of 59%.[68]

2.4 SACRIFICIAL ANODE-FREE CARBOXYLATION

One major drawback to electrocarboxylation reactions is that most systems rely on the use of sacrificial anodes. The metal cation generated oxidatively provides a stabilizing effect for the carboxylate product, preventing further nucleophilic reactions or reverse decarboxylation. Additionally, preferential oxidation of the anode prevents undesirable oxidation of the substrate, product or other organic species that would generate protons that are harmful to carboxylation performance. However, the constant need for anode regeneration prevents these systems from use in a continuous reaction setting and is often costly and non-environmentally friendly. Thus, the ability to perform electrocarboxylation reactions without the need for a sacrificial anode represents a positive step towards incorporating these processes in an industrial setting.

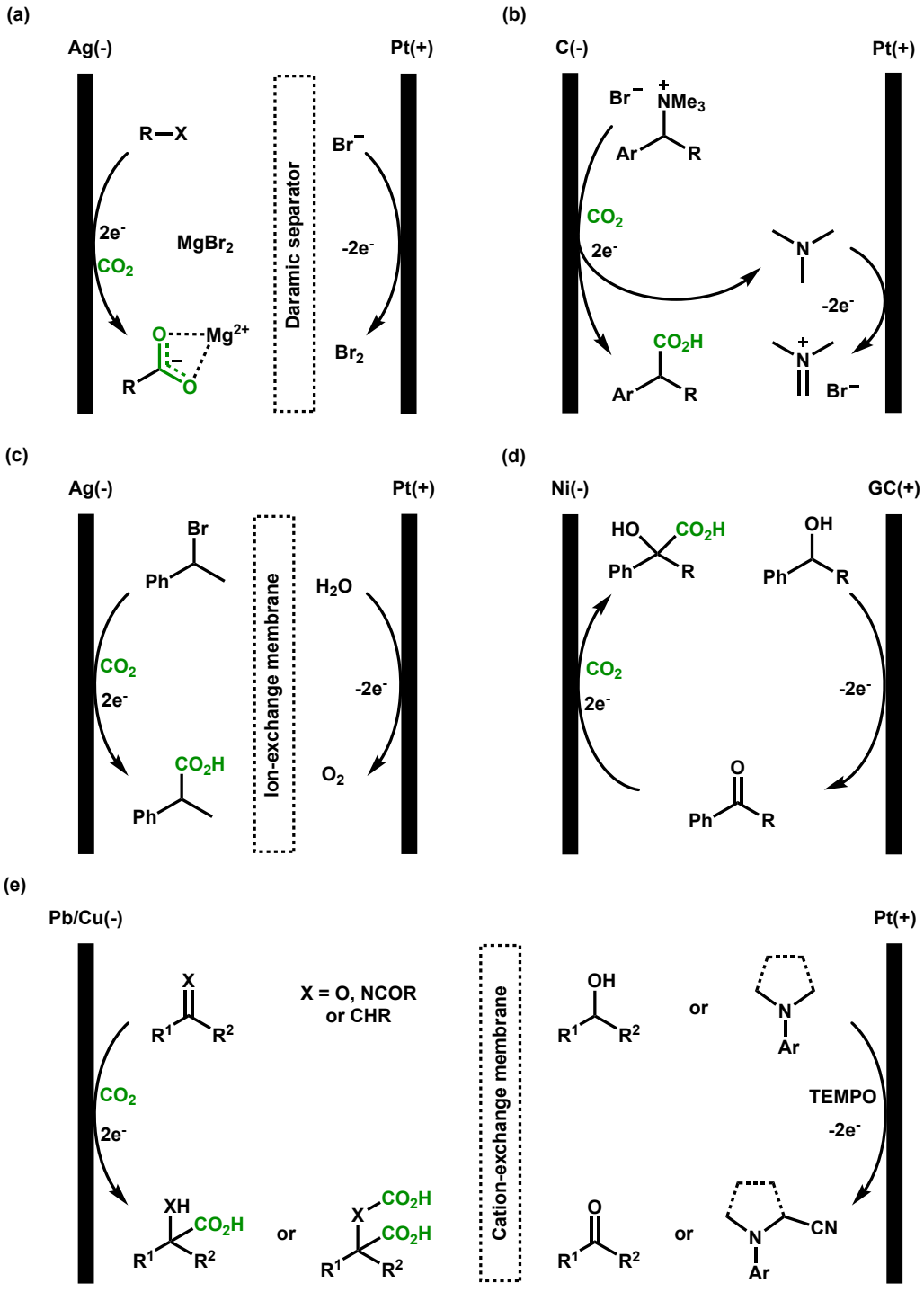

Figure 7. Sacrificial anode free electrochemical carboxylation. (a) Addition of exogeneous Mg salts replaces cations generated by a sacrificial anode, allowing for carboxylate protection without the use of a sacrificial anode. (b) The choice of substrate can circumvent the need for a sacrificial anode, such as the use of benzyltrimethylammonium salts. (c) Cell design strategies, such as the choice of membrane in divided cells, offer opportunities to explore the use of aqueous anolytes. (d, e) Paired electrosynthesis is a viable strategy to synthesize useful products at both electrodes.

2.4.1 Electrolyte Design

Rather than rely on the cation generated by the sacrificial anode for carboxylate protection, Manthiram et al. explored the ability to use exogenous Mg salts to control selectivity **(Figure 7a).**[32] When conducted in the absence of a sacrificial anode, facile bromine oxidation served as the counter reaction on the Pt anode, which avoids the generation of protons in the anodic counter reaction. Interestingly, inexpensive $MgBr_2$ served to match or improve process yields relative to the reaction in which a Mg anode was used across a variety of alkyl and aryl halides. A variety of spectroscopic techniques were used to reveal the ability of the carboxylate anion product to protect the cathode against detrimental passivation of insoluble $MgCO_3$ formed from CO_2 reduction.

2.4.2 Substrate Design

In addition to alkyl halides, benzyltrimethylammonium salts have been demonstrated as successful substrates for electrocarboxylation without the need for a sacrificial anode **(Figure 7b).**[33] A wide substrate scope was demonstrated for both primary and secondary starting materials, including the synthesis of racemic ibuprofen. The simple setup and reaction conditions avoid the need for complicated reaction purification procedures such as column chromatography, and the reaction was shown to proceed with similar yields on gram scale as on small scale. Although the starting materials required synthesis from the alkyl halides, a one-pot method was demonstrated using benzyl bromide and trimethylamine to yield the acid product without much loss in yield. Mechanistic studies using techniques such as Differential Electrochemical Mass Spectrometry (DEMS) supported the proposed mechanism, which included reductive cleavage of the C–N bond to form the carbon-based radical, followed by addition of the second electron and trapping with CO_2 to form the acid product, with trimethylamine oxidation at the anode.

2.4.3 Cell Design

Medvedev and coworkers investigated the use of aqueous anolytes in divided cells for sacrificial anode-free carboxylation **(Figure 7c)**.[69] A cation exchange membrane (CEM),

anion exchange membrane (AEM) and bipolar membrane (BPM) were studied at various potentials, and the AEM generally gave better yield and selectivity for the carboxylated product due to cathodic passivation with KBr when CEM or BPM were used. Three potential ranges were explored based on the dominant species identified by CV: (1) less negative than –1.0 V, where R–Br reduction to R$^{\bullet}$ is dominant, (2) between –1.0 and –1.5 V, where R$^{\bullet}$ reduction to R^{-} is dominant, and (3) more negative than –1.5 V, where CO_2 reduction is dominant. Concentration dependence studies revealed that a high CO_2/R–Br ratio was necessary for high selectivity for carboxylated product relative to dimerized product, and that lower temperatures favored carboxylated product due to the increased solubility of CO_2. DFT calculations were used to support the experimental results illustrating that at potentials more negative than –1.8 V, the barrier to CO_2 reduction is lower than that for alkyl halide reduction, whereas the trend switches above –1.8 V. The highest overall yields for carboxylated product were obtained using an AEM at –1.4 V in a dilute solution of alkyl halide.

2.4.4 Paired Electrosynthesis

The use of a linear paired electrosynthesis technique for α-hydroxycarboxylic acid synthesis was demonstrated by Muchez and coworkers in 2019.[70] A proposed mechanism involved TEMPO-mediated oxidation of the alcohol to the aldehyde or ketone, followed by reduction of the carbonyl and trapping with CO_2 **(Figure 7d)**. Not only did this method allow for sacrificial anode-free synthesis, but the use of alcohols represent a greener starting material than aldehydes or ketones. Both primary and secondary benzylic alcohols could be used, with bulkier secondary alcohols leading to higher yields due to minimized dimerization. For electrolyte conditions, the basic supporting electrolyte salt was used for deprotonation of the alcohol during oxidation, while water inclusion was explained by alcohol-to-TEMPO proton transfer, also during oxidation. Investigating various cathode materials led to the observation that for 1-phenylethanol and benzyl alcohol, catalysts with higher metal-hydrogen bond strengths led to higher yields.

Zhang et al. showed how the mono- or dicarboxylation of unsaturated bonds could be paired with TEMPO-mediated alcohol or amine oxidation, separated by a CEM **(Figure 7e)**.[71] With ketones or *N*-acyl imines in the cathodic chamber α-hydroxy- or aminocarboxylic acids were obtained, while alkenes and dienes led to the dicarboxylated products. On the anodic side, primary and secondary alcohol oxidation to aldehydes and ketones was explored, in addition to α-cyanation of tertiary amines. The ability to synthesize racemic Naproxen and Ibuprofen with one additional step following the electrocarboxylation was demonstrated. Mechanistic studies were conducted for the carboxylation reaction using CV and DFT revealed that while substrate reduction occurred prior to electrophilic attack of CO_2 for the ketone, CO_2 reduction followed by electrophilic attack of the substrate occurred for the alkene. For the model system, most of the >10 V cell potential was accounted for by ohmic resistance, with ~2.5 V being used to drive the reactions during constant current electrolysis.

2.5 CONCLUSIONS AND OUTLOOK

Much progress has been made on catalyst design efforts that allow for the electrocarboxylation of organic substrates at improved yields, FEs, and selectivity. While earlier catalyst design efforts have focused on the substrate activation mechanism, advances in the development of CO_2 reduction catalysts have led to emerging interest in performing electrocarboxylation via the CO_2 reduction route. Understanding of these two pathways is still nascent and further insight how to differentiate these pathways must be acquired. Developing this understanding will allow for the rational design of electrocatalysts with high activity, selectivity, and recyclability. Furthermore, understanding the anodic half-reaction of this system will be important in developing a truly sustainable electrocarboxylation system.

For electrocarboxylation to become industrially viable, the following challenges remain to be addressed:

1. Better understanding of the two different types of electrocarboxylation mechanisms and how they vary with different types of electrocatalysts: Experimental and computational methods should be used to better understand the different mechanistic pathways observed and favored on a wide range of electrocatalysts, such as metal foils, mixed metal alloys, metal oxides, and nanostructured catalysts. Specifically, there is little precedent of theoretical studies performed to better understand key intermediates observed in the different mechanistic pathways and how these intermediates might be favored or disfavored with the choice of catalyst. Additionally, advances in characterization techniques such as X-ray photoelectron spectroscopy (XPS), X-ray absorption spectroscopy (XAS), and vibrational spectroscopy may allow for in situ/operando characterization. To that end, these techniques should be used towards better understanding the relationship between electrocarboxylation catalyst and performance. Ultimately, this insight will allow for the electrocarboxylation of a wider range of substrates, producing carboxylic acids for applications in the pharmaceutical, polymer, and agrochemical industries.

2. *Asymmetric catalysis:* As previously mentioned, performing enantioselective electrocarboxylation is extremely challenging due to achiral nature of the electron. While there has been some progress made towards improving the enantioselectivity of electrocarboxylation reactions, many of these works involve the use of homogeneous catalysts that require costly separations. The development of a heterogeneous catalyst that is able to selectively produce the desired stereoisomer at high yields and FEs would dramatically improve the industrial capability of this process. To achieve this goal, further insight on the tradeoff between selectivity and activity must be developed, allowing for the development of hybrid catalysts that optimize both.

3. *Development of flow electrocarboxylation systems:* Flow systems offer the benefits of being more efficient, more scalable, and higher quality compared to batch systems. To make flow electrocarboxylation systems a reality, more robust electrocatalysts must be designed and studied. Additionally, passivation of the cathode material is a

common issue that must be addressed to improve the lifespan of the electrode. On the anodic side, the development of sacrificial anode free systems is promising, but greater understanding of anodic processes must be developed.

In conclusion, while many challenges remain to be addressed in the development of active, selective, and scalable electrocarboxylation catalysts, a great deal of progress has also been achieved to drive this technology towards industrial applications. We envision that with continued innovation informed by fundamental understanding, electrocarboxylation could contribute to a more sustainable carbon cycle.

Chapter 3

ELECTROCHEMICAL BENZALDEHYDE CARBOXYLATION FOR SUSTAINABLE MANDELIC ACID SYNTHESIS VIA RADICAL INTERMEDIATES

Ton, T. N.; Zhang, H.; Oyala, P. H.; Lee, G. S.; Manthiram, K.; Electrochemical Benzaldehyde Carboxylation for Sustainable Mandelic Acid Synthesis via Radical Intermediates. *Chem. Catal.* **2025**, 5(12), 101519. https://doi.org/10.1016/j.checat.2025.101519.

3.1 ABSTRACT

The electrochemical carboxylation of aldehydes with CO_2 is a sustainable strategy to synthesize industrially relevant *a*-hydroxycarboxylic acids under mild conditions while avoiding toxic sodium cyanide. However, this reaction remains hindered by low activity and selectivity due to a limited understanding of the reaction mechanism. In this work, we present a mechanistic study of electrochemical benzaldehyde carboxylation. In situ electron paramagnetic resonance spectroscopy demonstrated that the reaction occurs via a ketyl radical intermediate generated from the one electron reduction of benzaldehyde. Electrochemical kinetic analysis suggested the rate determining step to be the subsequent coupling of the surface-bound ketyl radical with CO_2. Finally, our investigation revealed that the optimal reaction rate and selectivity were achieved in the presence of Lewis acidic magnesium cations, resulting in the highest Faradaic efficiency of 79% and a partial current density of 12.9 mA/cm².

3.2 INTRODUCTION

a-hydroxycarboxylic acids (AHAs), including lactic acid (2-hydroxypropanoic acid) and mandelic acid (2-hydroxy-2-phenylacetic acid), are important precursors in the manufacturing of pharmaceuticals, personal care products, and plastics (**Figure 8a**). As of

2024, the AHA market in the United States was valued at 1.5 billion USD and is expected to grow to 2.4 billion by 2029.[72] Current processes to synthesize AHAs, such as mandelic acid, often require the use of harsh or toxic reagents. The most common method requires the use of toxic sodium cyanide to generate a cyanohydrin intermediate, followed by hydrolysis with hydrochloric acid (**Figure 8b**).[73,74] To improve the reaction conversion, the aldehyde or ketone must first react with sodium bisulfite to form an adduct, which then undergoes nucleophilic attack by cyanide–necessitating multiple steps. Consequently, an improved strategy is needed to eliminate hazardous reagents, offering a safer and more sustainable approach to synthesize valuable AHAs from ketones and aldehydes.

One such strategy is the electrochemical carboxylation of aldehydes with carbon dioxide (CO_2) to form the corresponding AHA (**Figure 8c**). CO_2 is a promising starting material for carboxylation because it is cheap, abundant, and nontoxic. However, the use of CO_2 in carboxylation processes is challenging due to its thermodynamic stability and kinetic inertness, requiring high temperature and pressure conditions that are energy-intensive and unsafe.[3] For instance, the industrial synthesis of urea from CO_2 and ammonia requires pressures of up to 350 bar and temperatures of up to 220 ºC.[28] The Kolbe-Schmitt reaction for the industrial synthesis of hydrobenzoic acid from phenol is performed at 100 bar of CO_2 pressure at 125 ºC.[6,7] To that end, electrochemical methods offer a milder route to activate CO_2 by supplying the necessary energy in the form of voltage-driven electrons.[75,76]

Despite the benefits offered by the electrocarboxylation of aldehydes to produce AHAs, this chemistry has remained underexplored compared to the electrocarboxylation of other substrates such as olefins, organic halides, and ketones.[9,77–79] This chemistry was first reported by Silvestri *et al.* in 1986 for the electrocarboxylation of benzaldehyde, with a mandelic acid yield of up to 40%.[23] More recent work has shown improved yields, with the highest reported yield for benzaldehyde carboxylation of 90%.[80,81] Although yield is a common metric for evaluating chemical reaction performance, it is also critical to consider the electron selectivity in electrocatalysis, which is captured by Faradaic efficiency (FE). A high FE indicates minimal energy waste, making the process more cost-effective by minimizing losses to undesired side reactions. However, only one prior study has reported

the FE of the aldehyde carboxylation process, with the highest value to date reaching just 35%.[23] Additionally, mechanistic understanding of aldehyde electrocarboxylation is still limited and mostly relies on the electrocarboxylation literature involving other substrates.

In this work, the electrocarboxylation of aldehydes was systematically studied using benzaldehyde as the model substrate (**Figure 8c**). Optimization efforts revealed that using tin as the working electrode, *N,N*-dimethylformamide as the solvent, and aluminum as the counter electrode resulted in high FE and partial current density towards the desired product. The addition of magnesium chloride as a Lewis acid additive was also crucial in improving the performance, leading to the highest FE of 79% and partial current density of 12.9 mA/cm^2. Mechanistic investigation indicated that the dominant carboxylation pathway involves a ketyl radical intermediate generated from the one-electron reduction of benzaldehyde, as confirmed by cyclic voltammetry and in situ electron paramagnetic resonance (EPR) spectroscopy using spin traps. With electrochemical kinetic analysis, it was shown that the rate limiting step is likely to be thermochemical coupling between the surface-bound ketyl radical and CO_2.

(a) Mandelic acid acts as a precursor for pharmaceuticals and polymers

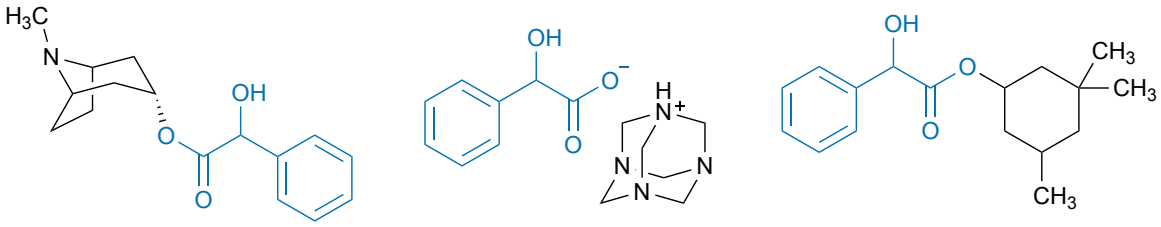

Homatropine Methenamine mandelate Cyclandelate

(b) Conventional route to synthesize mandelic acid using sodium cyanide

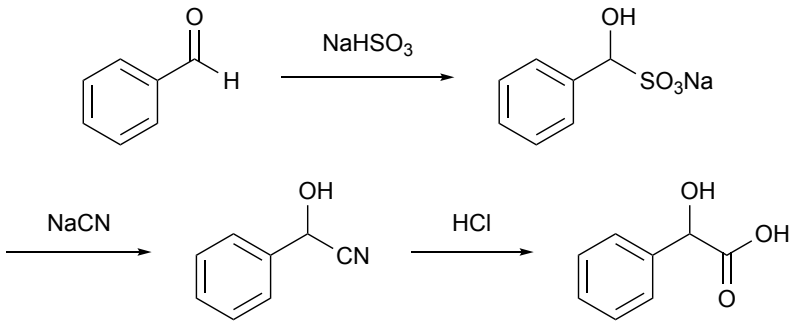

(c) This work: electrocarboxylation of benzaldehyde using CO_2

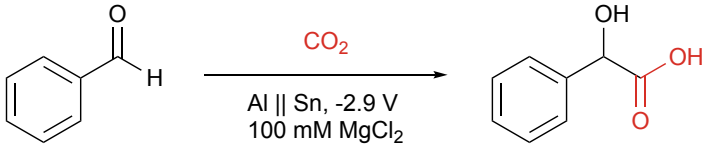

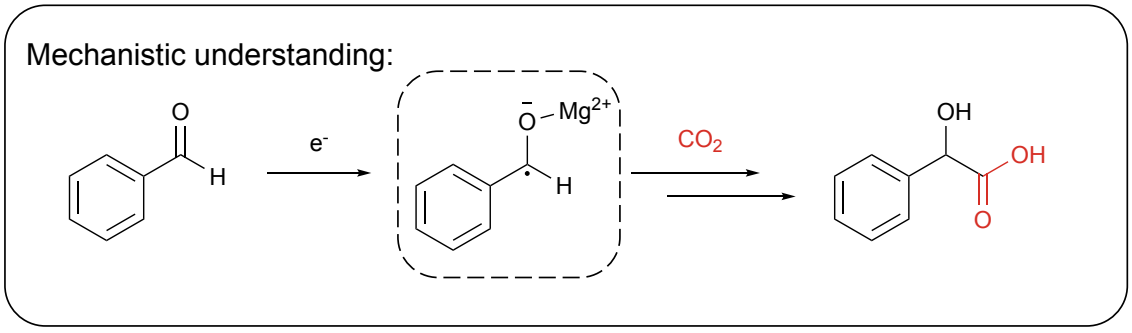

Figure 8. Background and overview for the electrochemical carboxylation of benzaldehyde. (a) Examples of pharmaceuticals synthesized using mandelic acid as a precursor. (b) The conventional route to synthesize mandelic acid from benzaldehyde which involves the use of toxic sodium cyanide. (c) Electrochemical carboxylation of benzaldehyde using CO_2.

3.3 RESULTS AND DISCUSSION

3.3.1 Optimization of Reaction Conditions

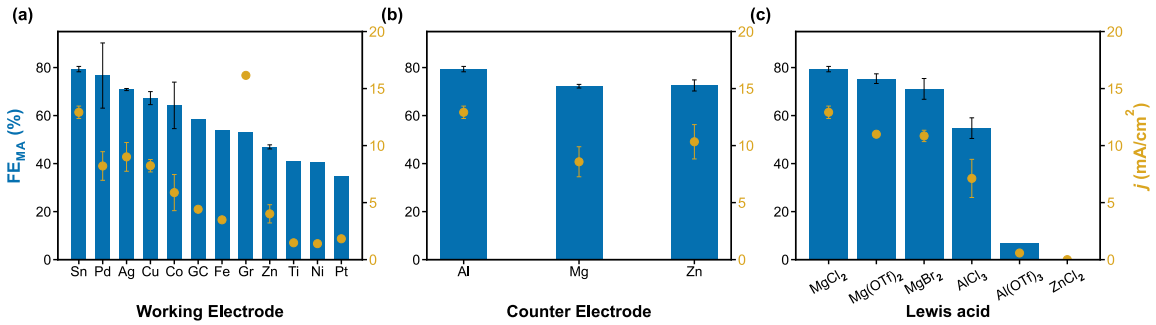

Figure 9. Effect of (a) working electrode (b) counter electrode, and c) Lewis acid additive on electrocarboxylation performance, as quantified by mandelic acid Faradaic efficiency and partial current density. Standard reaction conditions: 100 mM benzaldehyde, 100 mM Lewis acid additive, 20 sccm CO_2, 4 mL DMF, –2.9 V vs. $Me_{10}Fc^{0/+}$ for 30 minutes. Sn working electrode and Al counter electrode were used unless otherwise specified. $Me_{10}Fc$ = decamethylferrocene; GC = glassy carbon; Gr = graphite.

To systematically investigate the impact of reaction conditions on the electron balance, we quantified the FE and partial current density of benzaldehyde electrocarboxylation under varying reaction conditions, including working and counter electrodes, Lewis acid salts, solvents, and supporting electrolyte salts. The performance was evaluated by constant potential electrolysis in custom-made H-type PEEK cells (**Figure A1**) with continuous CO_2 purging (see Appendix A). Products were quantified using ultra performance liquid chromatography, using 1,3,5-trimethoxybenzene as an internal standard (**Figure A2**).

We screened 12 working electrodes, at –2.9 V vs. $Me_{10}Fc^{0/+}$ (all potentials are referenced against decamethylferrocene unless noted otherwise). The major product is mandelic acid with side products including phenylmethanol (benzyl alcohol) and 1,2-diphenylethane-1,2-diol (hydrobenzoin). FEs and partial current densities towards mandelic acid were largely dependent on the choice of working electrode materials (**Figure 9a**), suggesting its critical role in the reaction. This variation in performance likely arises from differences in how the organic substrates interact with each catalyst. We found that tin (Sn) produced the highest FE for mandelic acid of 79% (**Figure 9a**), outperforming graphite (Gr) and zinc (Zn), which

were previously shown to have high performance for the electrocarboxylation of benzaldehyde.[23] Gr gave the highest partial current density of 16.1 mA/cm^2 while Sn gave the second highest partial current density of 12.9 mA/cm^2. Sn was chosen as the working electrode for further investigation because it exhibited high FE and partial current density and is also abundant and cost-effective. We also observed that the FE for hydrobenzoin, which is formed via self-coupling of benzaldehyde, exhibited an opposite trend to that of mandelic acid (**Figure A3a**). This observed trend might be explained by the interaction of CO_2 with different electrode materials, such that materials with weaker CO_2 binding will have greater benzaldehyde coverage, favoring the self-coupling reaction to produce hydrobenzoin.[82]

Lewis acids (eg. $AlCl_3$, $TiCl_4$) have been shown to activate carbonyl species for electron transfer[83,84] and were hypothesized to promote benzaldehyde electrocarboxylation performance. Previously, Lewis acidic cations were introduced into the reaction system via the oxidation of sacrificial anodes (such as Al, Zn, Mg).[32] However, since the transport of these cations to the working electrode might be limiting, especially at early reaction times, a Lewis acid salt was also added to the system, in addition to the use of sacrificial anodes in our investigations. The screening of counter electrodes and Lewis acid salts was performed in parallel (**Figure 9b and c**). The choice of Lewis acid salts was limited to those that are soluble in the electrolyte and will not undergo electroplating under the applied negative potential. We found that Mg salts achieved the highest mandelic acid FEs and partial current densities, followed by Al salts, while $ZnCl_2$ completely shut down activity. Control experiments using $NaBF_4$ as a non-Lewis acidic additive produced no product, indicating that the observed trends can be attributed to the Lewis acidity of the additive, rather than non-Lewis acid effects such as ionic strength. Finally, scanning electron microscopy with energy dispersive X-ray spectroscopy (SEM-EDX)[85] of the pre- and post-electrolysis Sn electrode confirmed that no Mg plating occurred (**Figure A4**).

Interestingly, although Mg salts delivered the highest FEs and partial current densities for mandelic acid, using an Al counter electrode outperformed both Zn and Mg electrodes– achieving the highest mandelic acid FE and partial current density. Additional Al^{3+}

introduced by Al oxidation is unlikely to be the reason for this improvement because the final Al concentration is low (0.1 mM assuming 100% of anodic current goes to Al oxidation) compared to the added Lewis acid salt concentration (100 mM). Instead, a possible reason for the high mandelic acid FE and partial current density observed may be due to the facile kinetics of Al oxidation in DMF in comparison to the other electrode materials.[23] This is consistent of our observed carbon balance for the counter electrode materials (**Figure A5**). More specifically, a lower carbon balance closure was achieved for Mg (90%) and Zn (86%), which could be due undesired oxidation of starting material or products. Meanwhile, a higher carbon closure (96%) was achieved for Al, indicating that the self-oxidation process of the electrode is more favored over other oxidation processes.

We also investigated the effects of solvents and electrolyte salts which were suggested to have important influences on aldehyde electrocarboxylation reactions in previous studies.[80,81] The choice of solvent was limited to common aprotic solvents, including *N,N*-dimethylformamide (DMF), dimethyl sulfoxide (DMSO), acetonitrile (MeCN), and propylene carbonate (PC), to prevent the hydrogenation side reaction that forms benzyl alcohol. Out of the solvents tested, DMF gave the highest mandelic acid FE (**Figure A6**), followed by DMSO, MeCN and PC. A similar trend was reported in our previous study on the electrocarboxylation of organic halides. Our findings indicated that the more acidic the solvent, as quantified by the free energy of solvent deprotonation, the more it promoted the formation of the hydrogenation side product via solvent deprotonation, leading to lower carboxylation selectivity.[32,86] Comparing various tetrabutylammonium (TBA) salts, we observed that tetrabutylammonium tetrafluoroborate ($TBABF_4$) gave the highest FE and current density towards mandelic acid (**Figure A7**) while lower FEs were achieved for halide salts (Br^- and I^-). One reason that the presence of halide ions might affect the selectivity could be due to the evolution of halogens, Br_2 and I_2 respectively, at the counter electrode that can subsequently be reduced at the working electrode.

Following optimization efforts, a preliminary substrate scope (**Figure A8**) study was performed to demonstrate the broader application of the standard conditions.

3.3.2 Cyclic Voltammetry

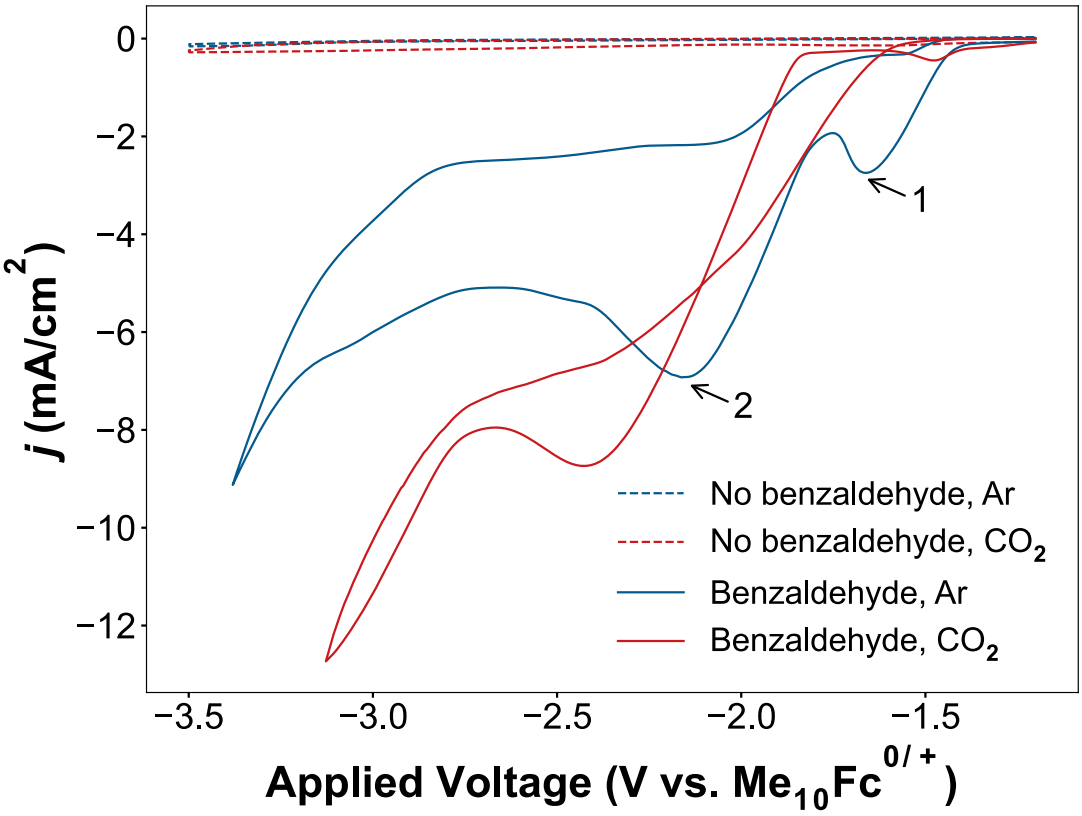

Figure 10. Cyclic voltammograms (CVs) at scan rate of 20 mV/s in DMF with and without 100 mM benzaldehyde, purged with Ar or CO_2. Reaction conditions: Sn working electrode, Al counter electrode, 100 mM $TBABF_4$, 100 mM $MgCl_2$ in DMF.

The electrocarboxylation mechanism was previously proposed to occur via the one electron reduction of the aldehyde.[80,81] To elucidate the reaction mechanism for our optimized system, cyclic voltammetry (CV) data was collected for benzaldehyde in the optimized conditions with and without the presence of CO_2.

As shown in **Figure 10**, with benzaldehyde under argon (Ar) atmosphere (solid blue trace), we observed two reduction peaks at –1.7 V and –2.2 V. The absence of these peaks without the addition of benzaldehyde suggests that they are correlated to benzaldehyde (dotted blue trace). To probe the nature of these two peaks, we performed control CV experiments with

varying $MgCl_2$ concentration (**Figure A9**). When the $MgCl_2$ is absent, only the peak at more negative potential (peak 2) was observed. Therefore, we assign peak 2 to the one-electron reduction of free benzaldehyde in DMF to form the ketyl radical intermediate, consistent with the assignment reported previously.[80] As $MgCl_2$ concentration increases from 0 to 150 mM, the intensity of the peak at less negative potential (peak 1) increases progressively (**Figure A9**). Based on these observations, peak 1 is assigned to the one-electron reduction of Mg^{2+}-coordinated benzaldehyde species to produce the Mg^{2+}-coordinated ketyl radical, as the coordination of benzaldehyde to Mg^{2+} makes it easier to be reduced compared to free benzaldehyde. Similar peaks were also observed in previous studies where benzaldehyde became easier to reduce in the presence of a protonating agent.[87] To provide further support for the peak assignment, density functional theory (DFT) calculations were performed (see Supplemental Information) to estimate the standard reduction potential of free benzaldehyde and Mg^{2+}-coordinated benzaldehyde. The standard reduction for free benzaldehyde was estimated to be –2.12 V vs. SCE, while coordination of Mg^{2+} to benzaldehyde dramatically shifted this value to –1.33 V vs. SCE). This substantial change in standard reduction potential is also consistent with the two distinct reduction peaks of benzaldehyde in the CVs.

Under a CO_2 atmosphere, prominent changes were observed in the benzaldehyde CV (**Figure 10**, solid red trace). First, a cathodic shift in the first reduction peak suggests that the presence of CO_2 made the electron transfer to benzaldehyde more unfavorable. This can be explained by the competitive adsorption between CO_2 and benzaldehyde on the electrode surface. The hysteretic crossing of the forward and reverse scans is characteristic of a two-electron transfer process that proceeds through an initial electron transfer step, a relatively slow chemical reaction step, and a subsequent second electron transfer step that occurs at a lower overpotential than the first electron transfer.[88] The increase in the current of the first reduction peak supports a chemical reaction between the generated ketyl radical and CO_2 (*vide infra*).

3.3.3 Detection of Radical Intermediates

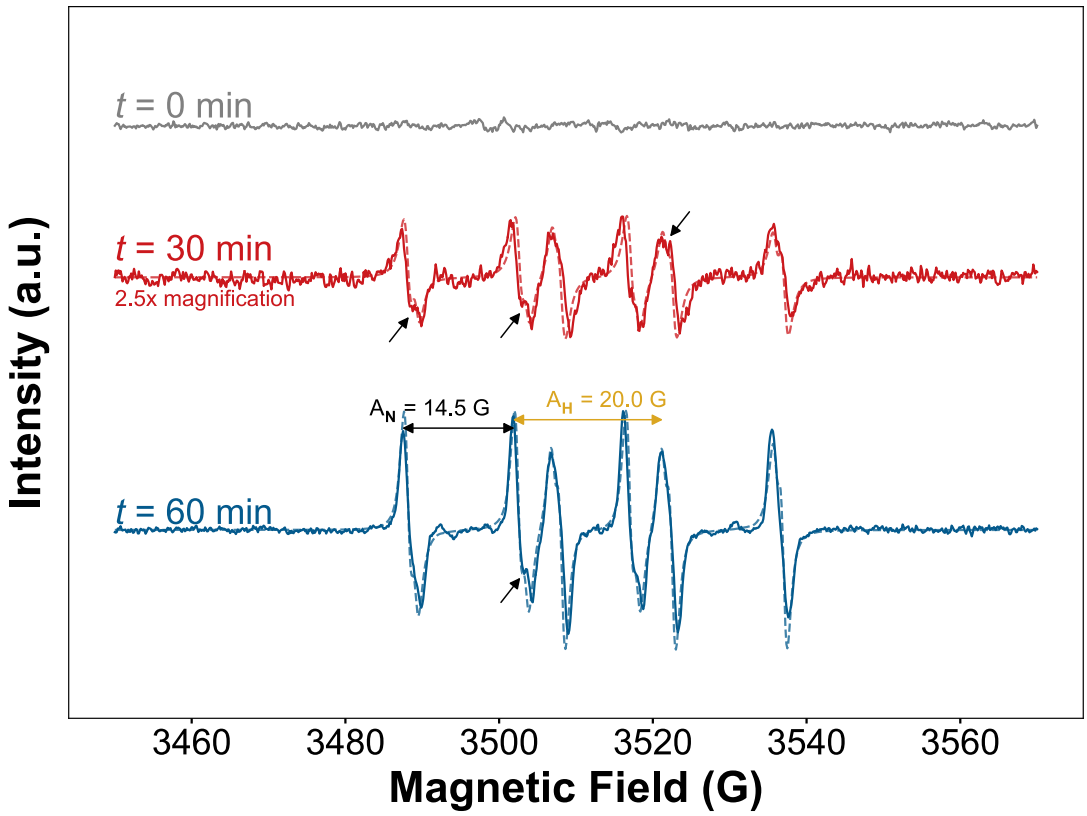

Figure 11. Experimental (solid) and simulated (dashed) EPR spectra from DMPO trapping experiments. EPR spectra were collected before potential is applied (t = 0 min, grey) and after electrolysis was performed at –2.9 V for 30 (red) and 60 minutes (blue). At t = 0 min, no radical species were detected. At t = 30 min and 60 min, the EPR spectrum contains DMPO-ketyl and DMPO-CO_2 species, leading to the split peaks (black arrows). Reaction conditions: Sn working electrode, Al counter electrode, divided cell, –2.9 V, 20 sccm of CO_2, 100 mM $TBABF_4$, 100 mM $MgCl_2$, DMF.

To identify intermediates involved in the electrocarboxylation, we turned to electron paramagnetic resonance (EPR) spectroscopy. Although EPR has been used to detect aldehyde-derived radicals,[89] it has not been applied toward understanding the aldehyde electrocarboxylation mechanism. In this study, quasi-in situ EPR was performed by adding 50 mM 5,5-dimethyl-1-pyrroline-N-oxide (DMPO) as a spin-trapping agent to the optimized electrolyte (100 mM benzaldehyde, 100 mM $TBABF_4$, and 100 mM $MgCl_2$ in DMF). Electrolysis was then performed at –2.9 V with a Sn working electrode. After 30 and 60 minutes of electrolysis, the reaction mixture was immediately transferred to capillary tubes

for EPR measurements. To assign the species detected, the EPR data collected were compared with EPR spectra simulated using the EasySpin Matlab toolbox.[90]

Under –2.9 V applied potential, a dominant sextet signal appeared, indicative of a carbon-centered radical, with isotropic hyperfine splitting values of A_N = 14.5 G and A_H = 20.0 G (**Figure 11**, *t* = 30 and 60 min, solid lines). This species was assigned as the trapped benzaldehyde ketyl radical (DMPO-ketyl) according to the simulation (**Figure 11**, *t* = 30 and 60 min, dashed lines). These hyperfine splitting patterns deviate slightly from previously reported values (A_N = 15.7 G and A_H = 22.5 G)[89] for the DMPO-trapped benzaldehyde ketyl radical, which is likely due to the coordination of Mg^{2+} ions to the radical species. When electrolysis was performed for a cell containing only benzaldehyde (no CO_2) as the starting material, the same sextet signal was observed, providing further support for the identity of the sextet as the DMPO-trapped benzaldehyde ketyl radical (**Figure A10**). The signal of the trapped ketyl radical became stronger overtime (from *t* = 30 min to *t* = 60 min) as enough of the ketyl radical accumulated, indicating that this is the primary species involved in the carboxylation mechanism.

Additionally, we observed that some of the hyperfine splitting features have split peaks (**Figure 11**, black arrows) that were attributed to a presence of a second, minor carbon radical. This species was fitted with anisotropic hyperfine splitting values of A_N = 14.0 and A_H = 18.0 and assigned as the CO_2 radical anion ($CO_2^{\bullet-}$) trapped by DMPO (DMPO-CO_2).[91] Control electrolysis experiment performed with only CO_2 as the starting material (no benzaldehyde) generated the same signal, further supporting the identity of the species as DMPO-CO_2 (**Figure A11**). Notably, the control experiment with CO_2 only produced minimal current (~20 μA/cm^2), suggesting that the CO_2 radical anion is generated in minor quantities under optimized reaction conditions and, therefore, unlikely to be involved the main carboxylation pathway (*vide infra*). Without electrolysis, no EPR signal was observed (**Figure 11**, *t* = 0 min), which validates that the observed radical species were generated electrochemically.

3.3.4 Electrochemical Kinetic Study

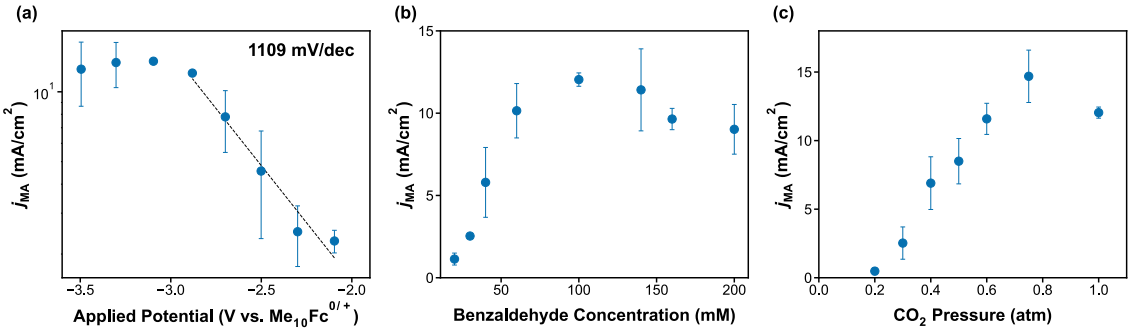

Figure 12. Kinetic data on the electrochemical carboxylation of benzaldehyde. (a) Tafel plot for benzaldehyde electrochemical carboxylation on Sn. (b) Benzaldehyde concentration and (c) CO_2 partial pressure dependence of the partial current density for mandelic acid (j_{MA}) at constant potential –2.9 V vs. $Me_{10}Fc^{0/+}$. Reaction conditions: Sn working electrode, Al counter electrode, undivided cell, 100 mM $TBABF_4$, 100 mM $MgCl_2$, DMF.

To further probe the electrocarboxylation mechanism, we investigated the potential dependence on mandelic acid partial current density (**Figure 12a**). In the potential range from –1.2 V to –2.9 V, the Tafel curve shows a linear region with a Tafel slope of ~1109 mV/dec, which indicates a weak potential dependence. Control experiments at –2.9 V with varying convection conditions (adjusted by CO_2 flow rates) suggest the reaction is kinetically controlled in this potential range (**Figure A12**). The large Tafel slope suggests that it is likely that a chemical reaction step is rate-limiting. Moreover, the unconventional value indicates that the formation of intermediates involved in the rate-limiting step (RDS) has a weak dependence on the applied potential, which we propose to be due to surface saturation of those intermediates. The partial current density plateaus at further increasing overpotentials, suggesting the reaction is influenced by the mass transport of reactants.

To gain more information on the kinetics, benzaldehyde concentration and CO_2 partial pressure dependence studies were conducted at constant potential (–2.9 V). As the benzaldehyde concentration increases from 20 mM to 100 mM, the mandelic acid partial current density increases monotonically (**Figure 12b**). Interestingly, the partial current density peaks at 100 mM, then decreases upon further increasing benzaldehyde concentration. This suggests that the further increase in benzaldehyde concentration will

negatively influence the concentration or coverage of other species involved in the rate-limiting steps for mandelic acid formation. In contrast, the partial current density for hydrobenzoin increased monotonically with benzaldehyde concentration (**Figure A13**).

A similar trend was also observed in the CO_2 pressure dependence study. The partial current density of mandelic acid shows an initial positive dependence on CO_2 partial pressure from 0.2 bar to 0.75 bar, followed by a negative dependence at the higher CO_2 partial pressures (**Figure 12c**). Combined, we propose that there is competitive adsorption between benzaldehyde and CO_2 on the catalyst surface. This is consistent with observed cathodic shift in the reduction peak of benzaldehyde in the presence of CO_2 compared to Ar atmosphere in the CV data (**Figure 10**). The proposed competitive adsorption also explains the strong dependence on working electrode material, where the best electrode material most likely has moderate binding affinity to both benzaldehyde and CO_2.

3.3.5 Mechanistic Interpretations

From the combined CV, EPR and kinetic study results, we propose a mechanism (**Scheme 1**) distinct from that previously reported for the electrocarboxylation of aldehydes.[80,81] Our mechanism invokes the initial one-electron reduction of benzaldehyde (A) to generate a ketyl radical (B) which is stabilized by Mg^{2+} over the Sn surface, as has been identified in our EPR and CV experiments (**Figures 10 and 11**). The surface-bound ketyl radical intermediate then reacts with CO_2 at the carbon atom to form a carboxylate radical species (C); this step is also the rate-limiting step (RDS). The previously reported mechanism invokes the addition of a second CO_2 molecule to species (C) to form a dicarboxylate species, followed by a second electron transfer step. We do not observe the involvement of a second CO_2 molecule and instead propose that the carboxylate radical species (C) directly undergoes the second electron transfer and is reduced to give the carboxylate (D). Finally, an acid workup leads to protonation of the carboxylate moiety to yield mandelic acid. Meanwhile, under protic conditions, the ketyl radical (B) can also undergo additional reduction or self-coupling to deliver the minor products benzyl alcohol and hydrobenzoin, respectively.

This mechanism is supported by the large Tafel slope (1109 mV dec^{-1}) calculated in the potential-dependence study, which suggests that a chemical–rather than an electrochemical–step is likely to be the RDS (**Figure 12a**). As the RDS is the coupling between the reduced benzaldehyde and CO_2 over the Sn surface, the reaction rate will increase with benzaldehyde concentration or CO_2 partial pressure at low coverage of reduced benzaldehyde or CO_2. Further increases in the benzaldehyde concentration or CO_2 partial pressure will decrease the coverage of the competing reactant due to competitive adsorption, thereby decreasing the reaction rate–consistent with the trends observed in substrate-dependence studies (**Figure 12b and c**). Based on these mechanistic findings, we believe that Sn gives the highest mandelic acid FE because it provides balanced adsorption of both benzaldehyde and CO_2, preventing either reaction from becoming limiting.

Based on the observation of a CO_2 radical anion DMPO-adduct in the EPR spectrum and detection of 1,2-ethanodioic acid (oxalic acid) (the CO_2 dimerization product) in the product distribution (**Figure 10**, t = 30 min), there is also a possibly of a minor pathway that occurs via CO_2 reduction (**Figure A14**). In this pathway, CO_2 is reduced to form the radical anion, followed by reaction with the aldehyde to form the coupled intermediate. Here, the two mechanisms converge to form the same carboxylate intermediate and final mandelic acid product. The lack of observable reductive current in the CV trace that only contains CO_2 indicates that this CO_2 reduction mechanism forms a very minor contribution to the final product formation.

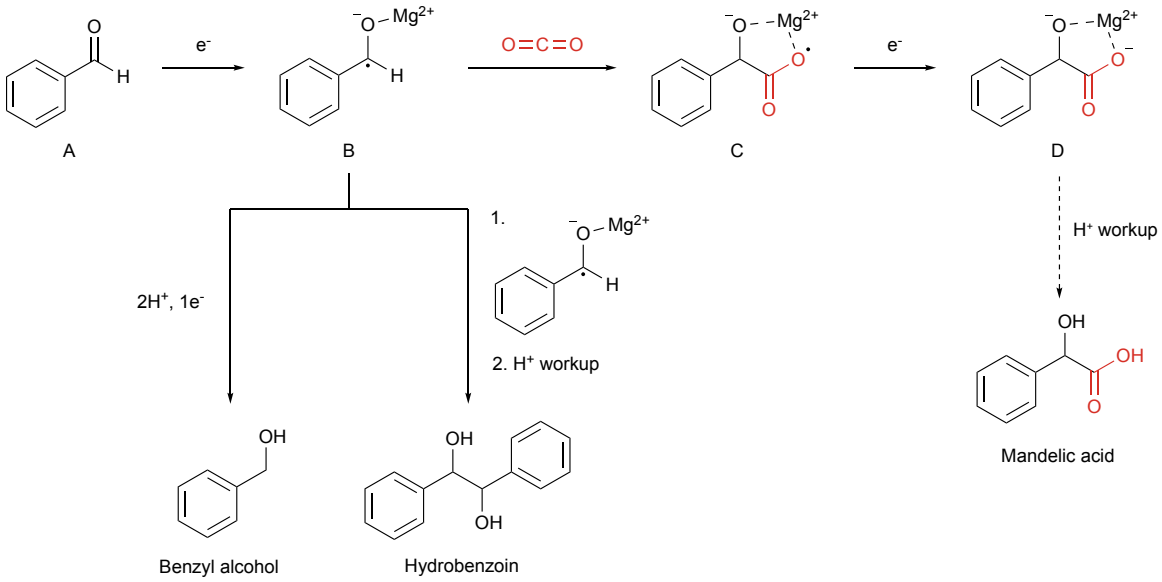

Scheme 1. Proposed mechanism for electrocarboxylation of benzaldehyde to form mandelic acid and side reaction pathways to form benzyl alcohol and hydrobenzoin.

3.4 CONCLUSIONS

This work investigated a system for the electrochemical carboxylation of benzaldehyde to synthesize mandelic acid using CO_2 as a non-toxic and abundant carbon source. Under optimized conditions (Sn working electrode, –2.9 V, 100 mM $MgCl_2$/DMF), an FE of 79% and partial current density of 12.9 mA/cm^2 were achieved. In situ EPR and kinetic measurements suggest that the reaction occurs via a one-electron reduction of benzaldehyde to generate a Mg^{2+}-stabilized ketyl radical intermediate that subsequently reacts with CO_2. To promote this key intermediate, magnesium chloride ($MgCl_2$) was added as a Lewis acid source to lower the overpotential of benzaldehyde reduction. Furthermore, coupling between the ketyl radical and CO_2 is determined to be the rate determining step in the reaction, which has not been previously reported. After the RDS, the coupled intermediate is proposed to undergo addition of a second electron, leading to the formation of the carboxylate product.

Looking forward, the detailed mechanistic insights into the aldehyde electrocarboxylation system established in this work will inform future strategies to enhance reaction efficiency and selectivity. Specifically, these insights can guide the rational design of more selective

electrocatalysts by balancing the binding of CO_2 and the aldehyde and the identification of Lewis acid additives that better stabilize the ketyl radical intermediate. Aside from selectivity, future improvements could also focus on increasing reaction rates by implementing continuous flow systems and scaling up the reactor design to enhance mass transport and electrode surface area, enabling industrial applications. Beyond this system, our conclusions significantly expand the mechanistic understanding of electrocarboxylation, paving the way for further advancements in related electrochemical transformations, including other electrocarboxylation reactions and reactions involving aldehydes.

3.5 METHODS

3.5.1 Electrode Preparation

Foils (Pd, Sn, Co, Ag, Fe, Zn, Ti, Ni, Pt, Al, Mg, graphite) were mechanically polished using 400 G silicon carbide sandpaper in a weigh boat lined with a piece of aluminum foil. The metal foil was submerged in Milli-Q water while polishing. The polishing procedure was as follows: small circular polishes were made for 1 min, followed by unidirectional polishing for 30 sec until discoloration is observed. After polishing, the foils were rinsed with Milli-Q water, followed by acetone, then wiped with a KimWipe before using right away.

Copper foils were first polished mechanically following the same procedure for other electrodes. Then, they were electrochemically polished with concentrated phosphoric acid (85% w/w) at 2.10 V vs. a Pt wire electrode for 5 minutes. The foils were rinsed with Milli-Q water, followed by acetone, then wiped with a KimWipe before using right away.

Glassy carbon (GC) electrodes were polished mechanically using an alumina slurry (0.05 μm) on a microcloth polishing pad. Polishing was performed using a figure-eight motion for 1 min to ensure uniform abrasion. Following polishing, the electrodes were thoroughly rinsed with Milli-Q water and sonicated in Milli-Q water for 5 min. The electrodes were removed from the sonication bath, rinsed with acetone, and sonicated in acetone for 5 minutes to get rid of residual polishing debris. The electrode was dried with a stream of nitrogen before using right away.

3.5.2 Electrolyte Preparation and Reaction Setup

Due to the sensitivity of the electrocarboxylation reaction to water, care was taken to ensure minimal water exposure of the electrochemical cell. All electrolyte components were stored in the glovebox. The electrolyte was prepared all in the glovebox day of usage and only taken out of the box right before the cell was assembled. Once taken out of the glovebox, the electrolyte was stored in a desiccator until it was ready to be added to the cell.

Electrochemical measurements were performed in custom-made H-type PEEK cells with continuous CO_2 purging. Aluminum foil was taped onto the PEEK backing plates to be used as current collectors. A leakless Ag/AgCl electrode was used as the reference electrode. The cell was filled with 4 mL of electrolyte solution and experiments were typically performed with 20 sccm of CO_2 gas bubbling through the electrolyte. Potential was applied using a potentiostat (Biologic SP-200).

3.5.3 EPR Experiments

EPR experiments were performed on a Bruker EMX X-band CW-EPR spectrometer at room temperature using an SHQE resonator at ~ 9.86 GHz. To collect EPR data, the electrolyte was taken from the H-Cell and added to 1.6 mm O.D. quartz capillary tubes for measurement. Spectra were collected using magnetic field ranges of 3411 to 3611 G with 20 scans averaged for each spectrum. Other acquisition parameters: MW power = 21.83 mW; Modulation amplitude = 1 Gauss; Conversion time = 10.0 ms.

EPR spectra were simulated using the EasySpin (v. 6.0.6) Matlab (v. R2023a) toolbox. The garlic function was used for computation of isotropic and fast-motional continuous-wave (cw) EPR spectra of radicals in solution.

Chapter 4

TOWARD ELECTROCHEMICAL CARBOXYLATION OF ALIPHATIC ALDEHYDES WITH CO_2

4.1 ABSTRACT

α-Hydroxycarboxylic acids (AHAs) are widely used in the pharmaceutical, cosmetic, and chemical industries, yet their synthesis often relies on hazardous reagents or energy-intensive processes. Electrochemical carboxylation of aldehydes with CO_2 offers a more sustainable alternative by using CO_2 as an abundant C1 feedstock under mild conditions, though its application to aliphatic substrates remains underexplored. Here, we systematically investigate the electrocarboxylation of aliphatic aldehydes, focusing on the influence of working electrode, solvent, and electrolyte on Faradaic efficiency (FE). Using 3-phenylpropanal as a model substrate, copper was identified as a cost-effective and efficient cathode material, enabling a maximum FE of 18.1% under optimized conditions. Solvent choice strongly influenced selectivity, whereas electrolyte identity had minimal effect. Electrochemical analysis supports a convergent mechanism involving aldehyde- and CO_2-derived radical intermediates, while significant aldehyde polymerization was identified as a competing side reaction limiting efficiency. Overall, this study expands the scope of electrochemical CO_2 incorporation to aliphatic aldehydes and provides mechanistic and practical insights for improving selectivity and efficiency in sustainable carboxylation chemistry.

4.2 INTRODUCTION

α-Hydrocarboxylic acids represent an important class of compounds with applications across the pharmaceutical, cosmetic, and polymer industries.[92–94] For instance, 2-hydroxypropanoic acid (lactic acid) and 2-hydroxylactic acid (glycolic acid) are widely used in skin care formulations as mild exfoliants.[93] Lactic acid is also used as a preservative and flavor

enhancer in the food industry.[95] Furthermore, the versatile functionality of the α-hydroxy group makes these molecules useful intermediates for high value chemical synthesis.

Industrial processes to synthesize AHAs often require the use of harsh or toxic reagents. One common method requires addition of toxic cyanide to a carbonyl precursor to generate a cyanohydrin intermediate, followed by an acid hydrolysis step to produce the desired acid (**Figure 13a**). Alternatively, catalytic oxidation methods using heavy metal catalysts such as thallic bromide have also been employed, but the use of these reagents pose significant risks to human health and the environment (**Figure 13a**).[93] As a result, there has been growing interest to develop safer and more sustainable routes to synthesize these valuable compounds.

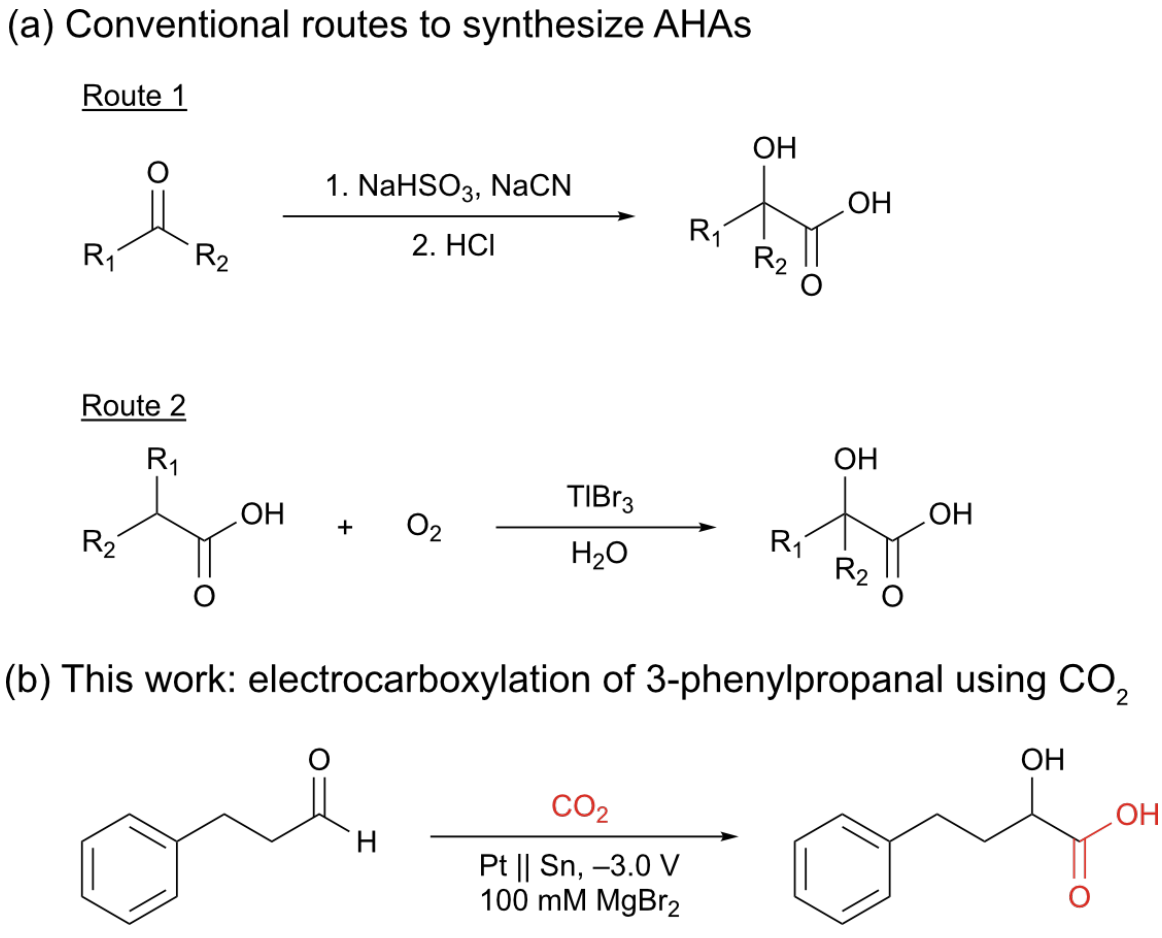

Figure 13. Background and overview for the electrochemical carboxylation of 3-phenylpropanal. (a) Examples of conventional routes to synthesize α-hydroxy carboxylic

acids from carbonyl species. (b) Electrochemical carboxylation of 3-phenylpropanal using CO_2.

A promising strategy is the electrochemical carboxylation of aldehydes with CO_2, which incorporates CO_2 into an existing organic backbone to produce the corresponding carboxylic acids. This strategy avoids the use of toxic reagents, while also taking advantage CO_2 as a safe and abundant C1 building block. It is also attractive because electricity can provide the necessary driving force to overcome the substantial energetic barrier associated with CO_2 activation. Compared to established industrial methods, such as the Kolbe-Schmitt reaction,[6,7] which typically require high temperatures and pressures to activate CO_2, electrochemical methods can be performed under milder and safer conditions.

While the electrochemical carboxylation of aldehydes presents a promising synthetic strategy, it remains limited in its reaction scope. Most literature reports focus on the synthesis of aromatic AHAs, leaving the production of aliphatic AHAs under explored, with only three reported studies to date. In 1986, Silvestri et al.[23] reported on the electrochemical carboxylation of acetaldehyde to synthesize lactic acid, which was achieved at 9% yield. It was not until 2023 that Waldvogel et al.[80] reported the synthesis of two aliphatic AHAs using graphite as both working and counter electrodes and propylene carbonate as a green solvent. More recently, Wirtanen and coworkers[96] reported the synthesis of seven different aliphatic AHAs, achieving the highest reported yield of 45% for glycolic acid.

Although yield is important parameter to optimize in chemical synthesis, it is also helpful to consider the Faradaic efficiency (FE) of an electrochemical reaction, which captures how much of the applied charge is going towards making the desired product. Improving the FE helps to minimize energy lost towards undesired side reactions, making the reaction more cost effective. With these considerations, this work systematically evaluated the influence of key reaction parameters on the FE of aliphatic aldehyde electrochemical carboxylation. It was found that both the choice of working electrode and solvent had a dramatic impact on FE, with the optimized conditions producing an FE of 18.1%. Mechanistic investigation was also performed to elucidate the underlying reaction pathway and identify key intermediates governing selectivity.

4.3 RESULTS AND DISCUSSION

4.3.1 Optimization of Reaction Conditions

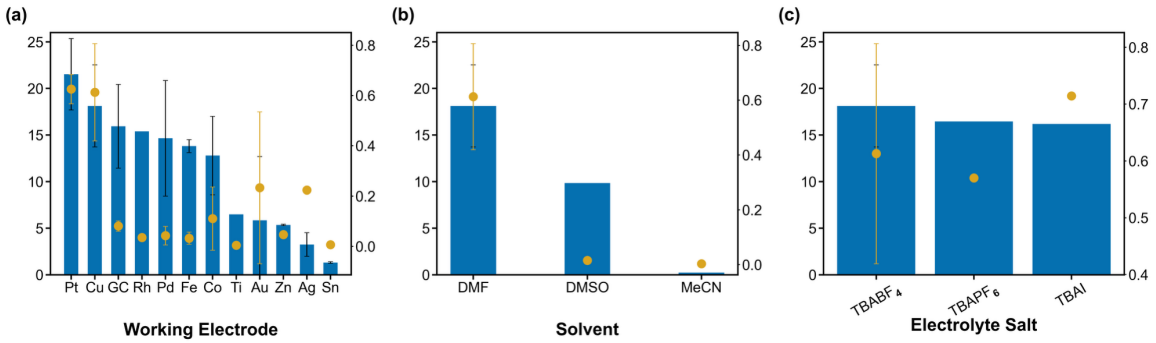

Figure 14. Effect of (a) working electrode (b) solvent, and (c) electrolyte salt on electrochemical carboxylation performance, as quantified by 2-hydroxy-4-phenylbutanoic acid Faradaic efficiency and partial currently. Catholyte: 100 mM 3-phenylpropanal, 100 mM $MgBr_2$, 100 mM electrolyte salt, 10 sccm CO_2, 2 mL DMF. Anolyte: 100 mM TBABr, 2 mL DMF. –3.0 V vs. $Me_{10}Fc^{0/+}$ for 2 hours. Cu working electrode and Pt counter electrode were used unless otherwise specified. $Me_{10}Fc$ = decamethylferrocene; GC = glassy carbon.

To evaluate how the reaction parameters (working electrode, solvent, and electrolyte salt) influence the electron selectivity, the FE and partial current density were quantified using the electrochemical carboxylation of 3-phenylpropanal (3P) to 2-hydroxy-4-phenylbutanoic acid (3PCOOH) as the model reaction. Bulk electrolysis was performed under constant applied potential of –3.0 V vs. $Me_{10}Fc^{0/+}$ (all potentials are reference against decamethylferrocene), under continuous CO_2 flow, using custom-made H-type PEEK cells (see Appendix B). To quantify the product, the electrolyte was diluted in Milli-Q water and was quantified using ultra-performance liquid chromatography (UPLC), with 1,3,5-trimethoxybenzene (TMB) as an internal standard (**Figure A14**).

The electrochemical carboxylation reaction has been performed on a wide range of working electrode materials, such as silver, zinc, and tin. In this study, the effect of 12 different working electrodes was investigated, and it was found that the choice of working electrode had a dramatic impact on the FE and partial current density (**Figure 14a**). In particular, platinum (Pt) produced the highest FE towards 3PCOOH at 21.5%, followed by copper (Cu)

which produced an FE of 18.1%. Pt and Cu also gave the highest partial current density towards products, at 0.63 mA/cm^2 and 0.61 mA/cm^2 respectively. Considering the cheaper cost of Cu compared to Pt, further studies were performed using Cu as the cathode material. The dramatic differences in selectivity among the different working electrode materials could be due to differences in the way reactants and intermediates are interacting with the electrode surface. Interesting, tin (Sn) showed the worst performance for 3P electrochemical carboxylation, resulting an FE of only 1.3% whereas our previous work on the electrochemical carboxylation of benzaldehyde showed that Sn gave the highest FE for that substrate. This observation may suggest that distinct mechanistic pathways are operative in the electrochemical carboxylation of aliphatic versus aromatic aldehydes. However, further studies are required to substantiate this hypothesis and fully elucidate the underlying differences in reactivity.

The effect of solvent and electrolyte salt was also investigated, as these parameters have previously been shown to have an influence on the electrochemical carboxylation reaction. As the presence of protons in solution can lead to the formation of the hydrogenation side product, the choice of solvent was limited to common aprotic solvents, including DMF, DMSO, and acetonitrile. It was observed that the choice of aprotic solvent has a dramatic effect on selectivity (**Figure 14b**). DMF gave the highest FE (15%) and partial current density (0.61 mA/cm^2), whereas performing the reaction in acetonitrile shut down reactivity. The observed trend is consistent with findings reported by Corbin et al.[86], who studied solvent effects in the electrochemical carboxylation of organic halides and found that selectivity toward the carboxylation product trends with the solvent's deprotonation energy. More specifically, the easier it is to deprotonate the solvent, the more it promotes the hydrogenation pathway, leading to a decrease in the carboxylation selectivity. The same trend was also observed in our work on the electrochemical carboxylation of benzaldehyde is hypothesized to be at play in this system. Aside from solvent, the effect of various tetrabutylammonium (TBA) salts were also investigated (**Figure 14c**). It was found that the electrolyte salt identity does not appear to have a dramatic impact on reaction selectivity,

suggesting that it is not a primary factor governing the reaction pathway under these conditions.

4.3.2 Cyclic Voltammetry

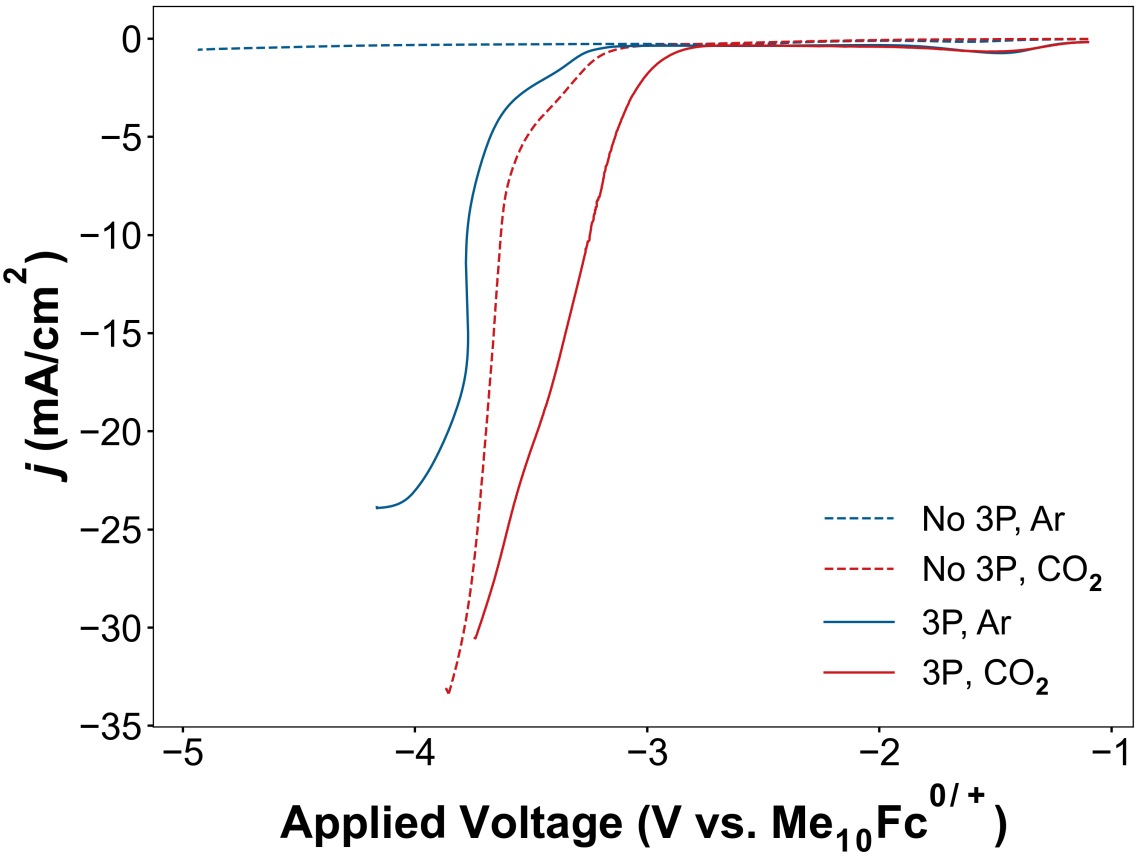

Figure 15. Linear sweep voltammograms (LSVs) at a scan rate of 50 mV/s in DMF with and without 100 mM 3-phenylpropanal (3P), purged with Ar or CO_2. Catholyte: 100 mM $TBABF_4$, 100 mM $MgBr_2$ in DMF. Anolyte: 100 mM TBABr in DMF. Cu working electrode, Pt counter electrode.

Following optimization efforts, linear sweep voltammetry (LSV) was performed to probe the reductive reaction mechanism. LSV data were collected for 3-phenylpropanal under optimized conditions with and without CO_2, with a scan rate of 50 mV/s.

When comparing the reductive traces of CO_2 versus 3-phenylpropanal, the onset reduce potential (defined here as the potential corresponding to a current density of –0.5 mA/cm^2)

of the two species show a difference of only 0.09 V, with the reduction of CO_2 being slightly more facile (**Figure 15**). When both species are present, the onset reduction potential shifts to a less negative value. The observed shift, together with the increase in reductive current, is consistent with an EC mechanism in which one species is undergoes an initial electron transfer, followed by a subsequent chemical reaction with the second substrate. Given the small difference in onset potentials between 3P and CO_2, it is likely that both species are activated, generating the ketyl radical and CO_2 radical anion respectively. Consequently, we propose two convergent reaction pathways leading to the formation of the carboxylic acid product.

In pathway 1 (**Scheme 2, top**), the first electron transfer to 3P generates a ketyl radical species, which then couples with a CO_2 molecule. This adduct undergoes a second electron transfer step to form a carboxylate product that is most likely stabilized by Mg^{2+} ions in solution. Meanwhile, in pathway 2 (**Scheme 2, bottom**), reduction of CO_2 forms a CO_2 radical anion that attacks the 3P electrophile. A second electron transfer step generates the same Mg carboxylate species observed in pathway 1, allowing the two pathways to converge. From the Mg carboxylation species, the carboxylic acid product is generated following an acid work-up step.

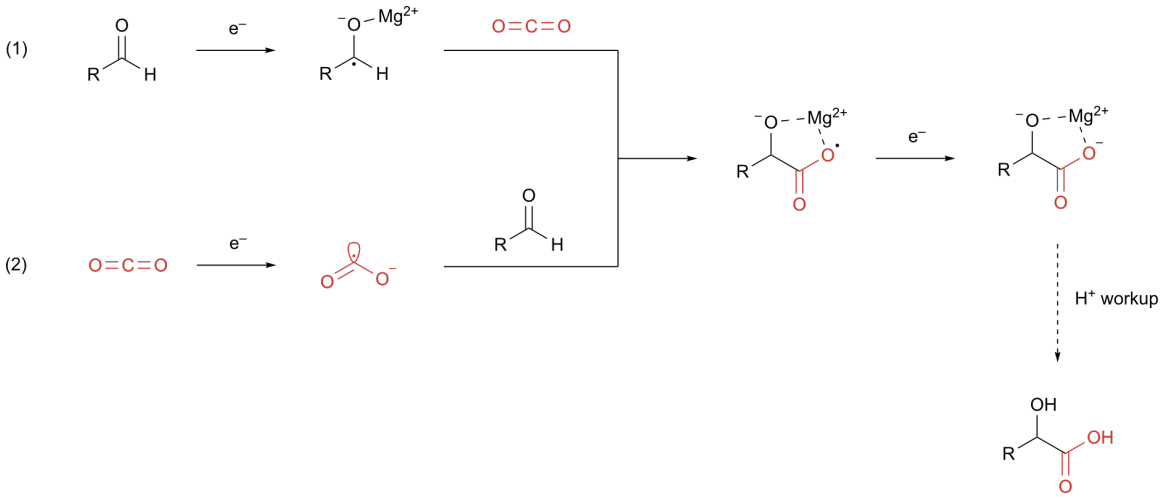

Scheme 2. Proposed mechanism for the electrochemical carboxylation of an aliphatic aldehyde to form the corresponding carboxylic acid. The reaction is proposed to occur via two convergent pathways: 1) substrate reduction and 2) CO_2 reduction.

4.3.3 Polymerization Side Reaction

Following bulk electrolysis, a gel was consistently observed on the cathodic side of the cell. After a few hours, the entire electrolyte became gel-like. ^{1}H NMR analysis of the gel showed that the 3-phenylpropanal starting material was completely consumed, indicating that the polymer is derived from the aldehyde (**Figures A15-17**). This observation is consistent with previous reports showing that aliphatic aldehydes can form polymers under either acidic or basic conditions.[97] Under the highly reductive conditions required for electrochemical carboxylation, it is possible that anionic species were generated that could initiate the polymerization process, lowering the carboxylation selectivity. To that end, further investigation of the polymerization process and strategies to avoid this side reaction is needed to improve the performance of aliphatic aldehyde electrocarboxylation.

4.4 CONCLUSIONS

This study demonstrates that electrochemical carboxylation of aliphatic aldehydes with CO_2 can provide access to α-hydroxycarboxylic acids under mild and sustainable conditions, though current efficiency remains limited. Systematic optimization of reaction parameters identified the working electrode and solvent as key factors controlling Faradaic efficiency, with copper emerging as a practical and effective cathode material. Under optimized conditions, a maximum Faradaic efficiency of 21.5% was achieved. Electrochemical and mechanistic studies support a convergent pathway involving both aldehyde and CO_2 activation, likely proceeding through ketyl radical and CO_2 radical anion intermediates. However, competitive polymerization of the aldehyde was identified as a major side reaction that reduces selectivity. Overall, this work establishes important structure-reactivity relationships for aliphatic aldehyde electrocarboxylation and highlights key challenges that must be addressed to improve efficiency and enable broader synthetic application.

Chapter 5

ENANTIOSELECTIVE ELECTROCHEMICAL CARBOXYLATION OF BENZALDEHYDE USING CHIRAL METAL SALEN CATALYSTS

5.1 ABSTRACT

The electrochemical carboxylation of aldehydes with CO_2 is a viable strategy for the sustainable synthesis of valuable α-hydroxycarboxylic acids, but achieving this transformation in an enantioselective manner remains challenging. In this work, the asymmetric electrocarboxylation of benzaldehyde catalyzed by chiral metal salen complexes was investigated for the first time. Using a chiral Ni(salen) complex, optically active mandelic acid was obtained in 43% enantiomeric excess. Systematic investigation of the reaction conditions revealed that both the applied potential and metal center identity exerted a strong influence on enantioselectivity, pointing to underlying electronic effects. Mechanistic studies using cyclic voltammetry suggest that the most effective catalysts readily undergo reductive activation under the applied conditions, enabling binding with CO_2 to initiate the enantioselective pathway. These findings provide a foundation for the rational design of improved asymmetric catalyst systems for electrochemical CO_2 incorporation.

5.2 INTRODUCTION

Rising energy demands coupled with our reliance on fossil fuels (coal, oil, natural gas) has led to unprecedent levels of atmospheric carbon dioxide (CO_2). This has contributed to worsening climate change, ocean acidification, habitat degradation and many other irreversible environmental problems. Faced with these challenges, research efforts have focused on the valorization of CO_2 into fuels and chemical products, which would simultaneously decrease society's reliance on fossil fuels and help sequester CO_2 from the atmosphere, allowing for the transition to a more sustainable carbon neutral economy. In addition, CO_2 is a promising C1 building block because it is cheap, abundant, and nontoxic. However, using CO_2 in chemical synthesis is challenging because it is thermodynamically

stable and kinetic inert. To that end, electrochemical activation of CO_2 has been of great interest. Compared to traditional methods requiring heat and pressure to activate CO_2, electrochemical methods provide a milder and safer route to activated CO_2 by applying the energy in the form of voltage-driven electrons.

Within this context, one subclass of electrochemical reactions involving CO_2 is the electrochemical carboxylation of carbonyls to form α-hydroxycarboxylic acids, which represent an important class of chemicals that find applications in the pharmaceutical, cosmetic, and polymer industries.[92,93] Many applications involving AHAs often require a specific enantiomer due to their relevance in biologically active molecules and chiral building blocks. For instance, (R)-(–)-mandelic acid is a key intermediate in the synthesis of penicillins, antitumor agents, and cephalosporins, whereas the S-enantiomer has been used for the synthesis of non-steroidal anti-inflammatory drugs.[93,98]

While there has been progress made in understanding the electrochemical carboxylation reaction to synthesize AHA, controlling stereochemistry is still challenging. Consequently, the development of enantioselective carboxylation strategies has attracted increasing interest. Asymmetric carboxylation remains limited to ketones, using chiral inductors such as chiral alkaloids[99,100] and metal salen complexes,[101–104]. Meanwhile, the asymmetric carboxylation of aldehydes has not been reported, despite their distinct reactivity and synthetic utility.

Guided by prior studies on the asymmetric carboxylation of ketones, we investigated the use of chiral metal salen catalysts for the enantioselective electrochemical carboxylation of benzaldehyde (**Scheme 3**). Metal salen catalysts offer an attractive platform due to their stability, ease of synthesis, and readily tunable structural and electronic properties.[105] Using a Ni(salen) catalyst, optically active mandelic acid was obtained in up to 43% enantiomeric excess (e.e.). Notably, both the applied potential and the identity of the metal center strongly influenced enantioselectivity, motivating further investigation into the underlying electronic effects.

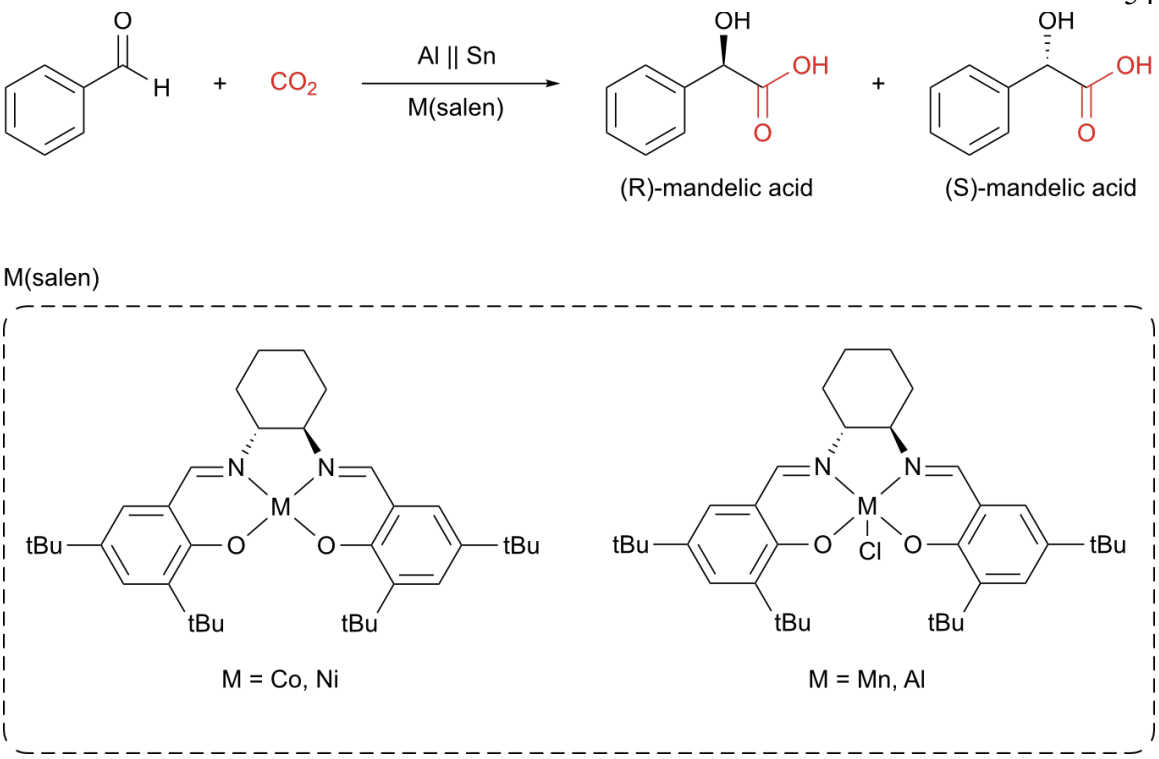

Scheme 3. Enantioselective electrochemical carboxylation of benzaldehyde using chiral metal salen complexes.

5.3 RESULTS AND DISCUSSION

5.3.1 Influence of Experimental Parameters

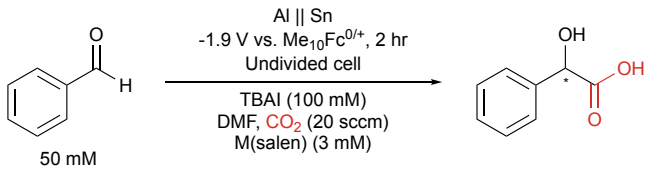

Entry	Deviation from Standard Conditions	Yield (%)	e.e. (%)
1	None	2.1	40
2	-2.0 V	1	30
3	-2.1 V	4	18
4	Ni(salen)	3	43
5	Mn(salen)	6	3
6	Al(salen)	7	2

Table 1. Screening of reaction conditions.

We began our investigation by examining the asymmetric electrochemical carboxylation of benzaldehyde using chiral metal salen catalysts. Drawing on our prior study on the electrochemical carboxylation benzaldehyde, tin (Sn) and aluminum (Al) foils were selected as the working and counter electrodes, respectively. The reaction was conducted in *N,N*-dimethylformamide (DMF) with tetrabutylammonium iodide (TBAI) as the supporting electrolyte under continuous CO_2 flow (see Appendix C). Products were quantified using ultra-performance liquid chromatography (UPLC) with a chiral column, using 4-chlorobenzoic acid as an internal standard (**Figure A18**).

Under these conditions, we observed that the applied potential had a pronounced effect on enantioselectivity. At −1.9 V vs. $Me_{10}Fc^{0/+}$ (all potentials are referenced against decamethylferrocene unless otherwise noted), the desired product was obtained with an e.e. of 40% with the use of a Co(salen) catalyst, whereas applying a more negative potential of −2.1 V led to a significant decrease in e.e. to 18% (**Table 1, entry 1-3**). One possible explanation for the decrease in enantioselectivity at more negative potentials is the involvement of competing non-selective pathways. However, further studies are required to elucidate the underlying potential dependence.

In addition to electrochemical parameters, the identity of the metal center was found to play a critical role in controlling enantioselectivity. Screening of different metal salen complexes revealed that Ni(salen) and Co(salen) afforded comparatively high e.e. of 43% and 40%, respectively (**Table 1, entry 4 and 1**). In contrast, the use of Mn(salen) resulted in poor e.e. (3%) despite its common use in asymmetric catalysis (**Table 1, entry 5**). These results indicate that the metal center exerts a significant influence on enantioselectivity under electrochemical conditions.

Together, these findings highlight that both applied potential and metal identity are key determinants of reaction outcome, motivating further mechanistic investigation into their roles in controlling reactivity and selectivity.

5.3.2 Cyclic Voltammetry

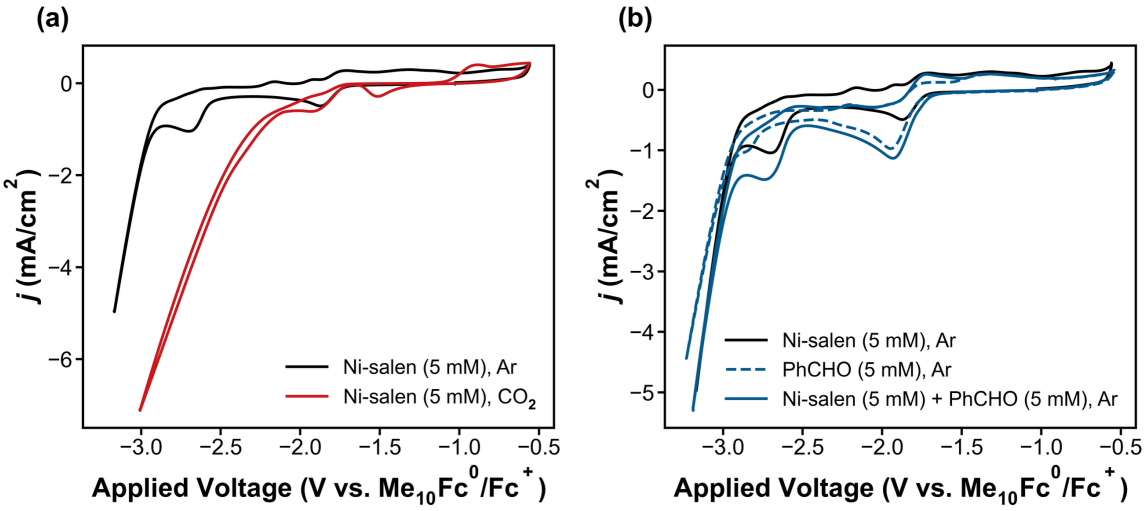

Figure 16. Cyclic voltammograms (CVs) at a scan rate of 20 mV/s in DMF for (a) Ni(salen) with and without CO_2 and (b) Ni(salen) with and without benzaldehyde. Reaction conditions: Sn working electrode, Al counter electrode, 100 mM TBAI in DMF.

To gain insight into the role of the metal salen complexes in controlling enantioselectivity, we investigated their electrochemical behavior using cyclic voltammetry. For the Ni(salen) complex, a reversible redox feature was observed with an $E_{1/2}$ value of –1.79 V (**Figure 16, black**), which is assigned to the reduction of Ni^{II}(salen) to $[Ni^{I}(salen)]^-$ based on literature precedent.[68,106] A second reduction peak at –2.70 V has also been reported and is attributed to reduction of the free Schiff base ligand generated via disproportionation of the $[Ni^{I}(salen)]^-$ species.[106]

To probe potential interactions with reactants, CVs were collected in the presence of CO_2 and benzaldehyde. In the presence of CO_2, the feature corresponding to the oxidation of $[Ni^{I}(salen)]^-$ to Ni^{II}(salen) was no longer observed, suggesting that the reduced $[Ni^{I}(salen)]^-$ species is consumed in a subsequent chemical step involving CO_2 (**Figure 16a, red**). This behavior is consistent with coordination of the reduced $[Ni^{I}(salen)]^-$ complex with CO_2, in line with prior studies on Ni(salen)-catalyzed CO_2 reduction.[107] In contrast, the electrochemical behavior of Ni(salen) remained largely unchanged in the presence of benzaldehyde (**Figure 16b**), suggesting minimal interaction between the reduced metal complex and the aldehyde substrate under reaction conditions.

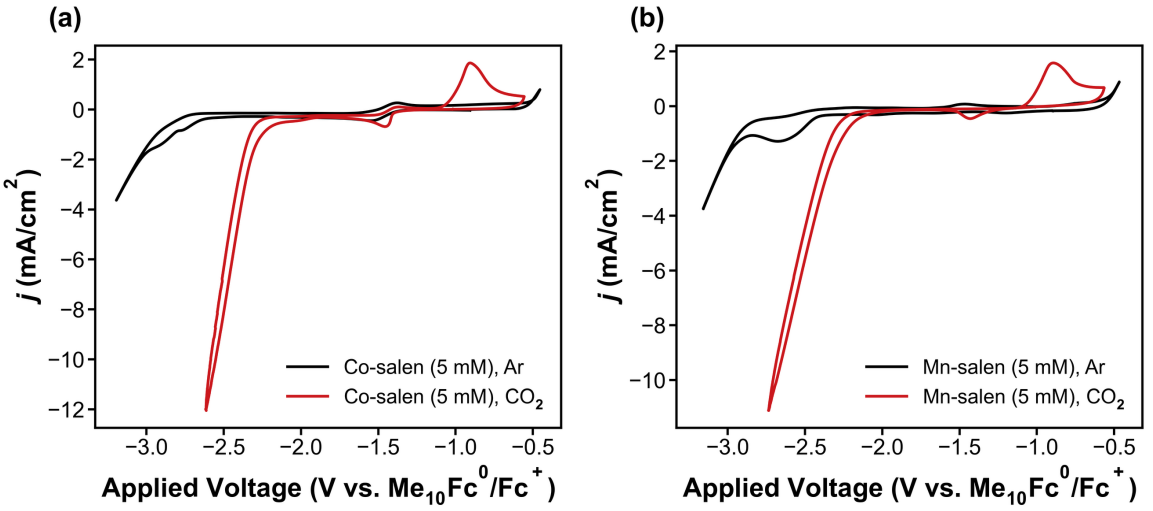

Figure 17. Cyclic voltammograms (CVs) at a scan rate of 20 mV/s in DMF for (a) Co(salen) with and without CO_2 and (b) Mn(salen) with and without CO_2. Reaction conditions: Sn working electrode, Al counter electrode, 100 mM TBAI in DMF.

We next examined the electrochemical behavior of Co(salen) and Mn(salen) to understand how metal identity influences reactivity and enantioselectivity. Similar to Ni(salen), the Co(salen) complex exhibited a redox feature corresponding to the Co^{II}(salen)/[Co^{I}(salen)]$^{-}$ couple ($E_{1/2}$ = –1.46 V) (**Figure 17a**). In contrast, reduction of Mn(salen) is observed only at significantly more negative potentials, with an onset at −2.4 V (**Figure 17b**). Consequently, under an applied potential of −1.9 V, both Ni- and Co-salen are expected to access their reduced M(I) states, whereas Mn(salen) remains in its higher oxidation state.

These observations suggest that access to a reduced metal center is important for reactivity under the reaction conditions, potentially enabling interaction with CO_2 and entry into the catalytic cycle. Consistent with this interpretation, since Mn(salen) is not reduced at the operating potential, it exhibits poor enantioselectivity. As a control, we performed the reaction with a redox-inactive Al(salen) complex, which showed no meaningful impact on enantioselectivity. Together, these results support a model in which electrochemical activation of the metal salen complex is required for it to participate in the reaction and exert stereocontrol.

5.3.3 Mechanistic Interpretations

Based on the observed potential dependence and CV data, a similar mechanistic pathway is proposed for both Ni(salen) and Co(salen) catalysts, with the Ni(salen) system shown as a representative example (**Scheme 4**). From CV analysis, it is suggested that Ni^{II}(salen) first undergoes a one-electron transfer step to generate the active $[Ni^{I}(salen)]^{-}$ species. This species is proposed to engage with CO_2, forming a $[Ni^{I}(salen)–CO_2]^{-}$ intermediate.

Notably, for both Ni(salen) and Co(salen), no product formation is observed at potentials more positive than −1.8 V, despite their distinct reduction onsets at −1.7 V and −1.35 V, respectively. Since the reduction of benzaldehyde also has an onset potential of approximately −1.7 V, these observations suggest that, in addition to activation of the metal salen catalyst, reduction of benzaldehyde is also required for product formation. Accordingly, we propose that the $[Ni^{I}(salen)–CO_2]^{-}$ intermediate intercepts the benzaldehyde-derived ketyl radical to form the carboxylated product, with the chiral metal complex governing the stereochemical outcome of this bond-forming step. The corresponding carboxylic acid is obtained following an acid workup step.

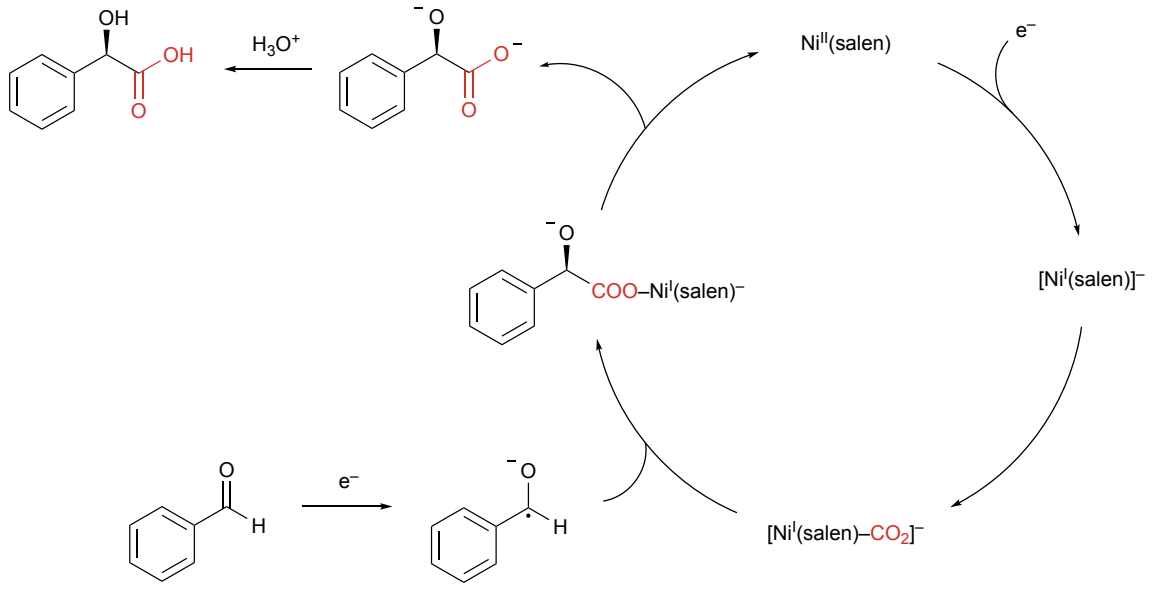

Scheme 4. Proposed mechanism for the enantioselective electrochemical carboxylation of benzaldehyde catalyzed by a chiral Ni(salen) complex.

5.4 CONCLUSIONS

This work investigated asymmetric electrochemical carboxylation of benzaldehyde using metal salen catalysts. It was found that the metal center identity has a significant effect on enantioselectivity, with a Ni-salen complex delivering in the highest e.e. of 43%. Cyclic voltammetry suggests that the best performing catalysts first undergo a reductive activation step under optimized reaction conditions. Formation of the active metal salen species is proposed to enable engagement with CO_2 and subsequent enantioselective coupling with the benzaldehyde-derived ketyl radical.

Looking forward, the insights into the asymmetric electrocarboxylation mechanism established in this work will inform future strategies to enhance enantioselectivity. Specifically, these insights can guide future studies to better understand how tuning the electronics of the metal salen complex through rational ligand design can further improve performance. Additionally, understanding the effect of sterics on the enantioselective is of continued interest. Beyond this system, these results expand the mechanistic understanding of asymmetric electrochemical carboxylation more broadly, providing a foundation for further development of other reactions involving electrochemical CO_2 incorporation.

Chapter 6

CONCLUSIONS AND OUTLOOK

6.1 CONCLUSIONS

This thesis focused on expanding both the scope and fundamental mechanistic understanding of the electrochemical carboxylation of aldehydes, a substrate class that remains underexplored relative to organic halides and olefins. Through a combination of catalyst screening, spectroscopic characterization, kinetic analysis, and asymmetric catalysis, this work has established new insights into how reaction conditions and catalyst identity govern selectivity and efficiency. Overall, this work advances the broader goal of developing electrochemical carboxylation as a practical and sustainable platform for the synthesis of value-added carboxylic acids.

A central theme throughout this work is the use of mechanistic insight to rationalize and improve reaction selectivity. For aromatic aldehydes, electroanalytical and spectroscopic studies support a mechanism in which a substrate-derived ketyl radical is generated at the cathode and couples with CO_2 to form the α-hydroxy carboxylic acid product. EPR spectroscopy provided direct evidence for ketyl radical formation under optimized reaction conditions, and electrokinetic studies identified the coupling step as rate-determining. These findings also highlighted the importance of Lewis acidic additives such as $MgCl_2$, which stabilize the ketyl radical intermediate and promote productive CO_2 coupling.

Extending the substrate scope from aromatic to aliphatic aldehydes revealed additional mechanistic complexity. The more negative reduction potentials of aliphatic aldehydes mean that CO_2 reduction becomes operative alongside substrate reduction, potentially contributing an additional pathway to the carboxylation product. However, aliphatic aldehydes were found to undergo polymerization under the reductive conditions of the reaction, introducing a competing decomposition pathway that substantially lowers FE. These observations highlight that improving selectivity in aliphatic aldehyde carboxylation will require strategies

to suppress anionic polymerization initiation alongside careful tuning of electrode and solvent identity.

Building on the mechanistic picture established for aldehyde electrochemical carboxylation, this thesis also demonstrated for the first time that enantioselective electrochemical carboxylation of an aldehyde is achievable. Using chiral metal salen complexes as homogeneous catalysts, optically active mandelic acid was obtained from benzaldehyde with up to 43% enantiomeric excess. Cyclic voltammetry revealed that the most effective catalysts, Ni(salen) and Co(salen), undergo reductive activation to their M^{I} states under the operating potential, enabling coordination with CO_2 and enantioselective coupling with the benzaldehyde-derived ketyl radical. In contrast, Mn(salen), which is not reduced at the same potential, showed negligible stereocontrol, and a redox-inactive Al(salen) control supports the conclusion that electrochemical activation is a needed for enantioselectivity. The applied potential was also found to influence stereoselectivity, with more negative potentials eroding enantioselectivity, possibly due to the onset of competing non-selective pathways.

Taken together, this body of work advances the fundamental understanding of electrochemical carboxylation and establishes new synthetic capabilities for aldehyde substrates. The mechanistic insights developed here provide a concrete framework for guiding future improvements in selectivity, efficiency, and stereochemical control in electrochemical CO_2 incorporation.

6.2 OUTLOOK

Despite the progress described in this thesis, several important challenges and opportunities remain. The following future research directions are proposed to build upon these findings and advance the field of electrochemical carboxylation.

Suppression of aldehyde polymerization in aliphatic aldehyde carboxylation. One of the central challenges identified in Chapter 4 is the competitive polymerization of aliphatic aldehydes under the reductive electrochemical conditions. A deeper understanding of the polymerization initiation mechanism, such as whether it is triggered by electrochemically

generated anionic intermediates, would be valuable for developing effective mitigation strategies. The goal would be to increase the carboxylation Faradaic efficiency for aliphatic substrates beyond the current maximum of approximately 18%, making this chemistry synthetically useful for a broader range of aliphatic α-hydroxy acids.

Mechanistic origins of electrode selectivity in aromatic versus aliphatic aldehydes. A striking and unexplained observation in this thesis is that tin is the optimal electrode for the carboxylation of aromatic aldehydes (Chapter 3), while copper performs best for aliphatic substrates (Chapter 4). This divergence suggests that the electrode plays a substrate-dependent role in stabilizing key intermediates, pointing to mechanistic differences between aromatic and aliphatic aldehyde carboxylation. Future work should employ in situ and operando spectroscopic techniques, such as surface-enhanced Raman spectroscopy (SERS) or attenuated total reflectance infrared (ATR-IR) spectroscopy, to characterize adsorbed intermediates on tin and copper surfaces during carboxylation. Complementary density functional theory (DFT) calculations could help elucidate how the binding energy and geometry of aldehyde-derived intermediates vary with electrode identity and substrate structure. Developing this mechanistic picture would provide guiding principles for identifying or designing optimal electrode materials for new substrate classes.

Improving enantioselectivity through rational ligand design. The proof-of-concept asymmetric electrochemical carboxylation results in Chapter 5 demonstrate that chiral metal salen complexes can impart meaningful stereocontrol, but the enantioselectivities achieved (up to 43% e.e.) are not yet at the level need for practical synthetic applications. Several strategies could be pursued to improve enantioselectivity. First, the electronic properties of the salen ligand can be systematically tuned through substitution at the phenol rings or imine backbone to modulate the reduction potential of the metal center and the binding geometry of the activated CO_2 species. Second, increasing the steric demand of the chiral diamine backbone could enforce a more defined chiral environment around the metal center and improve selectivity in the key C–C bond forming step. Beyond the salen scaffold, other classes of privileged chiral ligands, including BINAP-based systems and chiral N-

heterocyclic carbene (NHC) complexes, could be examined to identify platforms offering superior stereocontrol in electrochemical environments.

Development of heterogeneous asymmetric electrocatalysts. The homogeneous metal salen catalysts employed in Chapter 5, while effective for mechanistic studies, present practical challenges related to catalyst recovery and separation. The development of heterogeneous asymmetric electrocatalysts would dramatically improve the practical applicability of this chemistry. Strategies that can be explored include immobilization of chiral metal complexes on electrode surfaces via covalent tethering or incorporation into metal-organic frameworks (MOFs). A key challenge in this endeavor is preserving the enantioselectivity of the chiral catalyst after surface immobilization. Nonetheless, achieving a recyclable, surface-bound asymmetric electrochemical carboxylation catalyst would represent a significant milestone for the field and bring this technology closer to industrial relevance.

Scale-up and flow electrochemistry. All of the electrochemical carboxylation experiments described in this thesis were conducted in batch reactors at the milligram scale. Transitioning to continuous flow electrochemistry would offer significant advantages in terms of mass transport, scalability, and process control. However, implementing flow electrocarboxylation requires addressing challenges specific to this chemistry, including the tendency of certain electrode materials to passivate over time, the use of sacrificial anodes, and compatibility of the electrolyte with flow cell materials. Future work should explore the design of flow electrocarboxylation cells optimized for aldehyde substrates, with particular attention to mass transport of CO_2 and stability of the working electrode over extended operation.

In summary, the electrochemical carboxylation of aldehydes with CO_2 is a promising and mechanistically distinctive platform for sustainable carboxylic acid synthesis. This thesis has uncovered key principles governing selectivity in both aromatic and aliphatic aldehyde systems, provided spectroscopic evidence for critical radical intermediates, and demonstrated for the first time that enantioselective carboxylation of aldehydes is achievable under electrochemical conditions. The mechanistic insights and design principles established

here lay a strong foundation for future work aimed at improving efficiency, broadening substrate scope, and ultimately realizing the industrial potential of electrochemical CO_2 utilization in organic synthesis.

C h a p t e r 7

REFERENCES

(1) Liu, Q.; Wu, L.; Jackstell, R.; Beller, M. Using Carbon Dioxide as a Building Block in Organic Synthesis. *Nat. Commun.* **2015**, *6* (1), 5933. https://doi.org/10.1038/ncomms6933.

(2) *Carbon Dioxide as Chemical Feedstock*; Aresta, M., Ed.; Wiley-VCH: Zurich, 2010.

(3) Davies, J.; Lyonnet, J. R.; Zimin, D. P.; Martin, R. The Road to Industrialization of Fine Chemical Carboxylation Reactions. *Chem*. Elsevier Inc. November 11, 2021, pp 2927–2942. https://doi.org/10.1016/j.chempr.2021.10.016.

(4) Lamberth, C.; Dinges, J. Different Roles of Carboxylic Functions in Pharmaceuticals and Agrochemicals. In *Bioactive Carboxylic Compound Classes: Pharmaceuticals and Agrochemicals*; Wiley-VCH Verlag GmbH & Co. KGaA: Weinheim, Germany, 2016; pp 1–11. https://doi.org/10.1002/9783527693931.ch1.

(5) Maag, H. Prodrugs of Carboxylic Acids. In *Prodrugs: Challenges and Rewards*; Springer: New York, 2007.

(6) Schmitt, R. Beitrag Zur Kenntniss Der Kolbe'schen Salicylsäure Synthese. *Journal für Praktische Chemie* **1885**, *31* (1), 397–411. https://doi.org/10.1002/prac.18850310130.

(7) Kolbe, H. Ueber Synthese Der Salicylsäure. *Annalen der Chemie und Pharmacie* **1860**, *113* (1), 125–127. https://doi.org/10.1002/jlac.18601130120.

(8) Correa, A.; Martín, R. Metal-Catalyzed Carboxylation of Organometallic Reagents with Carbon Dioxide. *Angew. Chem. Int. Ed.* **2009**, *48* (34), 6201–6204. https://doi.org/10.1002/anie.200900667.

(9) Matthessen, R.; Fransaer, J.; Binnemans, K.; De Vos, D. E. Electrocarboxylation: Towards Sustainable and Efficient Synthesis of Valuable Carboxylic Acids. *Beilstein Journal of Organic Chemistry* **2014**, *10*, 2484–2500. https://doi.org/10.3762/bjoc.10.260.

(10) Ton, T. N.; Baker, R. J.; Manthiram, K. Recent Progress in the Development of Electrode Materials for Electrochemical Carboxylation with CO2. *J. Catal.* **2024**, *432*, 115371. https://doi.org/10.1016/j.jcat.2024.115371.

(11) Silvestri, G.; Gambino, S.; Filardo, G.; Gulotta, A. Sacrificial Anodes in the Electrocarboxylation of Organic Chlorides. *Angewandte Chemie International Edition in English* **1984**, *23* (12), 979–980. https://doi.org/10.1002/anie.198409791.

(12) Loveland, J. Electrolytic Production of Acyclic Carboxylic Acids from Hydrocarbons, 1962.

(13) Rondinini, S. Electrocatalytic Potentialities of Silver as a Cathode for Organic Halide Reductions. *Electrochem. commun.* **2000**, *2* (7), 491–496. https://doi.org/10.1016/S1388-2481(00)00065-5.

(14) Sock, O.; Troupel, M.; Perichon, J. Electrosynthesis of Carboxylic Acids from Organic Halides and Carbon Dioxide. *Tetrahedron Lett.* **1985**, *26* (12), 1509–1512. https://doi.org/10.1016/S0040-4039(00)98538-1.

(15) Niu, D.-F.; Xiao, L.-P.; Zhang, A.-J.; Zhang, G.-R.; Tan, Q.-Y.; Lu, J.-X. Electrocatalytic Carboxylation of Aliphatic Halides at Silver Cathode in Acetonitrile. *Tetrahedron* **2008**, *64* (46), 10517–10520. https://doi.org/10.1016/j.tet.2008.08.093.

(16) León, T.; Correa, A.; Martin, R. Ni-Catalyzed Direct Carboxylation of Benzyl Halides with CO $_2$. *J. Am. Chem. Soc.* **2013**, *135* (4), 1221–1224. https://doi.org/10.1021/ja311045f.

(17) Wang, H.; Lin, M.; Fang, H.; Chen, T.; Lu, J. Electrochemical Dicarboxylation of Styrene: Synthesis of 2-Phenylsuccinic Acid. *Chin. J. Chem.* **2007**, *25* (7), 913–916. https://doi.org/10.1002/cjoc.200790177.

(18) Gambino, S.; Gennaro, A.; Filardo, G.; Silvestri, G.; Vianello, E. Electrochemical Carboxylation of Styrene. *J. Electrochem. Soc.* **1987**, *134* (9), 2172–2175. https://doi.org/10.1149/1.2100846.

(19) Kim, Y.; Park, G. Do; Balamurugan, M.; Seo, J.; Min, B. K.; Nam, K. T. Electrochemical B-Selective Hydrocarboxylation of Styrene Using CO $_2$ and Water. *Advanced Science* **2020**, *7* (3). https://doi.org/10.1002/advs.201900137.

(20) Quan, Y.; Yu, R.; Zhu, J.; Guan, A.; Lv, X.; Yang, C.; Li, S.; Wu, J.; Zheng, G. Efficient Carboxylation of Styrene and Carbon Dioxide by Single-Atomic Copper Electrocatalyst. *J. Colloid Interface Sci.* **2021**, *601*, 378–384. https://doi.org/10.1016/j.jcis.2021.05.105.

(21) Bazzi, S.; Hu, L.; Schulz, E.; Mellah, M. Electrogenerated Sm(II)-Catalyzed Carbon Dioxide Reduction for β-Hydrocarboxylation of Styrenes. *Organometallics* **2023**, *42* (12), 1425–1431. https://doi.org/10.1021/acs.organomet.3c00076.

(22) Greenhalgh, M. D.; Thomas, S. P. Iron-Catalyzed, Highly Regioselective Synthesis of α-Aryl Carboxylic Acids from Styrene Derivatives and CO $_2$. *J. Am. Chem. Soc.* **2012**, *134* (29), 11900–11903. https://doi.org/10.1021/ja3045053.

(23) Silvestri, G.; Gambino, S.; Filardo, G. Electrochemical Carboxylation of Aldehydes and Ketones with Sacrificial Aluminum Anodes. *Tetrahedron Lett.* **1986**, *27* (29), 3429–3430. https://doi.org/10.1016/S0040-4039(00)84814-5.

(24) Scialdone, O.; Amatore, C.; Galia, A.; Filardo, G. CO2 as a C1-Organic Building Block: Electrocarboxylation of Aromatic Ketones. A Quantitative Study of the Effect of the Concentration of Substrate and of Carbon Dioxide on the Selectivity of the Process. *Journal of Electroanalytical Chemistry* **2006**, *592* (2), 163–174. https://doi.org/10.1016/j.jelechem.2006.04.009.

(25) Feng, Q.; Huang, K.; Liu, S.; Yu, J.; Liu, F. Electrocatalytic Carboxylation of Aromatic Ketones with Carbon Dioxide in Ionic Liquid 1-Butyl-3-

Methylimidazoliumtetrafluoborate to α-Hydroxy-Carboxylic Acid Methyl Ester. *Electrochim. Acta* **2011**, *56* (14), 5137–5141. https://doi.org/10.1016/j.electacta.2011.03.061.

(26) *Chemicals*. https://www.iea.org/energy-system/industry/chemicals (accessed 2023-09-04).

(27) August, G. Process for the Manufacture of Urea, 1958.

(28) KRASE, N. W.; GADDY, V. L. Synthesis of Urea from Ammonia and Carbon Dioxide. *Journal of Industrial & Engineering Chemistry* **1922**, *14* (7), 611–615. https://doi.org/10.1021/ie50151a009.

(29) Ebert, G. W.; Juda, W. L.; Kosakowski, R. H.; Ma, B.; Dong, L.; Cummings, K. E.; Phelps, M. V. B.; Mostafa, A. E.; Luo, J. Carboxylation and Esterification of Functionalized Arylcopper Reagents. *J. Org. Chem.* **2005**, *70* (11), 4314–4317. https://doi.org/10.1021/jo047731s.

(30) Cao, G.-M.; Hu, X.-L.; Liao, L.-L.; Yan, S.-S.; Song, L.; Chruma, J. J.; Gong, L.; Yu, D.-G. Visible-Light Photoredox-Catalyzed Umpolung Carboxylation of Carbonyl Compounds with CO2. *Nat. Commun.* **2021**, *12* (1), 3306. https://doi.org/10.1038/s41467-021-23447-8.

(31) Song, L.; Wang, W.; Yue, J.-P.; Jiang, Y.-X.; Wei, M.-K.; Zhang, H.-P.; Yan, S.-S.; Liao, L.-L.; Yu, D.-G. Visible-Light Photocatalytic Di- and Hydro-Carboxylation of Unactivated Alkenes with CO2. *Nat. Catal.* **2022**, *5* (9), 832–838. https://doi.org/10.1038/s41929-022-00841-z.

(32) Corbin, N.; Yang, D.-T.; Lazouski, N.; Steinberg, K.; Manthiram, K. Suppressing Carboxylate Nucleophilicity with Inorganic Salts Enables Selective Electrocarboxylation without Sacrificial Anodes. *Chem. Sci.* **2021**, *12* (37), 12365–12376. https://doi.org/10.1039/D1SC02413B.

(33) Yang, D.-T.; Zhu, M.; Schiffer, Z. J.; Williams, K.; Song, X.; Liu, X.; Manthiram, K. Direct Electrochemical Carboxylation of Benzylic C–N Bonds with Carbon Dioxide. *ACS Catal.* **2019**, *9* (5), 4699–4705. https://doi.org/10.1021/acscatal.9b00818.

(34) Schiffer, Z. J.; Limaye, A. M.; Manthiram, K. Thermodynamic Discrimination between Energy Sources for Chemical Reactions. *Joule* **2021**, *5* (1), 135–148. https://doi.org/10.1016/j.joule.2020.12.014.

(35) Kortlever, R.; Shen, J.; Schouten, K. J. P.; Calle-Vallejo, F.; Koper, M. T. M. Catalysts and Reaction Pathways for the Electrochemical Reduction of Carbon Dioxide. *J. Phys. Chem. Lett.* **2015**, *6* (20), 4073–4082. https://doi.org/10.1021/acs.jpclett.5b01559.

(36) Zhang, X.; Guo, S.-X.; Gandionco, K. A.; Bond, A. M.; Zhang, J. Electrocatalytic Carbon Dioxide Reduction: From Fundamental Principles to Catalyst Design. *Mater. Today Adv.* **2020**, *7*, 100074. https://doi.org/10.1016/j.mtadv.2020.100074.

(37) Boutin, E.; Robert, M. Molecular Electrochemical Reduction of CO2 beyond Two Electrons. *Trends Chem.* **2021**, *3* (5), 359–372. https://doi.org/10.1016/j.trechm.2021.02.003.

(38) Liang, H.; Beweries, T.; Francke, R.; Beller, M. Molecular Catalysts for the Reductive Homocoupling of CO_2 towards C_{2+} Compounds. *Angewandte Chemie* **2022**, *134* (19). https://doi.org/10.1002/ange.202200723.

(39) Somerville, R. J.; Martin, R. Relevance of <scp>Ni</Scp> (<scp>I</Scp>) in Catalytic Carboxylation Reactions. In *Nickel Catalysis in Organic Synthesis*; Wiley, 2020; pp 285–330. https://doi.org/10.1002/9783527813827.ch12.

(40) Rajagopal, V.; Manivel, P.; Nesakumar, N.; Kathiresan, M.; Velayutham, D.; Suryanarayanan, V. Ag_x Cu_y Ni_z Trimetallic Alloy Catalysts for the Electrocatalytic Reduction of Benzyl Bromide in the Presence of Carbon Dioxide. *ACS Omega* **2018**, *3* (12), 17125–17134. https://doi.org/10.1021/acsomega.8b02715.

(41) Yimin, D.; Lanli, N.; Hui, L.; Jiaqi, Z.; Linping, Y.; Qiuju, F. Cu-Ni Alloy Catalyzed Electrochemical Carboxylation of Benzyl Bromide with Carbon Dioxide in Ionic Liquid 1-Butyl-3-Methylimidazolium Tetrafluoroborate. *Int. J. Electrochem. Sci.* **2018**, *13* (1), 1084–1095. https://doi.org/10.20964/2018.01.85.

(42) Boro, B.; Kalita, P.; Vijayaprabhakaran, A.; Dao, D. Q.; Nandy, S.; Chae, K. H.; Nailwal, Y.; Kathiresan, M.; Mondal, J. Discrete Cu-Metalloporous Polycarbazole as a Nanoelectromediator for Effective Electrocarboxylation of Benzyl Bromide with CO_2. *ACS Appl. Nano Mater.* **2023**, *6* (13), 11788–11801. https://doi.org/10.1021/acsanm.3c01721.

(43) Sun, G.-Q.; Zhang, W.; Liao, L.-L.; Li, L.; Nie, Z.-H.; Wu, J.-G.; Zhang, Z.; Yu, D.-G. Nickel-Catalyzed Electrochemical Carboxylation of Unactivated Aryl and Alkyl Halides with CO2. *Nat. Commun.* **2021**, *12* (1), 7086. https://doi.org/10.1038/s41467-021-27437-8.

(44) Wang, Y.; Zhao, Z.; Pan, D.; Wang, S.; Jia, K.; Ma, D.; Yang, G.; Xue, X.; Qiu, Y. Metal-Free Electrochemical Carboxylation of Organic Halides in the Presence of Catalytic Amounts of an Organomediator. *Angew. Chem. Int. Ed.* **2022**, *61* (41). https://doi.org/10.1002/anie.202210201.

(45) Guan, A.; Quan, Y.; Chen, Y.; Liu, Z.; Zhang, J.; Kan, M.; Zhang, Q.; Huang, H.; Qian, L.; Zhang, L.; Zheng, G. Efficient CO2 Fixation with Acetophenone on Ag-CeO2 Electrocatalyst by a Double Activation Strategy. *Chinese Journal of Catalysis* **2022**, *43* (12), 3134–3141. https://doi.org/10.1016/S1872-2067(22)64116-0.

(46) Jones, J.; Prakash, G. K. S.; Olah, G. A. Electrochemical CO_2 Reduction: Recent Advances and Current Trends. *Isr. J. Chem.* **2014**, *54* (10), 1451–1466. https://doi.org/10.1002/ijch.201400081.

(47) Zhao, S.; Jin, R.; Jin, R. Opportunities and Challenges in CO_2 Reduction by Gold- and Silver-Based Electrocatalysts: From Bulk Metals to Nanoparticles and Atomically Precise Nanoclusters. *ACS Energy Lett.* **2018**, *3* (2), 452–462. https://doi.org/10.1021/acsenergylett.7b01104.

(48) Yuan, G.-Q.; Jiang, H.-F.; Lin, C.; Liao, S.-J. Efficient Electrochemical Synthesis of 2-Arylsuccinic Acids from CO2 and Aryl-Substituted Alkenes

with Nickel as the Cathode. *Electrochim. Acta* **2008**, *53* (5), 2170–2176. https://doi.org/10.1016/j.electacta.2007.09.023.

(49) Birdja, Y. Y.; Pérez-Gallent, E.; Figueiredo, M. C.; Göttle, A. J.; Calle-Vallejo, F.; Koper, M. T. M. Advances and Challenges in Understanding the Electrocatalytic Conversion of Carbon Dioxide to Fuels. *Nat. Energy* **2019**, *4* (9), 732–745. https://doi.org/10.1038/s41560-019-0450-y.

(50) Liu, S.; Yang, H. Bin; Hung, S.; Ding, J.; Cai, W.; Liu, L.; Gao, J.; Li, X.; Ren, X.; Kuang, Z.; Huang, Y.; Zhang, T.; Liu, B. Elucidating the Electrocatalytic CO_2 Reduction Reaction over a Model Single-Atom Nickel Catalyst. *Angew. Chem. Int. Ed.* **2020**, *59* (2), 798–803. https://doi.org/10.1002/anie.201911995.

(51) Yang, H. Bin; Hung, S.-F.; Liu, S.; Yuan, K.; Miao, S.; Zhang, L.; Huang, X.; Wang, H.-Y.; Cai, W.; Chen, R.; Gao, J.; Yang, X.; Chen, W.; Huang, Y.; Chen, H. M.; Li, C. M.; Zhang, T.; Liu, B. Atomically Dispersed Ni(i) as the Active Site for Electrochemical CO2 Reduction. *Nat. Energy* **2018**, *3* (2), 140–147. https://doi.org/10.1038/s41560-017-0078-8.

(52) You, Y.; Kanna, W.; Takano, H.; Hayashi, H.; Maeda, S.; Mita, T. Electrochemical Dearomative Dicarboxylation of Heterocycles with Highly Negative Reduction Potentials. *J. Am. Chem. Soc.* **2022**, *144* (8), 3685–3695. https://doi.org/10.1021/jacs.1c13032.

(53) Reductive Coupling. In *Organic Electrochemistry. Revised and Expanded*; Hammerich, O., Speiser, B., Eds.; CRC Press, 2015; pp 654–660.

(54) León, T.; Correa, A.; Martin, R. Ni-Catalyzed Direct Carboxylation of Benzyl Halides with CO_2. *J. Am. Chem. Soc.* **2013**, *135* (4), 1221–1224. https://doi.org/10.1021/ja311045f.

(55) Bazzi, S.; Schulz, E.; Mellah, M. Electrogenerated Sm(II)-Catalyzed CO_2 Activation for Carboxylation of Benzyl Halides. *Org. Lett.* **2019**, *21* (24), 10033–10037. https://doi.org/10.1021/acs.orglett.9b03927.

(56) Cao, Y.; Li, D.; Ding, C.; Ye, S.; Zhang, X.; Chi, H.; Liu, L.; Liu, Y.; Xiao, J.; Li, C. CO_2 Fixation with Aryl Bromide toward Carboxylic Acid Enabled by Bifunctional CuAg Electrocatalysts. *ACS Catal.* **2023**, 11902–11909. https://doi.org/10.1021/acscatal.3c02791.

(57) Seo, H.; Liu, A.; Jamison, T. F. Direct β-Selective Hydrocarboxylation of Styrenes with CO_2 Enabled by Continuous Flow Photoredox Catalysis. *J. Am. Chem. Soc.* **2017**, *139* (40), 13969–13972. https://doi.org/10.1021/jacs.7b05942.

(58) Yatham, V. R.; Shen, Y.; Martin, R. Catalytic Intermolecular Dicarbofunctionalization of Styrenes with CO_2 and Radical Precursors. *Angew. Chem. Int. Ed.* **2017**, *56* (36), 10915–10919. https://doi.org/10.1002/anie.201706263.

(59) Williams, C. M.; Johnson, J. B.; Rovis, T. Nickel-Catalyzed Reductive Carboxylation of Styrenes Using CO_2. *J. Am. Chem. Soc.* **2008**, *130* (45), 14936–14937. https://doi.org/10.1021/ja8062925.

(60) Shao, P.; Wang, S.; Chen, C.; Xi, C. Cp $_2$ TiCl $_2$ -Catalyzed Regioselective Hydrocarboxylation of Alkenes with CO $_2$. *Org. Lett.* **2016**, *18* (9), 2050–2053. https://doi.org/10.1021/acs.orglett.6b00665.

(61) Tummanapalli, S.; Gulipalli, K. C.; Endoori, S.; Bodige, S.; Kumar Pommidi, A.; Medaboina, S.; Rejinthala, S.; Choppadandi, S.; Boya, R.; Kanuka, A.; Valluri, M. A Highly Regio- and Stereoselective Pd-Catalyzed Electrocarboxylation of Baylis-Hillman Acetates: An Interesting Switchable Regioselectivity Based on Electrode Material. *Tetrahedron Lett.* **2022**, *104*, 154022. https://doi.org/10.1016/j.tetlet.2022.154022.

(62) Baiker, A. Crucial Aspects in the Design of Chirally Modified Noble Metal Catalysts for Asymmetric Hydrogenation of Activated Ketones. *Chem. Soc. Rev.* **2015**, *44* (21), 7449–7464. https://doi.org/10.1039/C4CS00462K.

(63) Chen, B.-L.; Zhu, H.-W.; Xiao, Y.; Sun, Q.-L.; Wang, H.; Lu, J.-X. Asymmetric Electrocarboxylation of 1-Phenylethyl Chloride Catalyzed by Electrogenerated Chiral [CoI(Salen)]− Complex. *Electrochem. commun.* **2014**, *42*, 55–59. https://doi.org/10.1016/j.elecom.2014.02.009.

(64) Yang, H.-P.; Yue, Y.-N.; Sun, Q.-L.; Feng, Q.; Wang, H.; Lu, J.-X. Entrapment of a Chiral Cobalt Complex within Silver: A Novel Heterogeneous Catalyst for Asymmetric Carboxylation of Benzyl Bromides with CO $_2$. *Chemical Communications* **2015**, *51* (61), 12216–12219. https://doi.org/10.1039/C5CC04554A.

(65) Yang, L.-R.; Zhang, J.-J.; Zhao, Y.-J.; Wang, Z.-L.; Wang, H.; Lu, J.-X. La1−xSrxFeO3 Perovskite Electrocatalysts for Asymmetric Electrocarboxylation of Acetophenone with CO2. *Electrochim. Acta* **2021**, *398*, 139308. https://doi.org/10.1016/j.electacta.2021.139308.

(66) Yang, L.-R.; Zhao, Y.-J.; Jiang, C.-J.; Xiong, R.; Wang, H.; Lu, J.-X. Perovskite La0.7Sr0.3Fe0.8B0.2O3 (B = Ti, Mn, Co, Ni, and Cu) as Heterogeneous Electrocatalysts for Asymmetric Electrocarboxylation of Aromatic Ketones. *J. Catal.* **2021**, *401*, 224–233. https://doi.org/10.1016/j.jcat.2021.08.001.

(67) Zhao, Y.-J.; Yang, L.-R.; Wang, L.-T.; Wang, Y.; Lu, J.-X.; Wang, H. Asymmetric Electrocarboxylation of 4′-Methylacetophenone over PrCoO $_3$ Perovskites. *Catal. Sci. Technol.* **2022**, *12* (9), 2887–2893. https://doi.org/10.1039/D2CY00116K.

(68) Xiong, R.; Wang, Y.; Zhu, J.; Li, M.; Lu, J.; Wang, H. Chiral Metal Salen Complexes as Chiral Electrocatalysts for Asymmetric Electrochemical Carboxylation of Acetophenone. *ChemistrySelect* **2023**, *8* (29). https://doi.org/10.1002/slct.202301126.

(69) Medvedev, J. J.; Medvedeva, X. V.; Li, F.; Zienchuk, T. A.; Klinkova, A. Electrochemical CO $_2$ Fixation to α-Methylbenzyl Bromide in Divided Cells with Nonsacrificial Anodes and Aqueous Anolytes. *ACS Sustain. Chem. Eng.* **2019**, *7* (24), 19631–19639. https://doi.org/10.1021/acssuschemeng.9b04647.

(70) Muchez, L.; De Vos, D. E.; Kim, M. Sacrificial Anode-Free Electrosynthesis of α-Hydroxy Acids via Electrocatalytic Coupling of Carbon Dioxide to

Aromatic Alcohols. *ACS Sustain. Chem. Eng.* **2019**, *7* (19), 15860–15864. https://doi.org/10.1021/acssuschemeng.9b04612.

(71) Zhang, X.; Li, Z.; Chen, H.; Shen, C.; Wu, H.; Dong, K. Pairing Electrocarboxylation of Unsaturated Bonds with Oxidative Transformation of Alcohol and Amine. *ChemSusChem* **2023**. https://doi.org/10.1002/cssc.202300807.

(72) *Alpha Hydroxy Acid Global Market Report 2025*. The Business Research Company. https://www.thebusinessresearchcompany.com/report/alpha-hydroxy-acid-global-market-report (accessed 2025-02-19).

(73) Benninga, H. A History of Lactic Acid Making: A Chapter in the History of Biotechnology; Springer Dordrecht, 1990; Vol. 11.

(74) Ritzer, E.; Sundermann, R. Hydroxycarboxylic Acids, Aromatic. In *Ullmann's Encyclopedia of Industrial Chemistry*; Wiley, 2000. https://doi.org/10.1002/14356007.a13_519.

(75) Deng, W.; Zhang, P.; Qiao, Y.; Kastlunger, G.; Govindarajan, N.; Xu, A.; Chorkendorff, I.; Seger, B.; Gong, J. Unraveling the Rate-Determining Step of C2+ Products during Electrochemical CO Reduction. *Nat. Commun.* **2024**, *15* (1), 892. https://doi.org/10.1038/s41467-024-45230-1.

(76) Zhang, G.; Zhao, Z.-J.; Cheng, D.; Li, H.; Yu, J.; Wang, Q.; Gao, H.; Guo, J.; Wang, H.; Ozin, G. A.; Wang, T.; Gong, J. Efficient CO2 Electroreduction on Facet-Selective Copper Films with High Conversion Rate. *Nat. Commun.* **2021**, *12* (1), 5745. https://doi.org/10.1038/s41467-021-26053-w.

(77) Liu, X.-F.; Zhang, K.; Tao, L.; Lu, X.-B.; Zhang, W.-Z. Recent Advances in Electrochemical Carboxylation Reactions Using Carbon Dioxide. *Green Chemical Engineering* **2022**, *3* (2), 125–137. https://doi.org/10.1016/j.gce.2021.12.001.

(78) Senboku, H.; Katayama, A. Electrochemical Carboxylation with Carbon Dioxide. *Curr. Opin. Green Sustain. Chem.* **2017**, *3*, 50–54. https://doi.org/10.1016/j.cogsc.2016.10.003.

(79) Ton, T. N.; Baker, R. J.; Manthiram, K. Recent Progress in the Development of Electrode Materials for Electrochemical Carboxylation with CO2. *J. Catal.* **2024**, *432*, 115371. https://doi.org/10.1016/J.JCAT.2024.115371.

(80) Seidler, J.; Roth, A.; Vieira, L.; Waldvogel, S. R. Electrochemical CO_2 Utilization for the Synthesis of α-Hydroxy Acids. *ACS Sustain. Chem. Eng.* **2023**, *11* (1), 390–398. https://doi.org/10.1021/acssuschemeng.2c06046.

(81) Singh, K.; Sohal, H. S.; Singh, B. Synthesis of α-Hydroxycarboxylic Acids from Various Aldehydes and Ketones by Direct Electrocarboxylation: A Facile, Efficient and Atom Economy Protocol. *Asian Journal of Chemistry* **2021**, *33* (4), 839–845. https://doi.org/10.14233/ajchem.2021.23090.

(82) Liu, X.; Sun, L.; Deng, W. Q. Theoretical Investigation of CO2 Adsorption and Dissociation on Low Index Surfaces of Transition Metals. *Journal of Physical Chemistry C* **2018**, *122* (15), 8306–8314. https://doi.org/https://doi.org/10.1021/acs.jpcc.7b12660.

(83) Lamm, V.; Pan, X.; Taniguchi, T.; Curran, D. P. Reductions of Aldehydes and Ketones with a Readily Available N-Heterocyclic Carbene Borane and Acetic

Acid. *Beilstein Journal of Organic Chemistry 9:76* **2013**, *9* (1), 675–680. https://doi.org/10.3762/BJOC.9.76.

(84) Liu, B.; Li, Y.; Liu, Q. Cobalt/Lewis Acid Cooperative Catalysis for Reductive Etherification of Ketones and Aldehydes with Alcohols. *Chem Catalysis* **2022**, *2* (4), 883–897. https://doi.org/10.1016/J.CHECAT.2022.03.001.

(85) Li, J.; Gong, J. *Operando* Characterization Techniques for Electrocatalysis. *Energy Environ. Sci.* **2020**, *13* (11), 3748–3779. https://doi.org/10.1039/D0EE01706J.

(86) Corbin, N.; Junor, G. P.; Ton, T. N.; Baker, R. J.; Manthiram, K. Toward Improving the Selectivity of Organic Halide Electrocarboxylation with Mechanistically Informed Solvent Selection. *J. Am. Chem. Soc.* **2023**, *145* (3), 1740–1748. https://doi.org/10.1021/jacs.2c10561.

(87) Chandrasekaran, M.; Noel, M.; Krishnan, V. Glassy Carbon Surface Effects on the Electroreduction of Aromatic Carbonyl Compounds. *J. Electroanal. Chem. Interfacial Electrochem.* **1991**, *303* (1–2), 185–197. https://doi.org/10.1016/0022-0728(91)85125-9.

(88) Bard, A. J.; Faulkner, L. R. Electrode Reactions with Coupled Homogeneous Chemical Reactions. In *Electrochemical Methods: Fundamentals and Applications*; John Wiley and Sons, Inc., 2001; pp 471–533.

(89) Yu, J.; Zhang, P.; Li, L.; Li, K.; Zhang, G.; Liu, J.; Wang, T.; Zhao, Z. J.; Gong, J. Electroreductive Coupling of Benzaldehyde by Balancing the Formation and Dimerization of the Ketyl Intermediate. *Nat. Commun.* **2022**, *13*, 7909. https://doi.org/10.1038/s41467-022-35463-3.

(90) Stoll, S.; Schweiger, A. EasySpin, a Comprehensive Software Package for Spectral Simulation and Analysis in EPR. *Journal of Magnetic Resonance* **2006**, *178* (1), 42–55. https://doi.org/10.1016/J.JMR.2005.08.013.

(91) Gimat, A.; Kasneryk, V.; Dupont, A. L.; Paris, S.; Averseng, F.; Fournier, J.; Massiani, P.; Rouchon, V. Investigating the DMPO-Formate Spin Trapping Method for the Study of Paper Iron Gall Ink Corrosion. *New Journal of Chemistry* **2016**, *40* (11), 9098–9110. https://doi.org/10.1039/C6NJ01480A.

(92) Yu, R. J.; Van Scott, E. J. Alpha-Hydroxyacids and Carboxylic Acids. *J. Cosmet. Dermatol.* **2004**, *3* (2), 76–87. https://doi.org/10.1111/j.1473-2130.2004.00059.x.

(93) Bhalla, T. C.; Kumar, V.; Bhatia, S. K. Hydroxy Acids: Production and Applications. In *AdvancesinIndustrialBiotechnology*; 2014; pp 56–76.

(94) Kornhauser, A. Applications of Hydroxy Acids: Classification, Mechanisms, and Photoactivity. *Clin. Cosmet. Investig. Dermatol.* **2010**, 135. https://doi.org/10.2147/CCID.S9042.

(95) Starr, J. N.; Westhoff, G. Lactic Acid. In *Ullmann's Encyclopedia of Industrial Chemistry*; Wiley-VCH Verlag GmbH & Co. KGaA: Weinheim, Germany, 2014; pp 1–8. https://doi.org/10.1002/14356007.a15_097.pub3.

(96) Oksanen, V.; Malinen, K.; Wirtanen, T. Synthesis of Aliphatic α-Hydroxy Carboxylic Acids *via* Electrocarboxylation of Aldehydes. *RSC Adv.* **2025**, *15* (53), 45724–45728. https://doi.org/10.1039/D5RA07885G.

(97) Martin, B. Y.; Schutz, L.; Claverie, J. P. Mechanistic Insights on the Anionic Polymerization of Aliphatic Aldehydes. *Macromolecules* **2021**, *54* (19), 9165–9173. https://doi.org/10.1021/acs.macromol.1c01003.

(98) Banerjee, A.; Mitra, A. K. Unlocking the Potential of Mandelic Acid Derivatives: Chemical and Biological Applications – a Comprehensive Review. *RSC Adv.* **2026**, *16* (2), 1509–1545. https://doi.org/10.1039/D5RA07369C.

(99) Zhang, K.; Wang, H.; Zhao, S.-F.; Niu, D.-F.; Lu, J.-X. Asymmetric Electrochemical Carboxylation of Prochiral Acetophenone: An Efficient Route to Optically Active Atrolactic Acid via Selective Fixation of Carbon Dioxide. *Journal of Electroanalytical Chemistry* **2009**, *630* (1–2), 35–41. https://doi.org/10.1016/j.jelechem.2009.02.013.

(100) Zhao, S.-F.; Zhu, M.-X.; Zhang, K.; Wang, H.; Lu, J.-X. Alkaloid Induced Asymmetric Electrocarboxylation of 4-Methylpropiophenone. *Tetrahedron Lett.* **2011**, *52* (21), 2702–2705. https://doi.org/10.1016/j.tetlet.2011.03.076.

(101) Yang, L.-R.; Zhang, J.-J.; Zhao, Y.-J.; Wang, Z.-L.; Wang, H.; Lu, J.-X. La1−xSrxFeO3 Perovskite Electrocatalysts for Asymmetric Electrocarboxylation of Acetophenone with CO2. *Electrochim. Acta* **2021**, *398*, 139308. https://doi.org/10.1016/j.electacta.2021.139308.

(102) Yang, L.-R.; Zhao, Y.-J.; Jiang, C.-J.; Xiong, R.; Wang, H.; Lu, J.-X. Perovskite La0.7Sr0.3Fe0.8B0.2O3 (B = Ti, Mn, Co, Ni, and Cu) as Heterogeneous Electrocatalysts for Asymmetric Electrocarboxylation of Aromatic Ketones. *J. Catal.* **2021**, *401*, 224–233. https://doi.org/10.1016/j.jcat.2021.08.001.

(103) Zhao, Y.-J.; Yang, L.-R.; Wang, L.-T.; Wang, Y.; Lu, J.-X.; Wang, H. Asymmetric Electrocarboxylation of 4′-Methylacetophenone over $PrCoO_3$ Perovskites. *Catal. Sci. Technol.* **2022**, *12* (9), 2887–2893. https://doi.org/10.1039/D2CY00116K.

(104) Xiong, R.; Wang, Y.; Zhu, J.; Li, M.; Lu, J.; Wang, H. Chiral Metal Salen Complexes as Chiral Electrocatalysts for Asymmetric Electrochemical Carboxylation of Acetophenone. *ChemistrySelect* **2023**, *8* (29). https://doi.org/10.1002/slct.202301126.

(105) Cozzi, P. G. Metal–Salen Schiff Base Complexes in Catalysis: Practical Aspects. *Chem. Soc. Rev.* **2004**, *33* (7), 410–421. https://doi.org/10.1039/B307853C.

(106) Ourari, A.; Aggoun, D.; Karce, H. E.; Berenguer, R.; Morallon, E.; Lanez, T.; Ouennoughi, Y. Electrochemistry and Study of Indirect Electrocatalytic Properties of a Novel Organometallic Schiff Base Nickel(II) Complex. *J. Organomet. Chem.* **2022**, *976*, 122441. https://doi.org/10.1016/j.jorganchem.2022.122441.

(107) Realista, S.; Costa, P. J.; Maia, L. B.; Calhorda, M. J.; Martinho, P. N. Mechanistic Insights into the Electrochemical Reduction of CO_2 to CO on Ni(Salphen) Complexes. *Inorg. Chem. Front.* **2023**, *10* (14), 4175–4189. https://doi.org/10.1039/D3QI00424D.

(108) Tomczyk, D.; Nowak, L.; Bukowski, W.; Bester, K.; Urbaniak, P.; Andrijewski, G.; Olejniczak, B. Reductive and Oxidative Electrochemical Study and Spectroscopic Properties of Nickel(II) Complexes with N2O2 Schiff Bases Derived from (±)-Trans-N,N′-Bis(Salicylidene)-1,2-Cyclohexanediamine. *Electrochim. Acta* **2014**, *121*, 64–77. https://doi.org/10.1016/j.electacta.2013.12.073.

Chapter 8

APPENDICES

APPENDIX A: ADDITIONAL CONSIDERATIONS FOR ELECTROCHEMICAL BENZALDEHYDE CARBOXYLATION FOR SUSTAINABLE MANDELIC ACID SYNTHESIS VIA RADICAL INTERMEDIATES

A.1 Materials

Name	Specifications	Vendor
Acetone	ACS, ≥99.5%	Thermo Fisher Scientific
N,N-Dimethylformamide (DMF)	Anhydrous, 99.8%	Sigma Aldrich
Acetonitrile (MeCN)	Anhydrous, 99.8+%	Thermo Fisher Scientific
Dimethylsulfoxide (DMSO)	ACS, ≥99.9%	Macron Fine Chemicals
Propylene carbonate (PC)	Anhydrous, 99.5%	Thermo Fisher Scientific
Ethyl acetate (EtOAc)	99.5+%	Thermo Fisher Scientific
Acetonitrile-d_3 (MeCN-d_3)	99.96%	Cambridge Isotopes Lab
Milli-Q Water	18.2 MΩ cm	EMD Millipore
Nitric acid (HNO_3)	ACS, 67-70%	Thermo Fisher Scientific
Hydrochloric acid (HCl)	ACS, 36.5-38.0 wt.%	VWR
Phosphoric acid (H_3PO_4)	85 wt% solution in water	Thermo Fisher Scientific
Carbon dioxide (CO_2)	99.5%	Airgas
Argon (Ar)	99.9999%	Airgas
Tin (Sn)	0.1 mm thick, 99.95% metals basis	Goodfellow
Palladium (Pd)	0.025 mm thick	
Cobalt (Co)	0.127 mm thick, 99.9% metals basis	Beantown Chemical
Silver (Ag)	99.998% metals basis, 0.1 mm thick, hard, Premion	Alfa Aesar
Copper (Cu)	0.15 mm thick, 99.9% metals basis	Goodfellow

Iron (Fe)	0.1 mm thick, 99% metals basis	Alfa Aesar
Zinc (Zn)	0.2 mm thick, 99% metals basis	Amazon
Titanium (Ti)	0.25 mm thick, 99% metals basis	Alfa Aesar
Nickel (Ni)	0.025 mm thick, 99% (metals basis)	Thermo Fisher Scientific
Platinum (Pt)	99.99% trace metal, 0.025 mm thick	Beantown Chemical
Aluminum (Al)	0.25 mm thick, Puratronic, 99.997% metal basis	Thermo Fisher Scientific
Magnesium (Mg)	0.05 mm thick, 99.9% metals basis	Alfa Aesar
Glassy carbon (GC)	2 mm thick,	Alfa Aesar
Graphite (Gr)	0.1 mm thick	Alfa Aesar
Platinum wire counter electrode	0.5 mm diameter	CH Instruments
1,3,5-Trimethoxybenzene (TMB)	99%	Thermo Fisher Scientific
Benzaldehyde	≥99.5%	Sigma Aldrich
Mandelic acid (MA)	≥99%	Fluka Chemicals
Meso-Hydrobenzoin (HB)	95%	Thermo Fisher Scientific
Benzyl alcohol (BA)	Anhydrous, 99.8%	Simga Aldrich
Magnesium sulfate ($MgSO_4$)	Anhydrous, 99.44%	Chem-Impex Int'L Inc.
Magnesium chloride ($MgCl_2$)	Ultra dry, 99.99% (metals basis)	Thermo Fisher Scientific
Magnesium bromide ($MgBr_2$)	Anhydrous, 98%	Thermo Fisher Scientific
Magnesium triflate ($Mg(OTf)_2$)	≥98.0%	TCI America
Aluminum chloride ($AlCl_3$)	Anhydrous, 99%	Sigma Aldrich
Aluminum triflate ($Al(OTf)_3$)	99.9%	Sigma Aldrich
Zinc chloride ($ZnCl_2$)	Anhydrous, 99.95% (metals basis)	Thermo Fisher Scientific
Tetra-n-butylammonium tetrafluoroborate ($TBABF_4$)	>98%	TCI America

Tetra-n-butylammonium hexafluorophosphate ($TBAPF_6$)	≥98.0%	Sigma Aldrich
Tetra-n-butylammonium bromide (TBABr)	98+%	Alfa Aesar
Tetra-n-butylammonium iodide (TBAI)	>98%	TCI America
Decamethylferrocene ($Me_{10}Fc$)	99%	Thermo Fisher Scientific
Molecular sieves (3Å)	4 to 8 mesh	Thermo Fisher Scientific
Oxalic acid	Anhydrous, 98%	Beantown Chemical

Table 2. List of materials used for electrochemical benzaldehyde carboxylation for sustainable mandelic acid synthesis via radical intermediates.

A.1.1 Electrolyte Salts

Electrolyte salts ($TBABF_4$, $TBAPF_6$, TBABr, TBAI, $Mg(OTf)_2$, and $Al(OTf)_3$) were dried overnight in a vacuum oven (80 °C) and stored in an argon-filled glovebox (Vacuum Atmospheres Genesis). $TBABF_4$ can also be dried in a regular drying oven at 100 °C. $MgBr_2$, $MgCl_2$, $AlCl_3$, and $ZnCl_2$ were purchased anhydrously and brought directly into the glovebox after receiving.

A.1.2 Solvents

Anhydrous solvents (DMF, MeCN, DMSO, PC) were brought into the glovebox after receiving. They were stored over 3 Å molecular sieves for at least 12 hours before use. The molecular sieves were activated by drying at 350 °C for at least 4 hours, cooling to 100 °C in the furnace, then cooling under vacuum and filling with argon before being brought into the glovebox.

A.1.3 Substrate

Benzaldehyde was brought into the glovebox after receiving and stored under septa seal until use.

A.2 Experimental Methods

A.2.1 Electrochemical Cell Setup

Electrochemical Cell Component Preparation

Before experiment, the PEEK cell components were rinsed with water and acetone before being stored in a drying oven (100 °C). Tubing was stored outside. The cell parts were allowed to dry for at least 3 hours before use, due to the water sensitive nature of the chemistry.

Cells were also cleaned with acid on a regular basis. The cells were sonicated in a solution of 20 wt% nitric acid (HNO_3) for at least 5 minutes. The cells were removed from the sonication bath, washed with copious amounts of Milli-Q water, and sonicated in Milli-Q water for 5 minutes. After sonication, the cells were washed with acetone and stored in a drying oven (100 °C) until use.

Electrochemical Cell Assembly

A PEEK sandwich cell was used for all electrolysis reactions. Aluminum foil was taped onto the PEEK backing plates to be used as current collectors. All cell parts were stored in the oven (100 °C) and assembled right before use. Cells were hand-tightened with socket head screws and wingnuts. The assembly procedure is shown in **Figure A1** for a one-compartment cell.

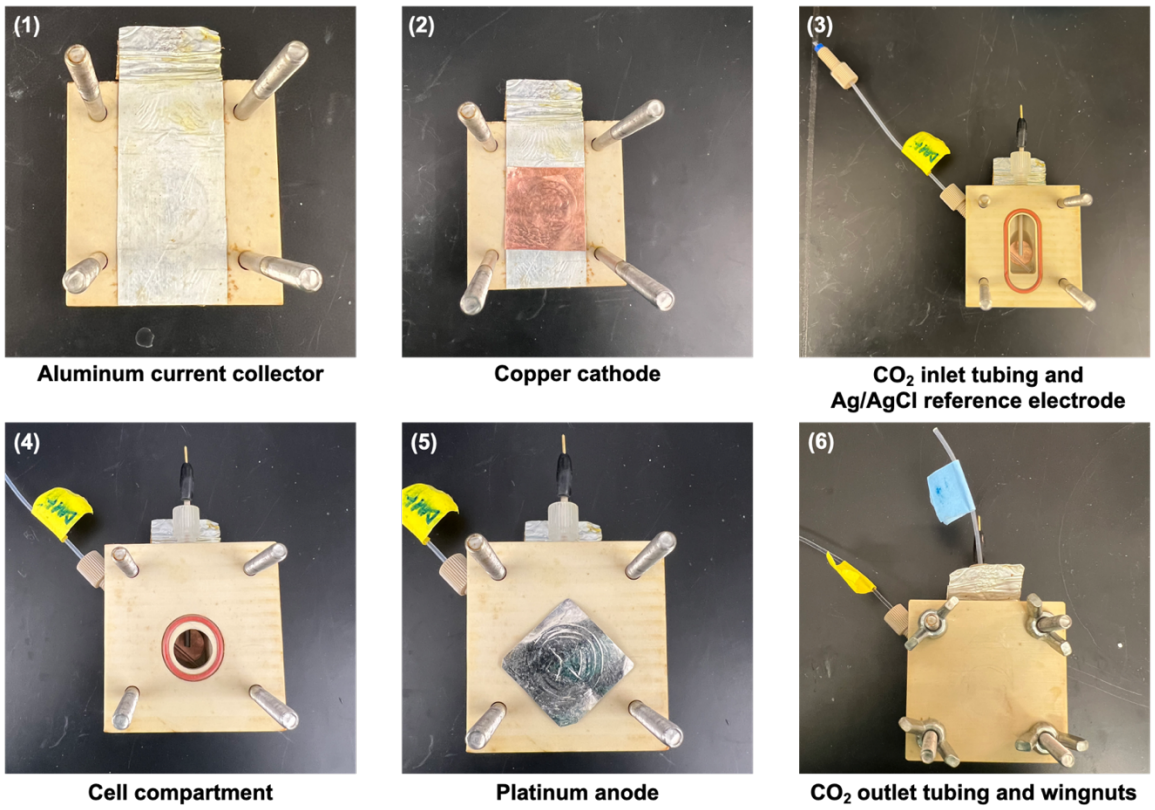

Figure A1. Assembly procedure for a one-compartment cell.

After the cell was assembled, it was connected to a gas source (either CO_2 or argon) via 1/16" O.D. FEP tubing through a side port closest to the cathodic side. A piece of 1/16" FEP O.D. tubing was used as an outlet on the anodic side. All other opening were closed with TEFZEL (ETFE) plugs. The cell was allowed to purge with gas for 2 minutes before the electrolyte was added. The electrolyte was allowed to saturate with the gas for 15 minutes before running the reaction.

A.2.2 Reference Electrode

A leakless Ag/AgCl reference electrode (eDAQ Incorporated, ET072-1) was used for all experiments involving a reference electrode. When not in use, the reference electrode was stored in Milli-Q water. The electrode was wiped with a KimWipe before use. The reference electrode was inserted into a flangeless fitting that was wrapped with Teflon tape to ensure secure positioning within the cell (see **Figure A1**).

The reference electrode was calibrated daily before use by referencing against the $Me_{10}Fc^{0/+}$ couple. The reference was done by performing 5 cyclic voltammetry (CV) cycles of a solution of $Me_{10}Fc$ dissolved in the electrolyte (usually 100 mM $TBABF_4$ and 100 mM of the appropriate Lewis acid). $Me_{10}Fc$ was sparingly soluble in DMF so only a small amount was added with some solid particles remaining undissolved; this was enough to give well defined CV data. The reference potential was determined by calculating the average of the peak potentials (cathodic and anode) to determine the $E_{1/2}$ value for that one scan, then averaging the $E_{1/2}$ values across all the scans of the CVs. The first scan was not included in the calculation.

A.2.3 Chronopotentiometry

Chronopotentiometry experiments were performed in one-compartment cells in a three-electrode setup (**Figure A1**). A BioLogic SP-200 potentiostat was used for all electrochemical experiments. After the cell was assembled, 4 mL electrolyte was added into the cell and purged with 20 sccm CO_2 for 15 min. The uncompensated resistance (Ru) was then measured using the electrochemical impedance spectroscopy. 85% Ru was compensated by the IR compensation function of the potentiostat and the final 15% was corrected manually during data processing.

A.2.4 Cyclic Voltammetry

Cyclic voltammetry experiments were performed in two-compartment cells with Daramic separator similar to the cell in the protocol described in **Figure A1**. After the cell was assembled, the cathodic chamber was purged with 20 sccm gas (Ar or CO_2) for 2-3 minutes before the electrolyte was added. 2 mL and 2 mL electrolyte were then added to the cathodic and anodic chambers, respectively. The electrolyte was purged for 15 minutes with 20 sccm gas. Voltammetry experiment was performed without IR compensation and 100% IR compensation was performed manually in the data processing step.

A.3 UPLC-UV Vis

A.3.1 Reaction Workup and Product Quantification

After electrolysis, a known amount of TMB stock solution (0.25 M in DMF) was added directly to the cell and was incorporated into the electrolyte by careful mixing via pipetting at least 10 times. Then, this mixture solution was diluted 1:19 into Milli-Q water. Products were identified and quantified on a UPLC-UV Vis spectrometer (Waters ACQUITY) fitted with a BEH C18 sorbent column (Waters ACQUITY) and photodiode array detector (Waters ACQUITY).

A.3.2 Calibration Curve

Calibration curves were constructed by making a stock solution of known compositions of the desired compounds in DMF. DMF was used to dilute the stock solution to generate standard solutions of various product concentrations. The typical work up procedure for UPLC-UV Vis was performed for each of the standard solution. Calibration curves were fit by using the area and moles of each compound relative to TMB.

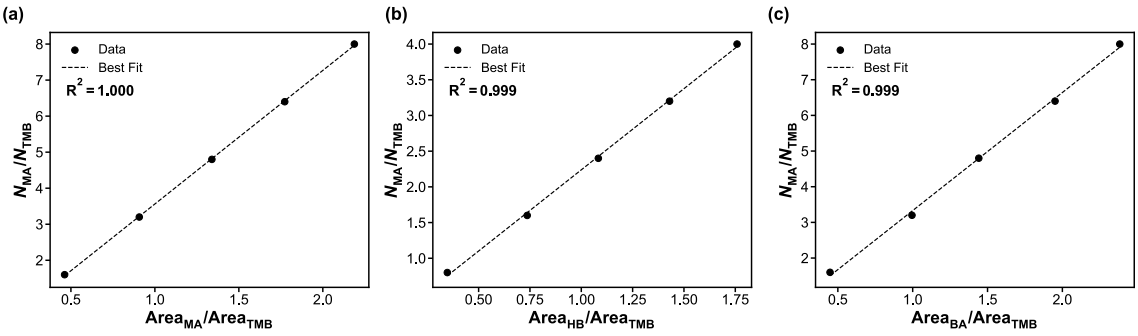

Figure A2. UPLC-UV Vis calibration curves for (A) mandelic acid, (B) hydrobenzoin, and (C) benzaldehyde.

A.4 Additional Optimization Data

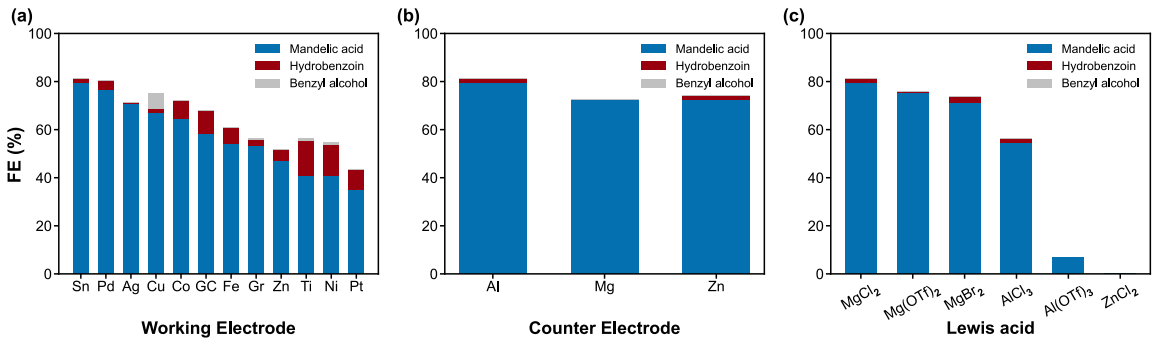

Figure A3. Effect of a) working electrode, b) counter electrode, and c) Lewis acid additive on the Faradaic efficiency of main product (mandelic acid) and side products (hydrobenzoin and benzyl alcohol).

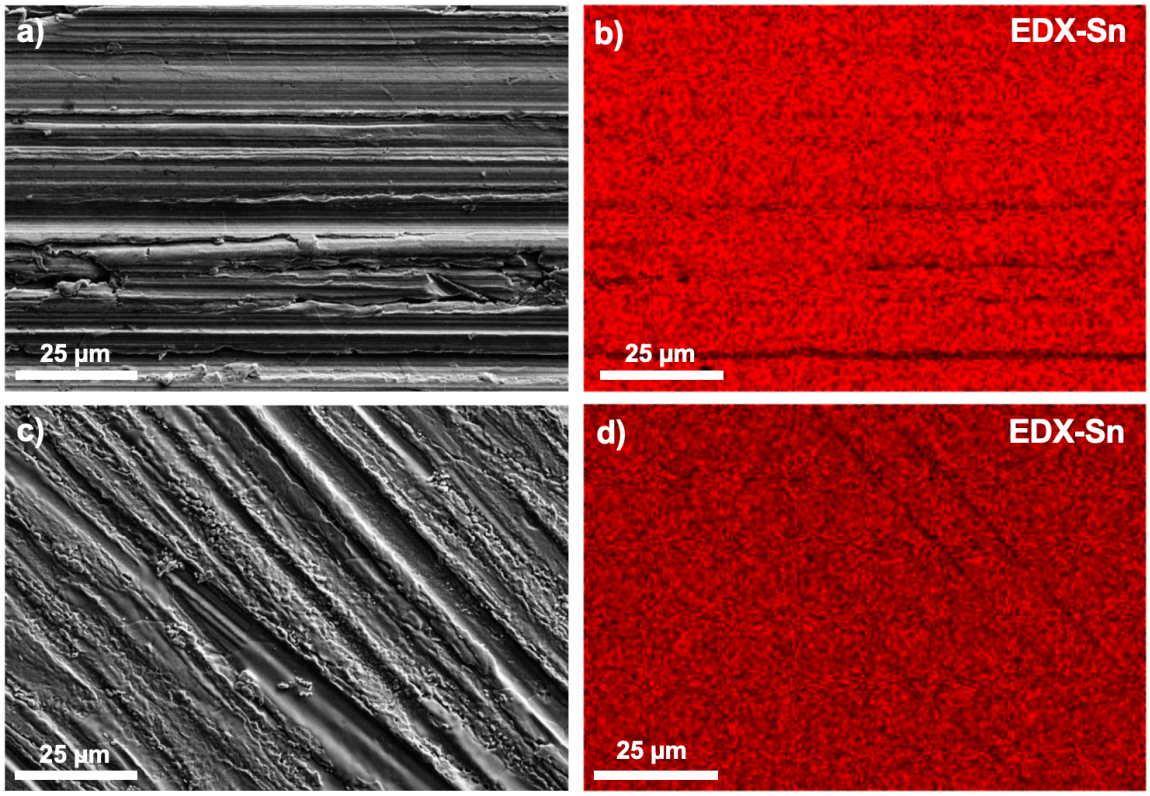

Figure A4. a) Scanning electron microscopy (SEM) image and b) EDX spectroscopy of the Sn electrode before electrolysis. c) SEM image and d) EDX spectroscopy of the Sn electrode after electrolysis.

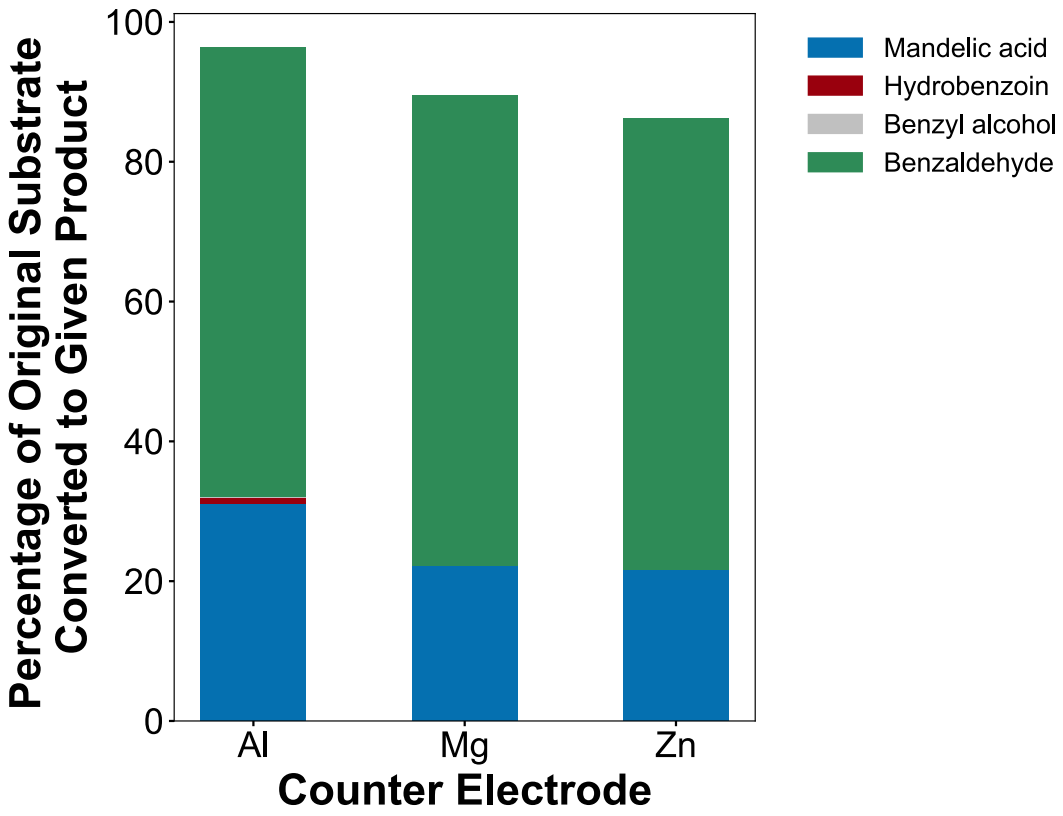

Figure A5. Carbon balance of the reaction as a function of counter electrode material. Standard reaction conditions: Sn working electrode, Al counter electrode, 100 mM benzaldehyde, 100 mM $TBABF_4$, 100 mM $MgCl_2$, 20 sccm CO_2, 4 mL DMF, –2.9 V vs. $Me_{10}Fc^{0/+}$.

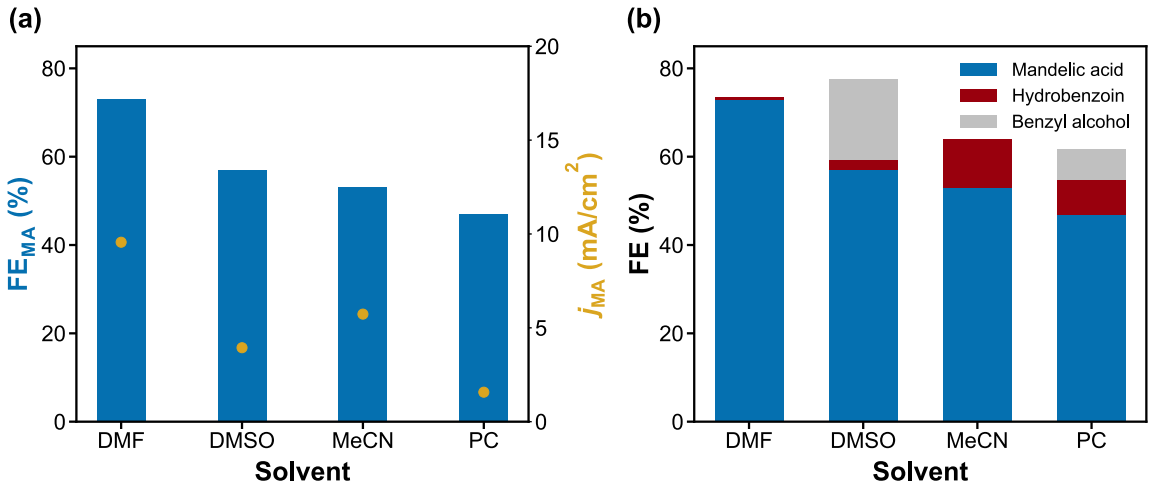

Figure A6. Solvent screening data. a) Effect of solvents on the FE and partial current density of mandelic acid. b) Effect of solvents on the FE of the main product (mandelic acid) and side products (hydrobenzoin and benzyl alcohol). Standard reaction conditions: Sn working electrode, Al counter electrode, 100 mM benzaldehyde, 100 mM $TBABF_4$, 100 mM $MgBr_2$, 20 sccm CO_2, 4 mL solvent, –2.9 V vs. $Me_{10}Fc^{0/+}$ for 30 minutes.

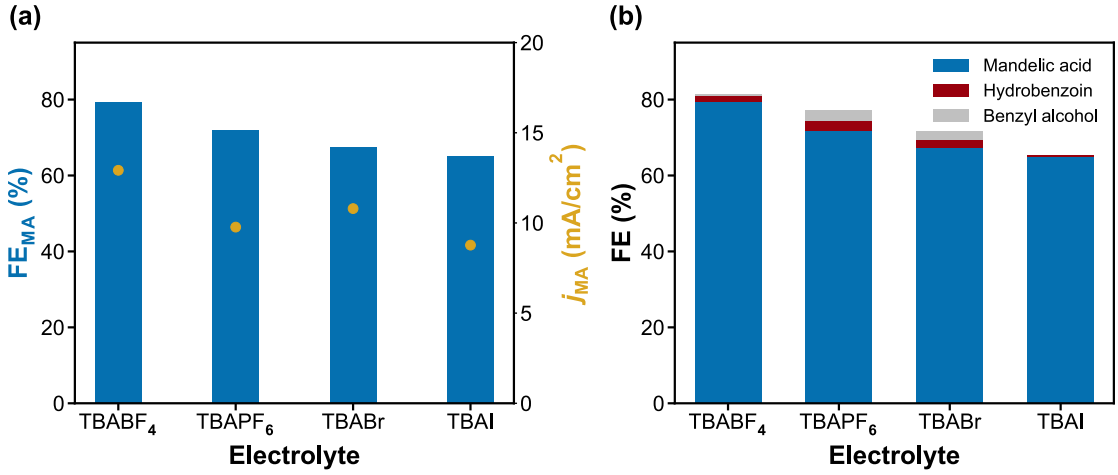

Figure A7. Electrolyte salt screening data. a) Effect of electrolyte salts on the FE and partial current density of mandelic acid. b) Effect of electrolyte salts on the FE of the main product (mandelic acid) and side products (hydrobenzoin and benzyl alcohol). Standard reaction conditions: Sn working electrode, Al counter electrode, 100 mM benzaldehyde, 100 mM electrolyte, 100 mM $MgCl_2$, 20 sccm CO_2, 4 mL DMF, –2.9 V vs. $Me_{10}Fc^{0/+}$ for 30 minutes.

A.5 Substrate Scope

A preliminary substrate scope was performed to investigate the electronic and steric effects of different substituents on the aromatic ring. Due to challenges in acquiring products standards for proper UPLC-UV Vis quantification, ^{1}H NMR was employed to perform quantification of the extracted product.

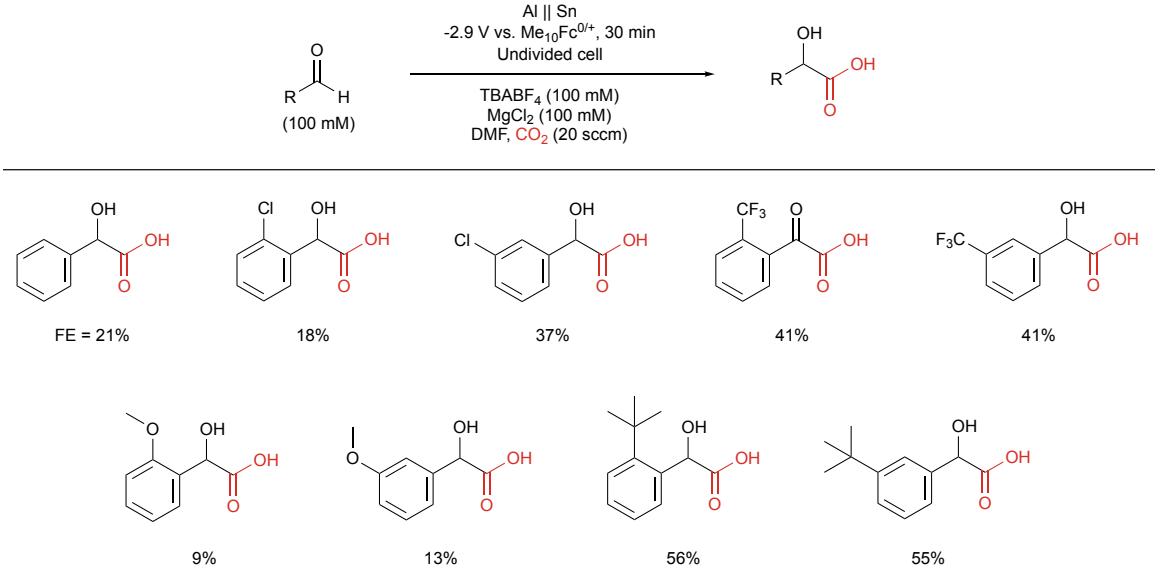

Figure A8. Substrate scope of the electrochemical carboxylation of aryl aldehydes. FEs are reported below each product. Standard reaction conditions: Sn working electrode, Al counter electrode, 100 mM benzaldehyde, 100 mM $TBABF_4$, 100 mM $MgCl_2$, 20 sccm CO_2, 4 mL DMF, –2.9 V vs. $Me_{10}Fc^{0/+}$.

A.6 Cyclic Voltammograms

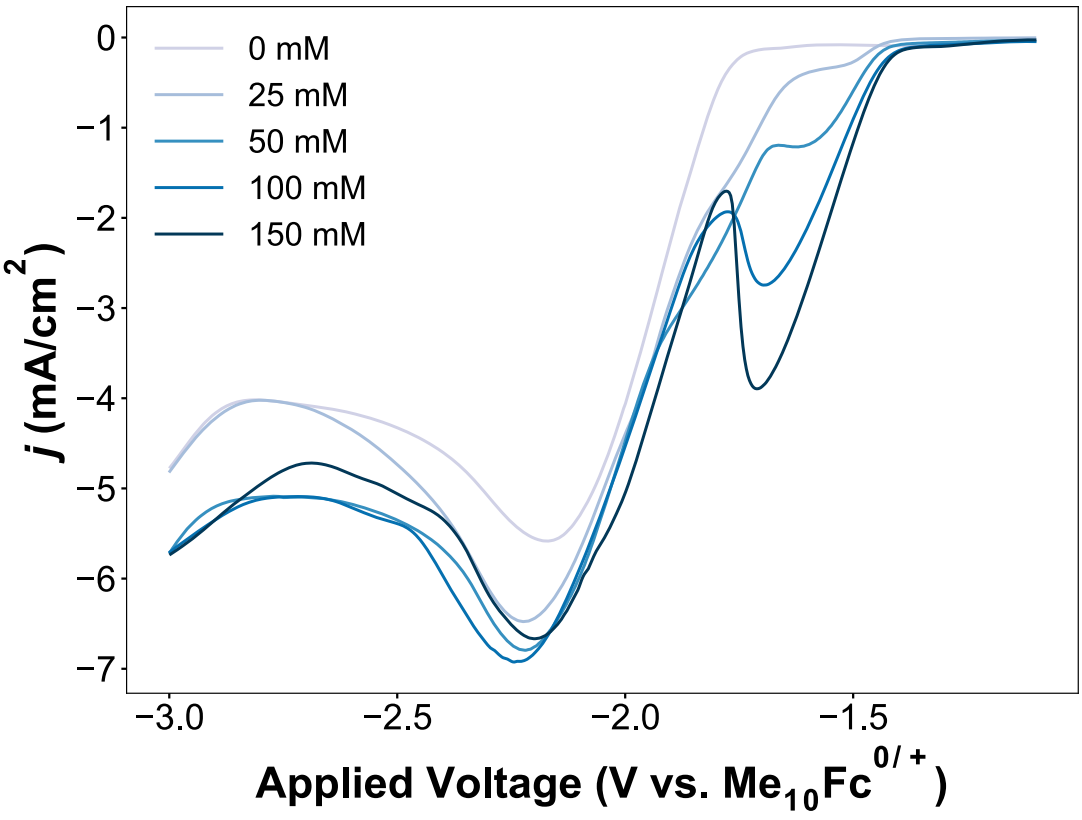

Figure A9. Cyclic voltammograms (CVs) of 100 mM benzaldehyde at 20 mV/s in DMF with various concentrations of $MgCl_2$, purged with argon. Reaction conditions: Sn working electrode, Al counter electrode, divided cell, 100 mM $TBABF_4$, DMF.

A.7 Electron Paramagnetic Resonances Spectroscopy

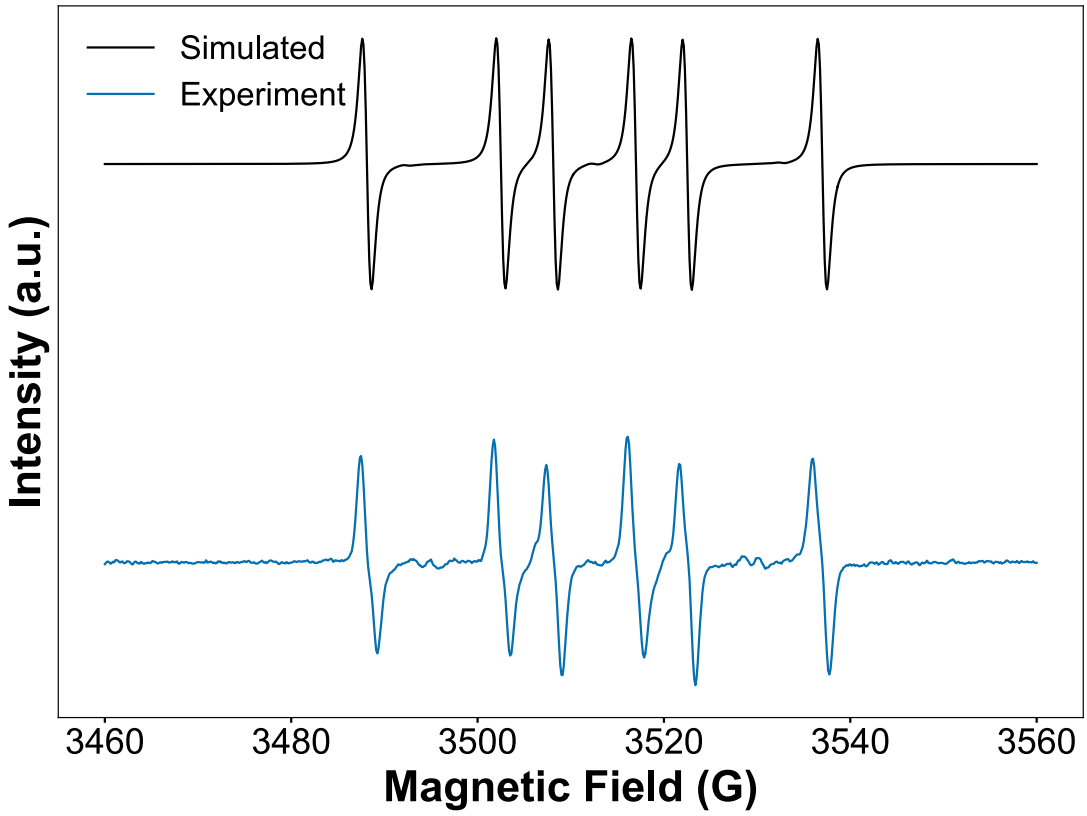

Figure A10. Simulated (black) and real (blue) EPR spectrum of an electrolytic cell containing only benzaldehyde at –2.9 V vs. $Me_{10}Fc^{0/+}$ after 30 minutes (t = 30 min) in the presence of DMPO as a radical trapping agent. The simulated spectrum is of the DMPO-ketyl species. Spectrum was collected at a frequency of 9.865624 GHz.

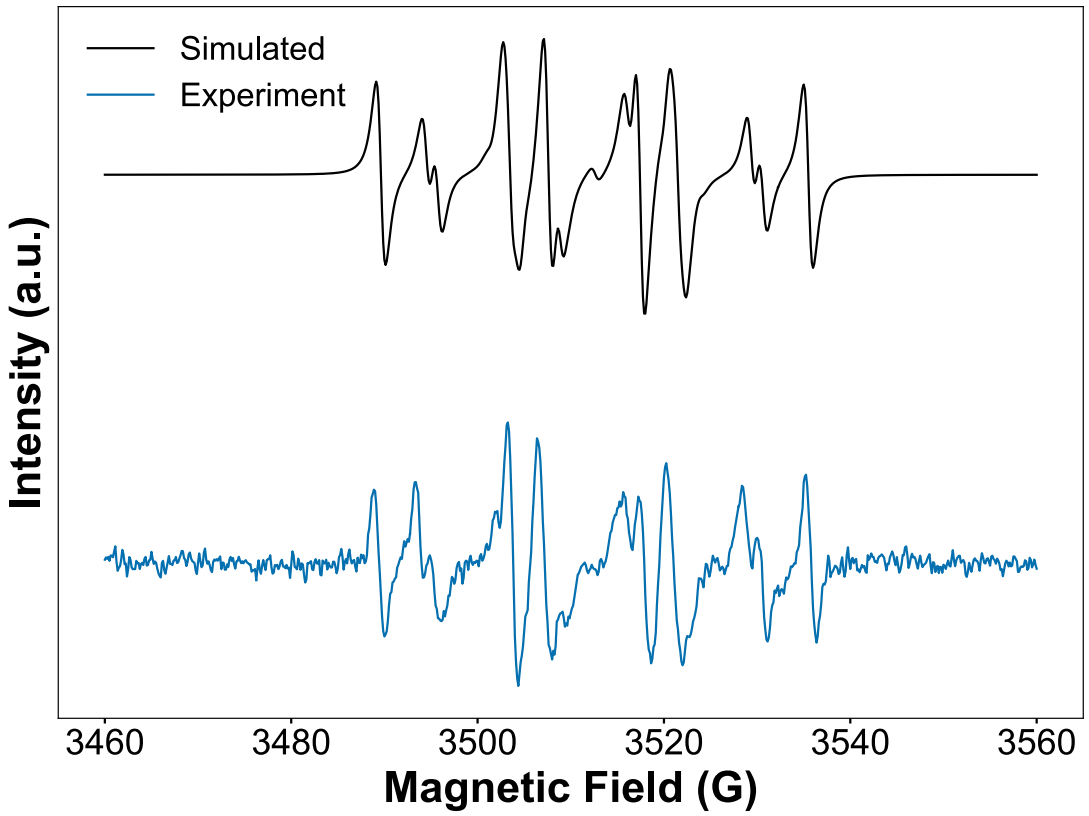

Figure A 11. Simulated (black) and real (blue) EPR spectrum of an electrolytic cell containing only CO_2 at –2.9 V vs. $Me_{10}Fc^{0/+}$ after 30 minutes (t = 30 min) in the presence of DMPO as a radical trapping agent. Notably, the DMPO-CO_2 signal is quite small and is similar in intensity to background signals corresponding to DMPO-trapped superoxide species (DMPO-OOH) and the oxidation product of DMPO (DMPOX). These background species were not considered in EPR spectra containing benzaldehyde due to the large signal of the DMPO-ketyl radical. Spectrum was collected at a frequency of 9.865553 GHz.

A.8 Density Functional Theory

Density functional theory (DFT) calculations were performed to estimate the standard reduction potential for the one-electron reduction of benzaldehyde to its corresponding ketyl radical anion in solution, with and without the presence of Mg^{2+} ions. All calculations were carried out using Gaussian 16 at the M06-2x/def2-TZVPD level of theory. Solvent effects (e.g. DMF) were included using the implicit solvation model (SMD).

For both the free and Mg^{2+}-coordinated forms, the Gibbs free energy in solution was computed as:

$$G_{sol} = E_{electronic} + G_{thermal} + \Delta G_{solvation}$$

The reduction free energy in solution was obtained via:

$$\Delta G_{red} = G_{sol}(reduced\ species) - G_{sol}(oxidized\ species)$$

The standard reduction potential (versus SHE) was calculated using:

$$E^{\circ} = -\frac{\Delta G_{red}}{F} + E^{\circ}_{SHE}$$

where F is Faraday's constant and E°_{SHE} is the absolute potential of the standard hydrogen electrode (take as 4.28 V). Potentials were converted to the saturated calomel electrode (SCE) scale by subtracting 0.241 V.

A.9 Supplementary Data and Figures

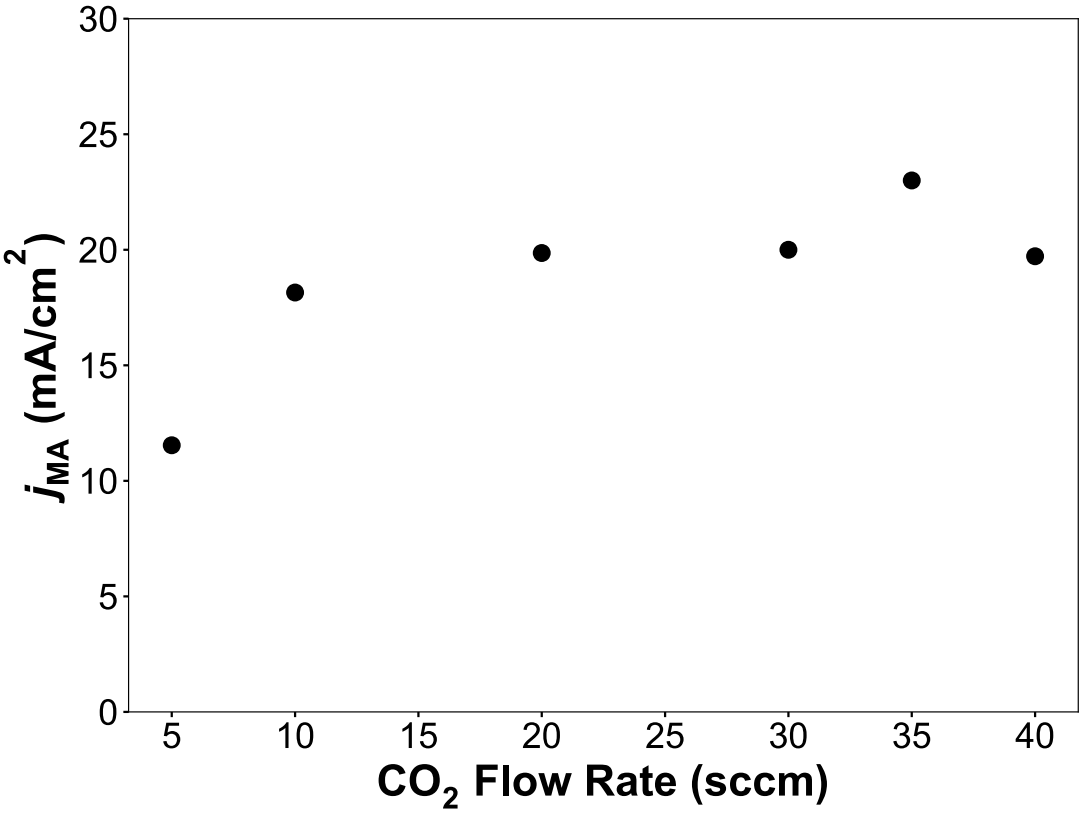

Figure A12. Partial current density of mandelic acid at varied CO_2 flow rates.

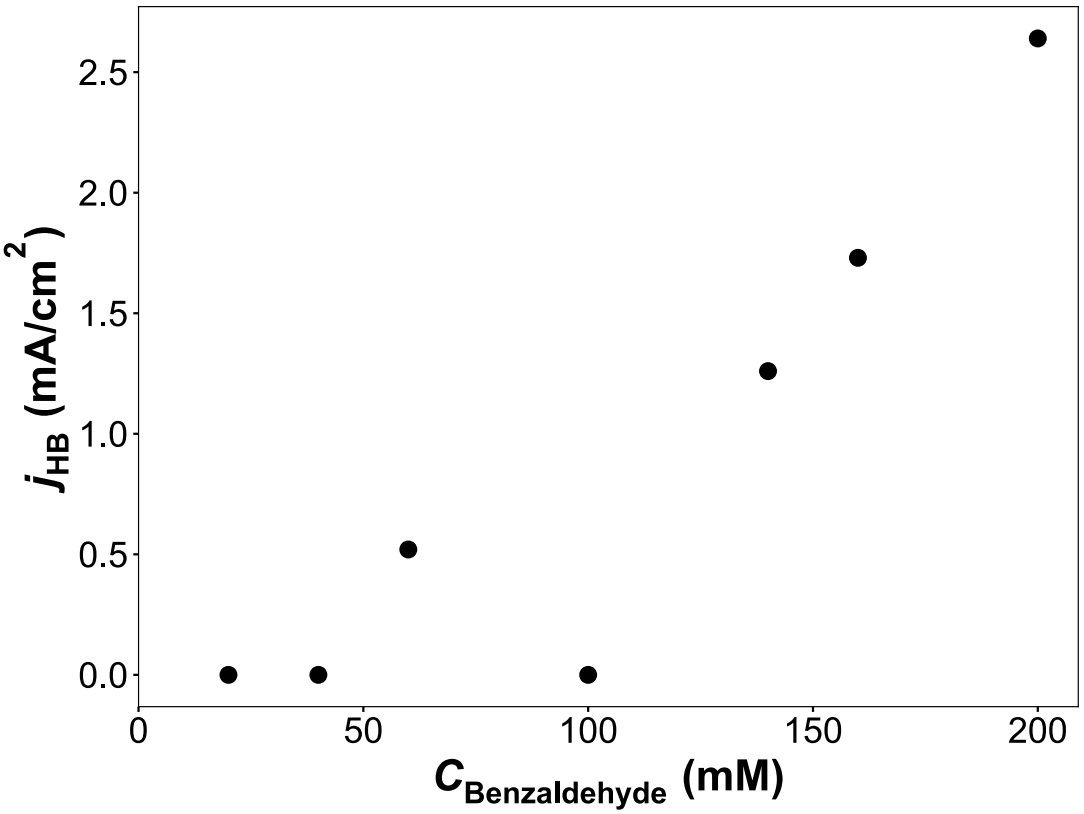

Figure A13. Partial current density towards hydrobenzoin as a function of benzaldehyde concentration.

A.10 Minor Mechanistic Pathways

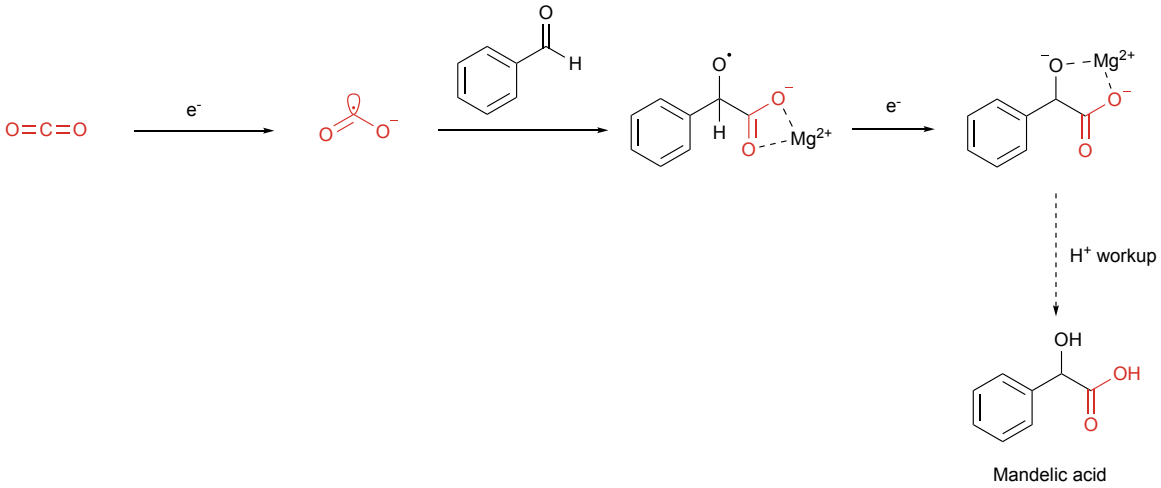

Scheme 5. Proposed minor mechanistic pathway proceeding via CO_2 reduction.

APPENDIX B: ADDITIONAL CONSIDERATIONS FOR TOWARD ELECTROCHEMICAL CARBOXYLATION OF ALIPHATIC ALDEHYDES WITH CO_2

B.1 Materials

Name	Specifications	Vendor
Acetone	ACS, ≥99.5%	Thermo Fisher Scientific
N,N-Dimethylformamide (DMF)	Anhydrous, 99.8%	Sigma Aldrich
Acetonitrile (MeCN)	Anhydrous, 99.8+%	Thermo Fisher Scientific
Dimethylsulfoxide (DMSO)	ACS, ≥99.9%	Macron Fine Chemicals
Chloroform-d ($CDCl_3$)	99.96%	Cambridge Isotopes Lab
Acetonitrile-d_3 (MeCN-d_3)	99.96%	Cambridge Isotopes Lab
Milli-Q Water	18.2 MΩ cm	EMD Millipore
Nitric acid (HNO_3)	ACS, 67-70%	Thermo Fisher Scientific
Phosphoric acid (H_3PO_4)	85 wt% solution in water	Thermo Fisher Scientific
Carbon dioxide (CO_2)	99.5%	Airgas
Argon (Ar)	99.9999%	Airgas
Tin (Sn)	0.1 mm thick, 99.95% metals basis	Goodfellow
Palladium (Pd)	0.025 mm thick	
Cobalt (Co)	0.127 mm thick, 99.9% metals basis	Beantown Chemical
Silver (Ag)	99.998% metals basis, 0.1 mm thick, hard, Premion	Alfa Aesar
Copper (Cu)	0.15 mm thick, 99.9% metals basis	Goodfellow
Iron (Fe)	0.1 mm thick, 99% metals basis	Alfa Aesar
Zinc (Zn)	0.2 mm thick, 99% metals basis	Amazon
Titanium (Ti)	0.25 mm thick, 99% metals basis	Alfa Aesar
Platinum (Pt)	99.99% trace metal, 0.025 mm thick	Beantown Chemical

Aluminum (Al)	0.25 mm thick, Puratronic, 99.997% metal basis	Thermo Fisher Scientific
Glassy carbon (GC)	2 mm thick,	Alfa Aesar
Platinum wire counter electrode	0.5 mm diameter	CH Instruments
1,3,5-Trimethoxybenzene (TMB)	99%	Thermo Fisher Scientific
3-phenylpropanal (3P)	95%	Thermo Fisher Scientific
2-hydroxy-4-phenylbutanoic acid (3PCOOH)	97	Sigma Aldrich
Magnesium bromide ($MgBr_2$)	Anhydrous, 98%	Thermo Fisher Scientific
Tetra-n-butylammonium tetrafluoroborate ($TBABF_4$)	>98%	TCI America
Tetra-n-butylammonium hexafluorophosphate ($TBAPF_6$)	≥98.0%	Sigma Aldrich
Tetra-n-butylammonium bromide (TBABr)	98+%	Alfa Aesar
Tetra-n-butylammonium iodide (TBAI)	>98%	TCI America
Decamethylferrocene ($Me_{10}Fc$)	99%	Thermo Fisher Scientific
Molecular sieves (3Å)	4 to 8 mesh	Thermo Fisher Scientific

Table 3. List of materials used for toward electrochemical carboxylation of aliphatic aldehydes with CO_2.

B.1.1 Electrolyte Salts

Electrolyte salts ($TBABF_4$, $TBAPF_6$, TBABr, TBAI) were dried overnight in a vacuum oven (80 °C) and stored in an argon-filled glovebox (Vacuum Atmospheres Genesis). $TBABF_4$ can also be dried in a regular drying oven at 100 °C. $MgBr_2$, was purchased anhydrously and brought directly into the glovebox after receiving.

B.1.2 Solvents

Anhydrous solvents (DMF, MeCN, DMSO) were brought into the glovebox after receiving. They were stored over 3 Å molecular sieves for at least 12 hours before use. The molecular sieves were activated by drying at 350 °C for at least 4 hours, cooling to 100 °C in the furnace, then cooling under vacuum and filling with argon before being brought into the glovebox.

B.1.3 Substrate

3-phenylpropanal was brought into the glovebox after receiving and stored under septa seal until use.

B2. Experimental Methods

Experiments were conducted according to the procedures outline in Chapter 3 (see Chapter 3, 3.5 Methods) and Appendix A (see Appendix A, A.2 Experimental Methods).

B3. UPLC-UV Vis

B.3.1 Reaction Workup and Product Quantification

After electrolysis, a known amount of TMB stock solution (0.25 M in DMF) was added directly to the cell and was incorporated into the electrolyte by careful mixing via pipetting. Then, this mixture solution was diluted 1:19 into Milli-Q water. Products were identified and quantified on a UPLC-UV Vis spectrometer (Waters ACQUITY) fitted with a BEH C18 sorbent column (Waters ACQUITY) and photodiode array detector (Waters ACQUITY).

A.3.2 Calibration Curve

Calibration curves were constructed by making a stock solution of known compositions of the desired compounds in DMF. DMF was used to dilute the stock solution to generate standard solutions of various product concentrations. The typical work up procedure for UPLC-UV Vis was performed for each of the standard solution. Calibration curves were fit by using the area and moles of each compound relative to TMB.

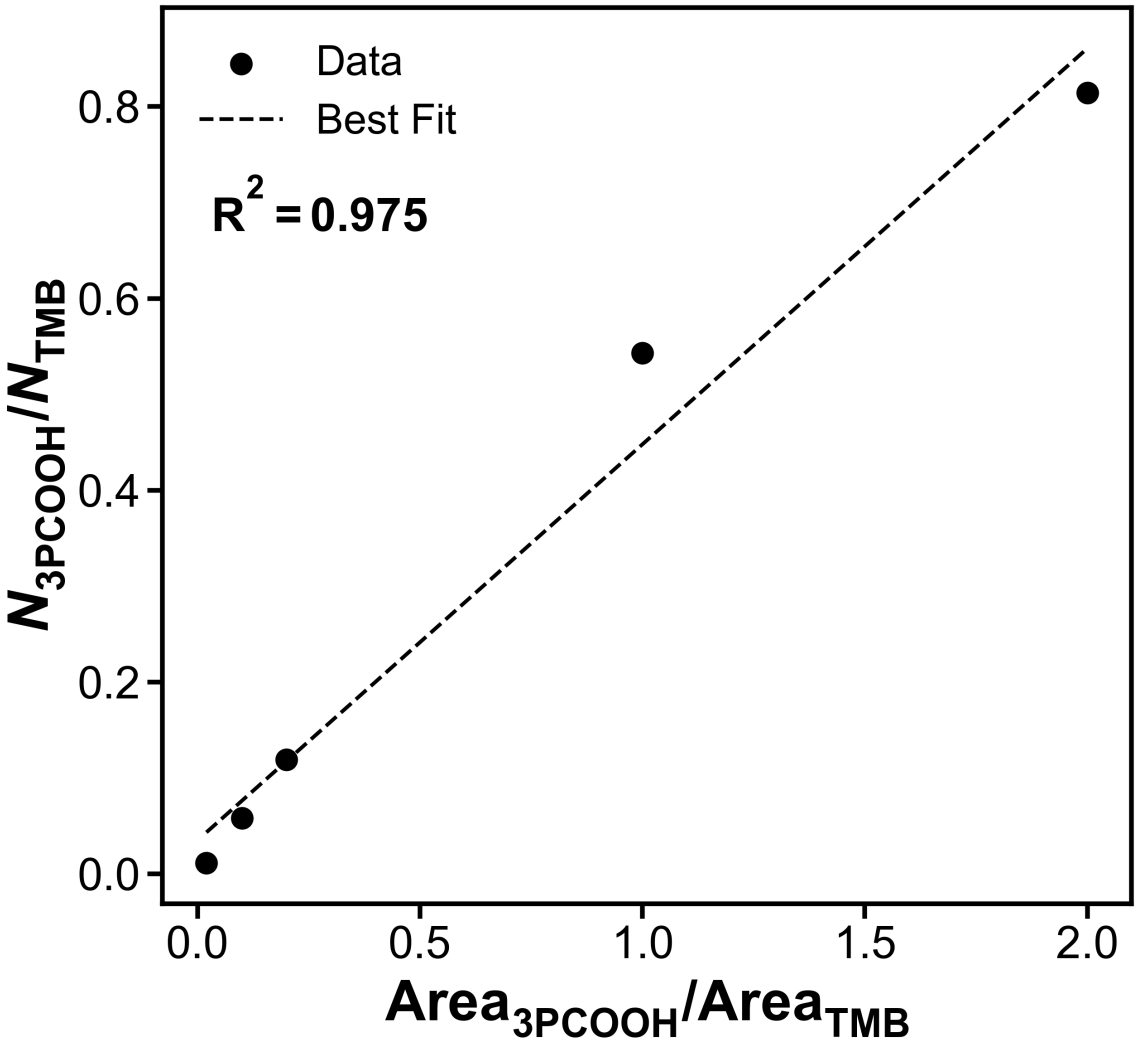

Figure A14. UPLC-UV Vis calibration curves for 2-hydroxy-4-phenylbutanoic acid (3PCOOH).

B.5 Nuclear Magnetic Resonance Spectra

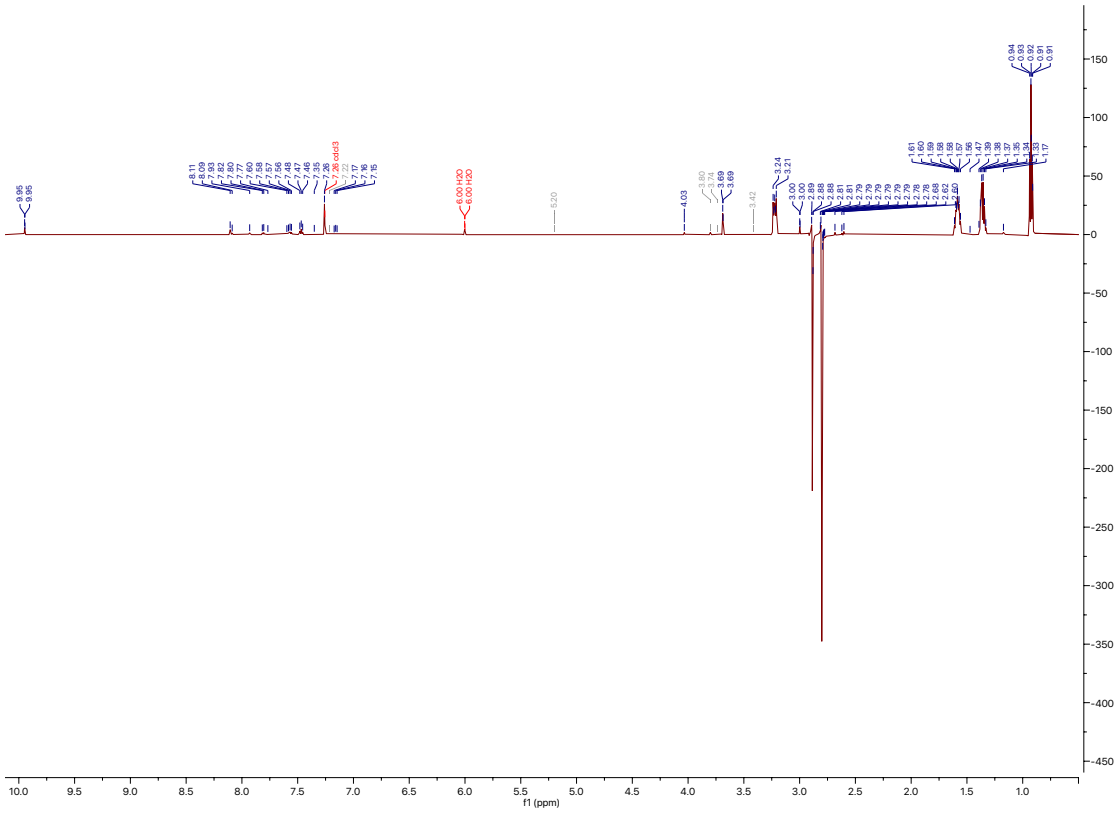

Figure A15. ^{1}H NMR spectrum of polymer formed during electrolysis in chloroform-d_3.

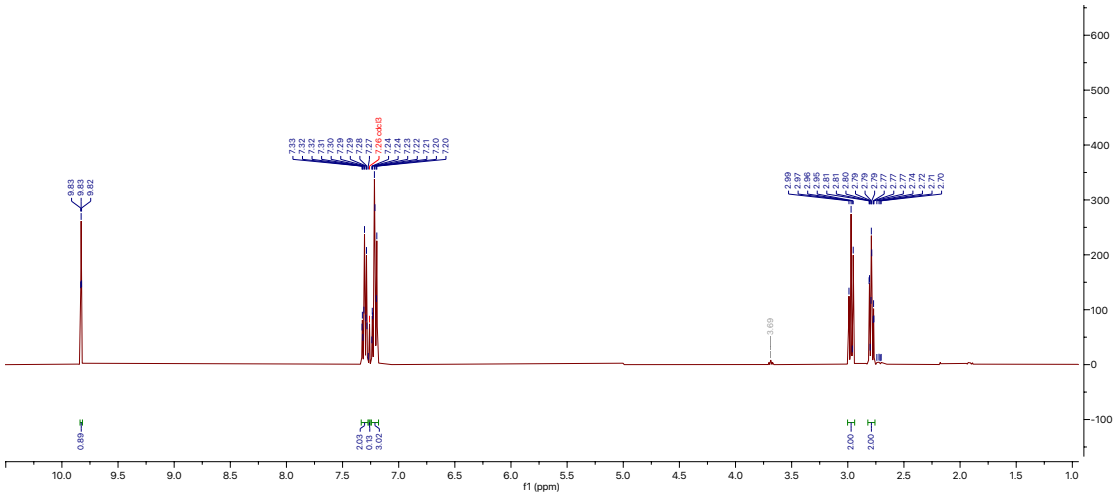

Figure A16. ^{1}H NMR spectrum of 3-phenylpropanal in chloroform-d_3.

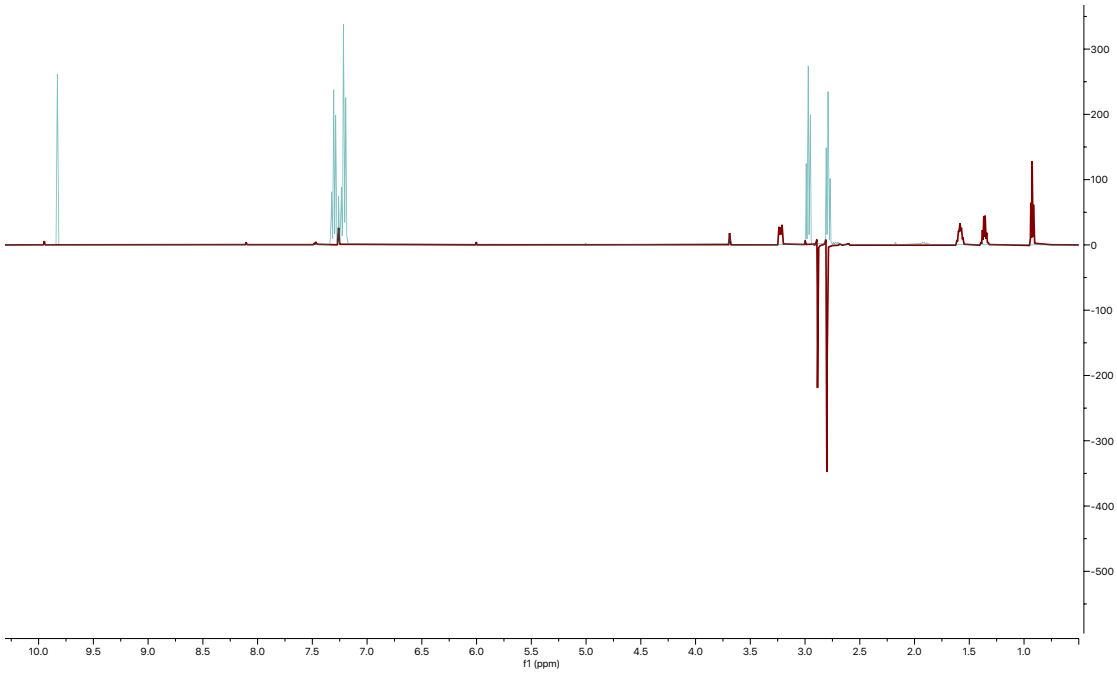

Figure A17. Overlay of ^{1}H NMR spectra from Figure A15 and A16.

APPENDIX C: ADDITIONAL CONSIDERATIONS FOR ENANTIOSELECTIVE ELECTROCHEMICAL CARBOXYLATION OF BENZALDEHYDE USING CHIRAL METAL SALEN CATALYSTS

C.1 Materials

Name	Specifications	Vendor
Acetone	ACS, ≥99.5%	Thermo Fisher Scientific
N,N-Dimethylformamide (DMF)	Anhydrous, 99.8%	Sigma Aldrich
Chloroform-d ($CDCl_3$)	99.96%	Cambridge Isotopes Lab
Acetonitrile-d_3 (MeCN-d_3)	99.96%	Cambridge Isotopes Lab
Dichloromethane-d_3 (CD_2Cl_2)	99.9%	Millipore Sigma
Milli-Q Water	18.2 MΩ cm	EMD Millipore
Nitric acid (HNO_3)	ACS, 67-70%	Thermo Fisher Scientific
Carbon dioxide (CO_2)	99.5%	Airgas
Argon (Ar)	99.9999%	Airgas
Tin (Sn)	0.1 mm thick, 99.95% metals basis	Goodfellow
(*R,R*)-(–)-*N,N'*-Bis(3,5-di-*tert*-butylsalicylidene)-1,2-cyclohexanediamine	98%	Sigma Aldrich
(*R,R*)-(–)-*N,N'*-Bis(3,5-di-*tert*-butylsalicylidene)-1,2-cyclohexanediaminocobalt(II)		Sigma Aldrich
(*S,S*)-*N,N'*-Bis(3,5-di-*tert*-butylsalicylidene)-1,2-cyclohexanediaminoaluminum chloride		Sigma Aldrich
(R,R)-(–)-N,N'-Bis(3,5,-di-tert-butylsalicylidene)-1,2-cyclohexanediamino manganese(III) chloride		Sigma Aldrich

Platinum (Pt)	99.99% trace metal, 0.025 mm thick	Beantown Chemical
Aluminum (Al)	0.25 mm thick, Puratronic, 99.997% metal basis	Thermo Fisher Scientific
Platinum wire counter electrode	0.5 mm diameter	CH Instruments
4-chlorobenzoic acid (CBA)	98+%	Thermo Fisher Scientific
Benzaldehyde	≥99.5%	Sigma Aldrich
Mandelic acid (MA)	≥99%	Fluka Chemicals
(R)-(–)-Mandelic acid	≥99%	Sigma Aldrich
(S)-(+)-Mandelic acid	≥99%	Simga Aldrich
Tetra-n-butylammonium tetrafluoroborate ($TBABF_4$)	>98%	TCI America
Tetra-n-butylammonium bromide (TBABr)	98+%	Alfa Aesar
Tetra-n-butylammonium iodide (TBAI)	>98%	TCI America
Decamethylferrocene ($Me_{10}Fc$)	99%	Thermo Fisher Scientific
Molecular sieves (3Å)	4 to 8 mesh	Thermo Fisher Scientific

Table 4. List of materials used for enantioselective electrochemical carboxylation of benzaldehyde using chiral metal salen catalysts.

C.1.1 Electrolyte Salts

Electrolyte salts ($TBABF_4$, TBABr, TBAI) were dried overnight in a vacuum oven (80 °C) and stored in an argon-filled glovebox (Vacuum Atmospheres Genesis). $TBABF_4$ can also be dried in a regular drying oven at 100 °C.

B.1.2 Solvents

Anhydrous DMF was brought into the glovebox after receiving. DMF was stored over 3 Å molecular sieves for at least 12 hours before use. The molecular sieves were activated by drying at 350 °C for at least 4 hours, cooling to 100 °C in the furnace, then cooling under vacuum and filling with argon before being brought into the glovebox.

B.1.3 Substrate

Benzaldehyde was brought into the glovebox after receiving and stored under septa seal until use.

C.2 Experimental Methods

Experiments were conducted according to the procedures outline in Chapter 3 (see Chapter 3, 3.5 Methods) and Appendix A (see Appendix A, A.2 Experimental Methods).

C.3 UPLC-UV Vis

C.3.1 Reaction Workup and Product Quantification

After electrolysis, a known amount of CBA stock solution (0.25 M in DMF) was added directly to the cell and was incorporated into the electrolyte by careful mixing via pipetting at least 10 times. Then, this mixture solution was diluted 1:19 into a H_3PO_4/MeOH solution (90% H_3PO_4 pH 3 buffer and 10% MeOH). The sample was spun down in a centrifuge for 15 minutes at 9000 rpm. Products were identified and quantified on a UPLC-UV Vis spectrometer (Waters ACQUITY) fitted with a CHIRALPAK ID-U 3.0 x 100 mm, sub-2 micron column (Daicel Chiral Technologies) and photodiode array detector (Waters ACQUITY).

A.3.2 Calibration Curve

Calibration curves were constructed by making a stock solution of known compositions of the desired compounds in DMF. DMF was used to dilute the stock solution to generate standard solutions of various product concentrations. The typical work up procedure for UPLC-UV Vis was performed for each of the standard solution. Calibration curves were fit by using the area and moles of each compound relative to CBA.

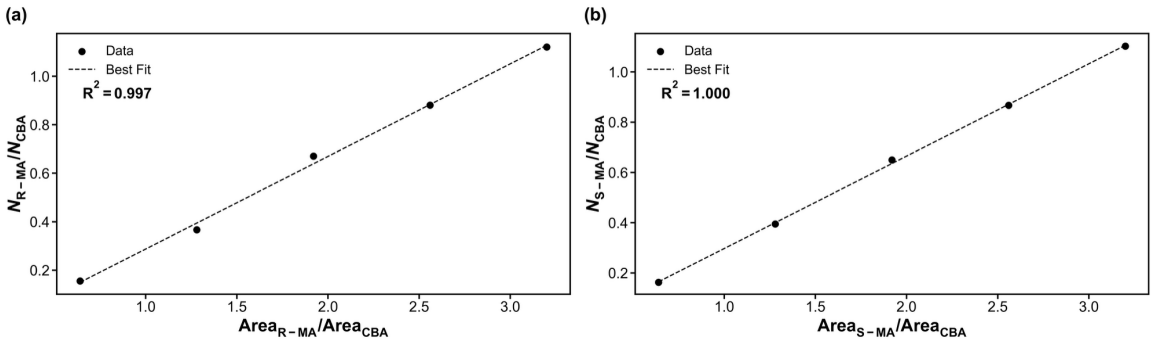

Figure A18. UPLC-UV Vis calibration curves for (a) (R)-(–)-mandelic acid and (b) (S)-(+)-mandelic acid.

C.4 Cyclic Voltammograms

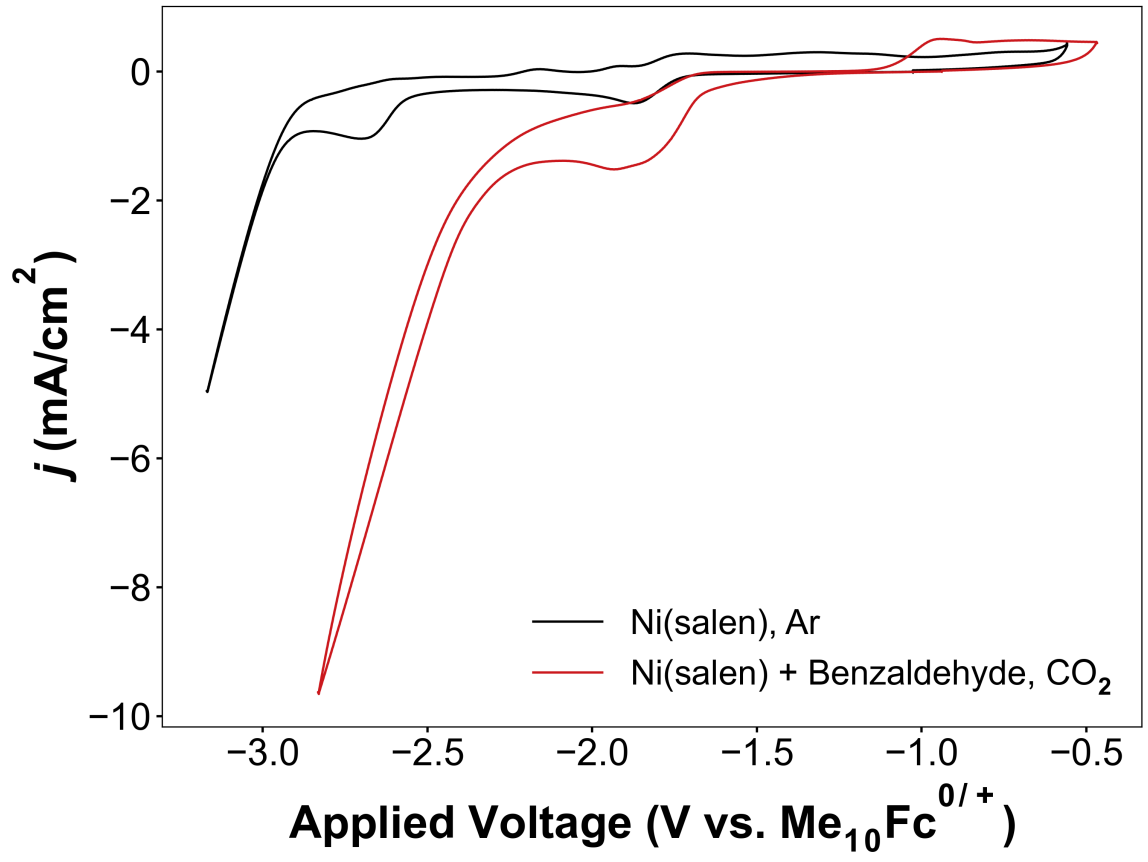

Figure A19. Cyclic voltammograms (CVs) at a scan rate of 20 mV/s in DMF for (a) Ni(salen) and (b) Ni(salen) in the presence of benzaldehyde and CO_2. Reaction conditions: Sn working electrode, Al counter electrode, 100 mM TBAI, 5 mM substrates in DMF.

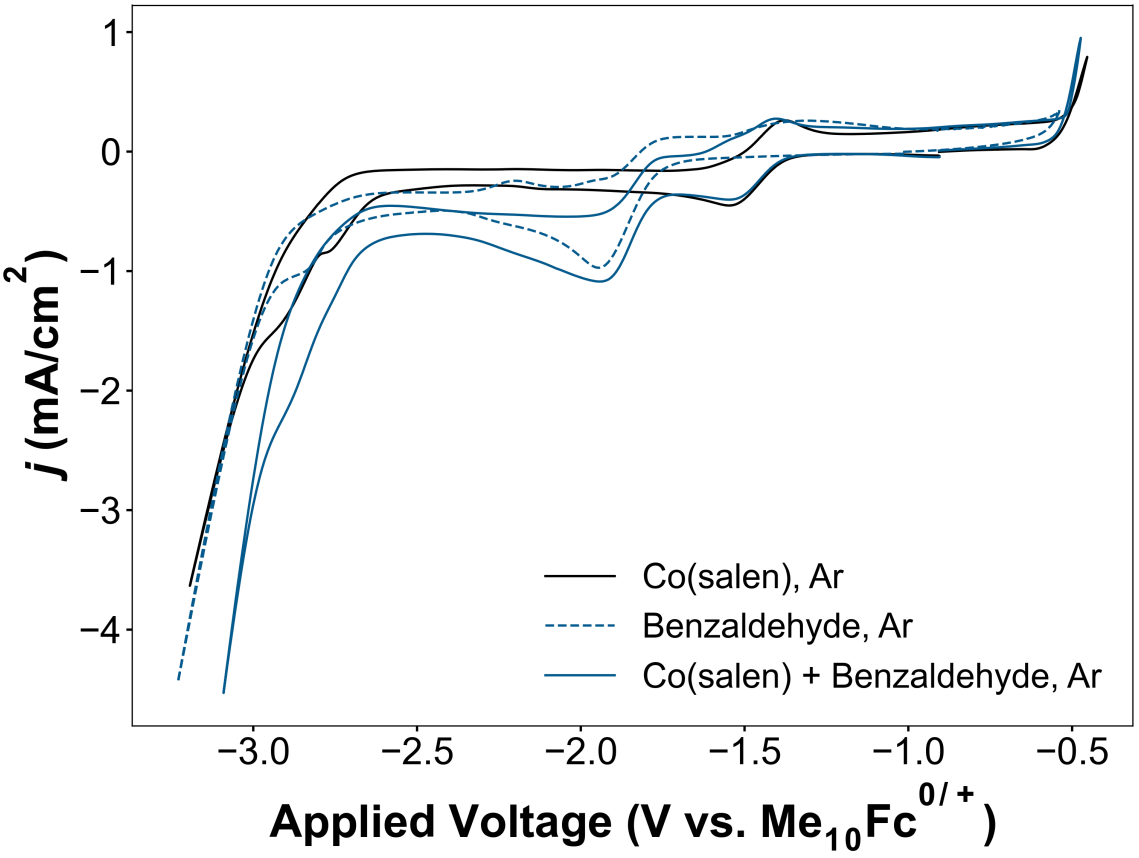

Figure A20. Cyclic voltammograms (CVs) at a scan rate of 20 mV/s in DMF for Co(salen) with and without benzaldehyde. Reaction conditions: Sn working electrode, Al counter electrode, 100 mM TBAI, 5 mM substrates in DMF.

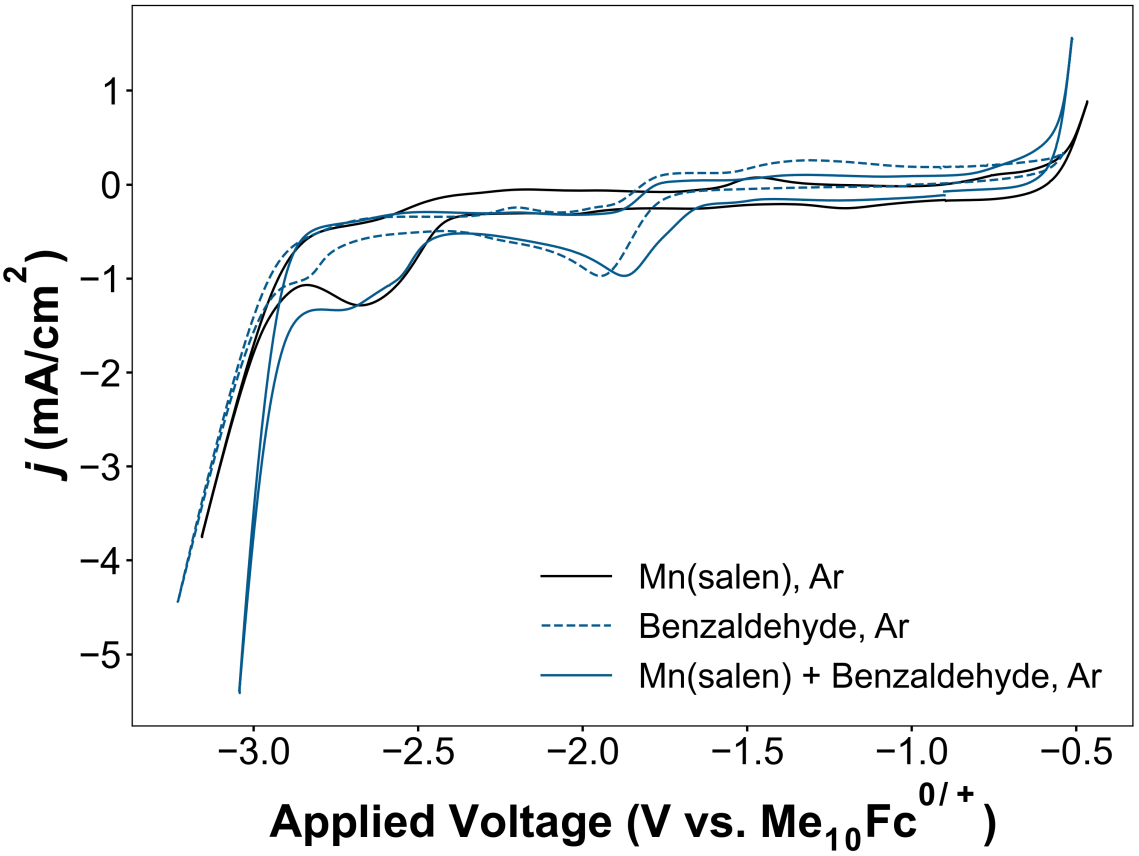

Figure A21. Cyclic voltammograms (CVs) at a scan rate of 20 mV/s in DMF for Mn(salen) with and without benzaldehyde. Reaction conditions: Sn working electrode, Al counter electrode, 100 mM TBAI, 5 mM substrates in DMF.

C.5 Synthesis of Salen Complexes

Ni(salen) complex was synthesized following reported synthetic procedures.[68,108] In a three-neck round-bottomed flask, 1.3 mmol of $Ni(OAc)_2 \cdot 4H_2O$ was mixed with 1 mmol of the chiral ligand in 40 mL of EtOH. The solution was allowed to reflux overnight at 80 ºC. Following the reflux, the reaction was left to cool to room temperature. The resulting solid was collected via vacuum filtration and washed with ethanol. The solid was dried overnight in a vacuum oven at 80 ºC to give the chiral metal catalyst.

(R,R)-(–)-N,N'-Bis(3,5-di-tert-butylsalicylidene)-1,2-cyclohexanediaminocobalt(II)

^{1}H-NMR (CD_2Cl_2): δ=7.44 (s, 2H), 7.29 (s, 2H), 6.95 (s, 2H), 2.99 (s, 2H), 2.44 (s, 2H), 1.90 (s, 2H), 1.38 (s, 18H), 1.32 (m, 4H), 1.27 (s, 18H).

C.6 Nuclear Magnetic Resonance Spectra

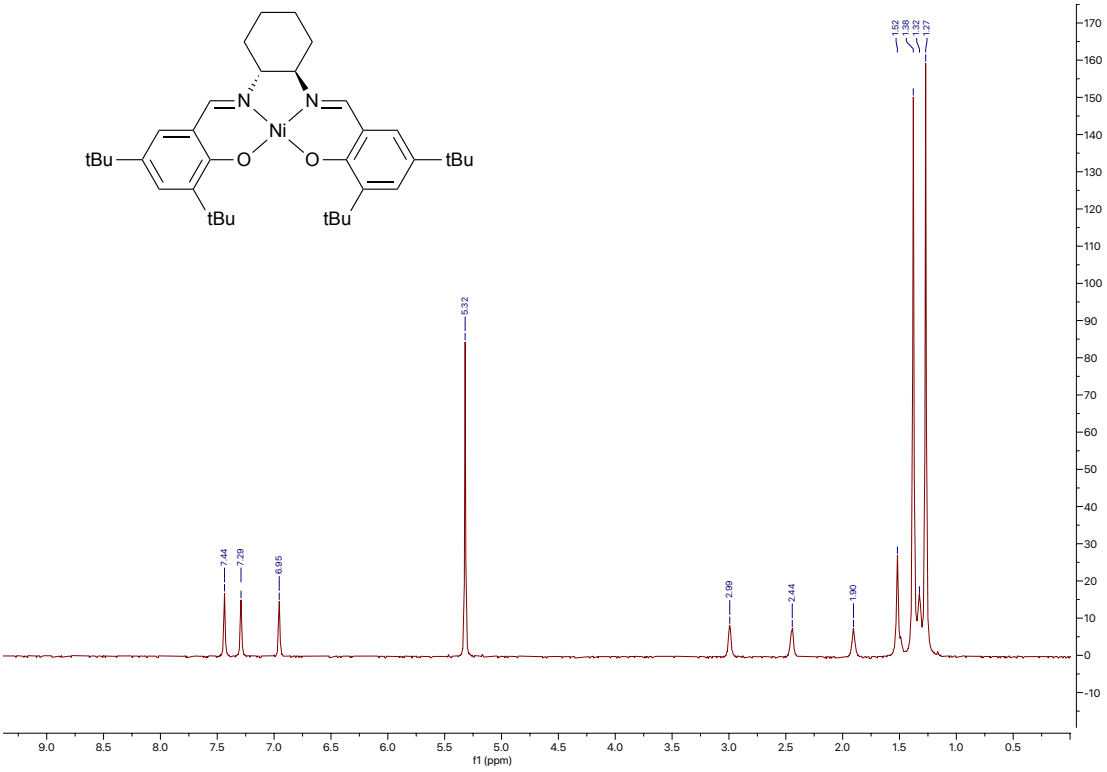

Figure A22. ^{1}H NMR spectrum of Ni(salen) complex in CD_2Cl_2.